GeoArch

Report 2012/18

Archaeometallurgical residues from the Brecon to Tirley gas pipeline

Dr Tim Young
4th July 2012
Revised 4th June 2013

Archaeometallurgical residues from the Brecon to Tirley gas pipeline

Dr T.P. Young

Abstract

This report details the analytical investigation of selected samples of archaeometallurgical residues from plots 331 and 430.Materials from plots 454 and 496 were also examined, but not analysed. Selected materials had been sub-sampled, with cut pieces mounted in resin, ground and polished, for inspection on the analytical scanning electron microscope. Data presented here are mainly backscattered electron photomicrographs (BSEM) and energy dispersive X-Ray spectroscopic (EDS) microanalyses.

The samples from Plot 331 had been taken from whole or fragmented smithing hearth cakes (SHCs). Brief re-examination of the material suggests that the cakes ranged from about 400g to a little over 1000g. The cakes have a high iron content, some contain evidence for formerly having contained metallic iron and many show evidence for 'clasts' of iron oxides, in one case of coarsely dendritic magnetic. These features indicate a high rate of iron loss in the hearth, which suggests that they were generated during bloomsmithing (primary smithing as part of the process of iron production) rather than blacksmithing (the end use of iron).

Samples from Plot 430 are entirely from bloomery iron smelting; they include tapped smelting slags, smelting slags that cooled inside the furnace and a small fragment of bloom. The chemical composition of the slags indicates that they were produced during the smelting of iron ores from the Forest of Dean. The localised distribution of the high-grade ore of Dean meant that smelting took place in locations with woodland resources well outside the area of ore outcrops. This hinterland extends at least 20km from Dean to NW and SE and35Km to SW and NE, in which directions river transport may have had a significant role. Plot 430 is well within this sphere of influence. The tapslag composition compares very closely with previously described from Ariconium *and so, although analyses of ore and furnace ceramic were not available from Plot 430, it is likely that the efficiency and mass balance of the Plot430 smelting would have been similar to that previously described there. The physical evidence from the slags also suggests similar smelting technology to that described from other smaller sites in the hinterland, rather than the different technology that appears to have been employed at the major, possibly military, smelting sites in S Wales and the SW of Dean.*

Contents

Abstract 1

Methods 2

Plot 331
- General nature of material 3
- Results 3
  - Description of residues 3
  - Details of samples 3
  - Chemical composition 4
- Interpretation 4
- Discussion 4

Plot 430
- General nature of material 6
- Results 6
  - Description of residues 6
  - Details of samples 6
  - Chemical composition 9
- Interpretation 9
- Discussion 10

Plot 454
- General nature of material 12

Plot 496
- General nature of material 13

References 14

Glossary 16

Illustration Captions 18

Table 1: Samples from Plot 331 20
Table 2: Average compositions, Plot 331 21
Table 3: Samples from Plot 430 22
Table 4: Average compositions, Plot 430 23
Table 5: comparison of Plot 331 SHCs 24

Plate 1: 25
Plate 2: 26

Figure 1: 27
Figure 2: 28
Figure 3: 29
Figure 4: 30
Figure 5: 31
Figure 6: 32

Appendix A: SEM image archive 33
Appendix B: SEM/EDS data archive 67

Methods

Samples for further investigation had been identified at the assessment stage and a methodology for their investigation on the SEM agreed between Network Archaeology and their specialist for the assessment. The methodology for this project does not follow the usual GeoArch approach and was entirely based around investigation using the analytical SEM.

Electron microscopy was undertaken on the Cambridge Instruments (LEO) S360 analytical electron microscope in the School of Earth and Ocean Sciences, Cardiff University. Microanalysis was undertaken using the system's Oxford Instruments INCA ENERGY energy-dispersive x-ray analysis system (EDX). All petrographic images presented in this report are backscattered electron photomicrographs. The polished blocks for investigation on the SEM were supplied already-prepared.

Locations of analyses are presented as sample-area-analysis (e.g. A2 SOI2 #3), where the samples (up to two) were mounted in resin blocks A to L. The area of the sample in a particular image is referred to as SOIn (SOI = Site Of Interest in the terminology of the INCA microanalysis software) and individual analyses (points or areas) are labelled #m. Images of all SOIs are included in Appendix A, including , where appropriate, details of the analysed points/areas. The scale of the images is mostly indicated by the included scale bar. For samples I,J,K and L, a problem with the instrument meant that the scale bars on the images are given incorrectly. The correct scales are quoted in the figure captions.

All analyses were collected with all elements analysed (including oxygen, but not carbon). Analytical totals were frequently far from 100%, because the analytical system is designed to provide totals of 100% from spot analyses in the centre of the field. The area analyses required for this project are not standardised in the same way and will diverge from a total of 100% (either above or below, depending on the location of the area with respect to the centre of the field).In order to make the microanalytical results simply comparable across materials (and also sites), no attempt has been made to adjust for the oxidation state of elements with variable valency. The figures employed in the report have therefore been constructed with elements expressed as oxides in weight% calculated stoichiometrically, except for mineral structure calculations, where the measured oxygen has been used. Iron is reported in the report expressed as FeO and manganese as MnO.

Throughout this report standard mineral terminology is applied to both natural and anthropogenic materials – although artificial phases are no longer strictly considered to be minerals.

The convention adopted in this report is to describe olivine bearing Fe, Mg, Ca and Mn in terms of an olivine on the forsterite-fayalite join (using the notation for instance of Fa95Fo5 for an olivine that is 95% fayalite and 5% forsterite; where Fe/(Fe+Mg) = 0.95) plus figures for the overall percentage replacement by calcium and manganese.

This project was undertaken for Network Archaeology.

Plot 331

General nature of material

Plot 331 (NGR 336993 236156) was located 1.3km to the south west of Kingstone, in Herefordshire. Most of the assemblage from Plot 331 derives from contexts investigated during initial assessment of the site and not during the subsequent excavation phase; this material does not therefore appear in the assessment catalogue (McKenzie 2008, tables E10.1 and E10.2). The site is of greater significance than might be anticipated from that document alone. The material found is described as occurring in 'dumps', with slag, hearth lining and hammerscale, associated with pottery of the late Iron Age to c. AD70. The 'dumps' lay close to a pit, also containing slag, which was c. 7.5m NE of a late Iron Age/Roman ring ditch, which also contained slag.

The site yielded a moderate number of smithing hearth cakes (SHCs), of which fifteen were either complete or were sufficiently so to be able to have the original weight estimated (230, 264, 270, 298, 310, 336, 386, 557, 606, 636, 786, 890, 920, 944 and 1035g). They thus ranged in weight from 230g up to 1035g, with mean weight of 565g and with seven (47%) weighing less than 500g and one (7%) weighing more than 1000g. Several of the examples have 'exploded' since excavation because of the corrosion of metallic iron within them.

Results

Description of residues

The five mounted samples were derived from four separate SHCs, selected as part of the assessment process.

The four SHCs sampled are all slightly different and provide a spectrum of iron content:

SHC K: this material was very iron rich and contained a zone formed of coarse-grained magnetite overgrown by wustite, several inclusions dominantly of wustite and some unusual lobe-margins comprised of wustite, magnetite and some iscorite. Other parts of the slag showed a slightly lower iron content, with a more conventional texture of wustite dendrites, followed by fayalite, with an interstitial glass.

SHC H/I: this very iron-rich slag was entirely dominated by wustite, ranging from blebby to dendritic forms. There were vesicles, probably tubular and vertical, partially occluded by fayalitic slag. The slag contained possible corroded iron blebs near its base and, less certainly, at its top.

SHC J: was somewhat heterogeneous, with a dense wustite-rich core. Both upper and lower surfaces had a higher content of silicate, with inclusions of melted hearth ceramic present on what was probably the upper surface.

SHC L: was the most silicate-rich of the four samples and therefore more fayalitic with an abundant interstitial leucite-wustite cotectic. It contained some hammerscale inclusions and ceramic influenced zones, around which there were complex intergrowths of calcic olivines and leucite, with a rhönite-bearing interstitial glass.

Details of samples

Sample H & Sample I
Context 3021
(Plates A21, A22, A23, A24)

These two samples are believed to have been taken from the same specimen, with Sample H being from the upper part of the cake and Sample I the lower.

The overall structure shows vesicles near the upper surface (which has a weathered 'crust' lying on in hand specimen, not represented in the polished mounts). The vesicularity decreases rapidly downwards to dense central section. Vesicles are again present near the somewhat lobate base.

Both samples show a texture dominated by wustite, typically in blebby to rounded stubbily dendritic forms. Typical dense parts of the slag shows 80-92% FeO. The dense wustitic slag shows pores, probably mainly vertically tubular, which often are partially filled with a material of lower iron concentration. These fills are glassy or finely crystalline olivine with an FeO content of approximately 50%.

Near the top of the cake (Sample H) the texture is complex, and rather corroded (Plate A22 f-h) Some of the secondary iron oxides have textures similar to that seen in the corroded iron in other specimens and so it is possible that the top of the SHC was originally marked by iron inclusions. Within one of these zones there are rounded areas of slag showing olivines with compositions from F96 with 4% calcium substitution in the core to Fa98 with 7% calcium substitution on the outside. A second generation of olivine is seen in the interstitial spaces, apparently with a higher calcium content.

Olivine-bearing slags are also well seen near the base of the specimen (Sample I; Plate A22, b-c). Again, these areas appear to have contained iron blebs, now entirely oxidised.

Sample J
Context 3021
(Plates A25, A26)

This sample comprised a dense, wustite-rich slag which became increasingly heterogeneous towards one surface (interpreted as the base, since vesicles appear to be generated off the siliceous inclusions, but the way up is not certain). The centre of the piece is dense and wustite-rich. The opposing surface is more siliceous again with large, delicate wustite dendrites.

In a typical, central, heterogeneous area the olivine is elongate, with crystal lengths of several millimetres. The olivine has cores of Fa93 with 4-5%Ca substitution and about 0.4% Mn substitution. These cores grade out to Fa95 with up to 10% Ca substitution and 0.4% Mn, which is then abruptly overlain by calcic olivines of Fa97 with 35% Ca substitution (i.e. 70% kirschsteinite). The interstitial spaces show fine dendrites, probably also of a calcic olivine.

The heterogeneous area show wustite-rich enclaves and zones, typically with fine textures, in associated with more siliceous, coarse grained areas, bearing vesicles with leucite –rich marginal zones.

The contact between the iron-rich slag and the partially melted hearth ceramic includes patches of kirschsteinitic olivine (expressable as Fa98 with 31% calcium substitution, i.e. 62% kirschsteinite) in an apparent cotectic with leucite (or a leucite-wustite cotectic).

Sample K
Context 3050
(Plates A27, A28, A29)

This sample shows a complex texture. The location and orientation of the sample within the SHC is difficult to reconstruct, but may be from its base.

This sample is differentiated from the others from this site by its relatively oxidised nature. Although parts of the slag are fairly conventional, with wustite dendrites, followed by elongate olivines(Fa95-96 with 4-5% Ca substitution and 0.3-0.4% Mn substation) and glass (e.g. Plate A26b), other parts show a strong development of magnetite (as equant euhedral grains and as stocky dendrites, typically with about 12% hercynite). The slag shows a strong differentiation into lobes of different levels of magnetite content, locally bounded by oxide rims, themselves of both magnetite and wustite – and locally iscorite (Plate A27 d,e,f).

The presumed basal layer in the section is dominantly of magnetite – as coarse dendrites (Plate A28). Here, too, the magnetite shows evidence over overgrowth by wustite.

Sample L
Context 3052
(Plates A30, A31)

This sample is rather different from most of the other samples from this site. The slag shows a relatively low wustite content, moderately large elongate olivine and abundant interstitial leucite-wustite cotectic. As with Sample J, where there are inclusions of glass derived from the hearth ceramic, this is associated with the development of complex intergrowths of calcic olivines and leucite, with a rhönite-bearing interstitial glass (Plate A29b).

Dense wustite inclusions occur rarely and are suggestive of flake hammerscale (Plate A29h).

Chemical composition

The overall range of composition within the samples is large, with the analysed areas from Samples H/I, Sample J and Sample L all spanning the FeO-SiO_2-anorthite ternary diagram (Figures 1 and 2) from the wustite to tridymite fields. Sample K shows less variation – possibly as a result of less sampling, but shows a similar range of variation to that of Sample I (the lower part of the section represented by Samples H and I).

The analyses mostly form a tight linear array across the FeO-SiO_2-anorthite ternary diagram, reflecting a narrow range of molar silica to alumina ratio (average of 4.0).

Interpretation

The range of textures and mineralogy demonstrated by these samples is unusual, compared with smithing slags in general, but there is little data available on comparably-dated material. The general chemical composition of the samples is however, broadly in line with other Iron Age and Roman smithing slags from the area.

The weight distribution of the SHC assemblage may be compared with those of just a few other sites. Neither the present assemblage, nor most of the comparative ones, is sufficiently large to be statistically significant, but general comparison may be made.

A compilation of the available data or comparative sites is presented in Table 5. Sample sizes are typically small, so for most sites the statistical parameters are unreliable. Nonetheless it is possible to see two groups of Roman smithing assemblages – one group with SHCs mainly less than 500g and none greater than1000g and a second group with examples of SHCs over 1000g and an average weight of over 500g. The first group is interpreted as the residues from blacksmithing operations (secondary smithing; the end use of iron), whereas the second group is interpreted to include residues from bloomsmithing (primary smithing involved in transforming a raw bloom into usable iron).

The SHC assemblage from Plot 331 fits best with this second group and although the maximum SHC size is less than on the other sites involved in bloomsmithing, the SHCs are larger than those on the middle to late Iron Age iron-production site at Crawcwelt in North Wales (Crew 1998). Other sites in the hinterland of the Forest of Dean where there was iron production also show the presence of large SHCs (e.g. Frocester Court, Thomas 2000). Other such sites in the area may have gone unrecognised; recent attempts by Allen (2009, 2010) to propose non-slag tapping furnaces from the Romano-British period around the Severn Estuary are probably erroneous, for the so-called furnace bottoms of his papers (mainly with weights less than 1kg) are extremely similar to the SHCs from bloomsmithing at Miskin and elsewhere. The site at School Road, Miskin (author's unpublished data) has an assemblage of particularly large SHCs, but this may have been a specialist site, with no secondary smithing.

The only assemblage of material available for direct comparison of the detailed analytical data is that from Coldfurrow, Lyonshall, Herefordshire (approximately 22km NNW of Plot 331). The assemblage (Young 2006b) included a number of large, dense, iron-rich SHCs from deposits associated with a smithy in a small, enclosed, Romano-British farmstead. The assemblage was interpreted as being from bloomsmithing, but there is no identified local source of iron or known smelting sites. Transport of iron ore, or part finished blooms from the Forest of Dean area is possible, but unlikely given the 50km distance. Other, as yet unknown, local sources are more likely. The Milford Haven to Brecon gas pipeline (Young 2011d) produced evidence for Roman smelting in the valley of the Afon Honddu just north of Brecon. This location would suggest a local, probably bog iron ore, source was being exploited. If such sources exist in the river valleys around Brecon, then they may well exist in the Wye valley to the NE too.

The Lyonshall assemblage shows internal structures that are broadly similar to the Plot 331 materials, but the overall chemical compositions appear more iron-rich. It is likely, however, that because investigation of the samples has focused on informative textures and mineral relationships, the large areas of rather simple wustite- and magnetite- dominated textures are possibly somewhat under-represented amongst the area analyses and therefore the calculated averages (Table 2 and Figure 3) are likely to show less iron than is actually the case. The implication of this would be that the Lyonshall smithing slags and those from Plot 331 may be more similar than the average compositions would suggest.

The weight range of the SHCs, together with the high iron contents, therefore suggests that the SHCs from Plot 331 are the residues from the processes broadly known as bloomsmithing or bloom-refining. In detail, these classes of residues are poorly understood at present, for it is clear that not all bloom refining was undertaken purely as a smithing (reheating, working) process. The present material is however suggestive of bloomsmithing in the conventional sense – the samples show oxidised pieces of iron and hammerscale.

Discussion

The subsequent interventions at this site avoided some of the slag-rich deposits located in the evaluation phase, but none-the-less it is clear that this site was of enormous significance. Very few Iron Age bloomsmithing sites have been described; none with both full residue descriptions accompanying physical evidence for the nature of the hearth and process. It is unfortunate that full investigation of the metalworking at Plot 331 was not attempted (macroresidues, microresidues, e.g. hammerscale, and structures).

Iron Age bloomsmithing structures have been described in North Wales (Crew 1987, 1989, 1998), and early to middle Iron Age bloomsmithing residues have been described from southern England from Risely (McDonnell 1984) and from Truro (Young 2008). The occurrence of early Roman (1st century AD) bloomsmithing residues at sites such as Caergwanaf (Young 2010b), and Cardiff Castle (Young & Kearns 2011) is known, but these materials have not yet been analysed in detail. Later Roman bloomsmithing has been identified at Lyonshall (Young 2006b), Dymock (Young & Kearns 2010b) and Caerwent (Young 2006a). At none of these Roman sites is there yet good evidence for the physical nature of the bloomsmithing facility.

The distance of Plot 331 from the Forest of Dean, and its general similarity with the residues from Lyonshall even further away, hints that other sources of iron ore may have supplied so-far unrecognised smelting in this area. One possibility is that there are local bog iron ore resources.

The evidence from Plot 331 therefore falls within a complete gap in existing knowledge, making the site significant on a national basis.

Plot 430

General nature of material

Plot 430 (NGR 35590 22514) was located north of the A49, about 1km northwest of Peterstow.

The site produced archaeometallurgical residues from a wide variety of contexts. The key area was area 430C, a subsection of the site lying at the top of the hill above the two enclosures (area A and B). In Area C metalworking appears to have been undertaken in the 1st-2nd centuries AD.

The current description of the field remains suggests that area C included the remains of two 'bloomeries'. The presented field evidence is insufficiently detailed to comment in detail, but the description resembles to some extent that of two 'furnace settings' – locations in which a furnace may be built and then reconstructed as required over time. The succession, in each setting, of intercutting pits may indicate the changing location of the furnace., but it is unclear what element of the furnaces the 'pits' might represent. Further detailed consideration of (and archaeometallurgical input to?) the interpretation of these structures will be needed before publication, as discussed further below.

Results

Description of residues

The fourteen samples investigated in detail included eight samples of tapped slag, one sample of a slag 'rod', four samples of furnace slags and one fragment of bloom.

The tapped slag (tapslags) showed some textural variability, with some examples with a very fine texture, in small lobes (e.g. sample F1), others with 'classic' textures with chilled lobe margins, sheaf-like bundles of olivine crystals nucleating from the margins and thin 'crusts' on the lobes formed of wustite and/or magnetite (e.g. sample A1) and others still with coarser textures and less well-formed lobe boundaries suggestive of slow cooling (e.g. sample B1).

The tapslags showed elongate olivine, with composition close to fayalite (the total substitution by cations other than iron is almost always less than 10%), with only slightly magnesian cores grading to slightly calcic margins. The interstitial spaces are usually filled by other a glass bearing very fine-grained calcic olivine, or by strongly calcic olivine (70% kirschsteinite) in association with a leucite-wustite cotectic. Such textures were described more generally in the region by Thomas (2000) and it is possible that the origin of the variation lies in a degree of immiscibility within the last fraction to crystallise.

The furnace slags show, as typical, a much less homogeneous texture, with a very variable distribution of primary wustite, forming a network with holes, some of which become occluded by more fayalitic slag, others of which remain open as vesicles. The vesicles, and the margins of charcoal inclusions, often show the development of leucite-rich rims. This is a result of the capture of potassium from the fuel gasses by the adjacent slag. The adjacent olivine is also often moderately to strongly calcic, probably reflecting the addition of calcium from the fuel too. The olivine in the bulk of the slag shows similar low levels of substitution to those in the tapslags.

The bloom fragment was unfortunately too corroded for recovery of any information about the iron. The metal was in contact with a variable, but commonly very wustite-rich slag.

The slag 'rod' (Sample E1) had a structure and mineralogy similar to those of the more iron-rich furnace slags.

Details of samples

Sample A1
Context 86104
(Plates A1, A2, A3)

This sample was taken from a block of fine-grained tap slag in well-formed flow lobes. The flow lobes have smooth, maroon surfaces. In section, the lobe surfaces are seen to be thin horizons of oxides.

The lobes are formed of slag which is variably vesicular. It has fine, sparse, but large dendrites of wustite, forming around 5%. The slag is variably vesicular, both between and within lobes, from just approximately 2% on chilled lobe edges to over 20% in some lobe cores.

The olivine ranges in composition from cores of Fa95 with about 2% of calcium substitution and 0.4% manganese substitution to outer parts of up to Fa98 with 8% Ca and 0.4%Mn. The interstitial glass occasionally bears crystals that are probably a kirschsteinitic olivine.

The olivine crystals form radiating sheaves nucleated on the chilled margins of lobes (Plate A3a, c). The crystals are at least 2mm in length and probably up to 5mm. At their widest individual crystals reach 80µm.

Sample A2
Context 86001
(Plate A4)

Sample A2 resembles A1 in many ways, but the internal lobe surfaces are less well marked, commonly show small protuberances (Plate a3b, d, f) and in some instances (Plate A3d) show continuity of olivine crystals across the boundary. These features suggest that the lobes seen were formed in rapid succession with the earlier (lower) lobe incompletely solidified before imposition of the later (upper) lobe.

The primary wustite is very similar, with sparse, delicate, large dendrites. The olivine is similar in morphology and composition to that in A1 (Fa95 with 2% Ca and 0.4% Mn substitution grading outwards to Fa99 with 0.9% Ca substitution.

Sample B1
Context 86131
(Plate A5)

Sample B1 is a coarser-grained tap slag than samples A1 and A2. The internal lobe boundaries are marked by textural changes in the slightly coarser-grained olivine, with no indication of a wustite/magnetite lobe crust – suggesting that these lobes may have accumulated in the absence of significant oxygen and with a lower cooling rate – so perhaps within the

furnace mouth or low in a rapidly accumulating stack of lobes.

The main phase olivine shows a similar range of composition to that in A1 and A2, ranging outwards from Fa93 with 2% Ca and 0.3% Mn substitution to Fa98 with up to 13% Ca substitution and 0.3 Mn substitution.

The interstitial areas are of two distinct varieties. In one there is an interstitial glass bearing fine dendrites of a late-stage calcic olivine. In the other there is a development of a leucite-wustite cotectic in association with a kirschsteinitic overgrowth (Fa100 with 35%Ca substitution) on the main olivine.

Sample B2
Context 86131
(Plates A6, A7)

Sample B2 is porous, charcoal-bearing slag. In section there is very little primary wustite, and the little that is present is concentrated in particular areas. There are some substantial vesicles, with well-developed leucite-rich margins and localised development of grains of metallic iron nearby. The leucite occurs as rounded masses of a leucite-wustite cotectic and also as equant euhedral crystals.

Near to the leucite-rich areas, observed olivine compositions ranged from Fa89 with 1% Ca and 0.4% Mn substitution through to Fa99 with 10% Ca and 0.4%Mn on the margin. In one area the olivine was associated with minor hercynite. The olivine is typically present as 80-300 µm equant, euhedral grains, but in some cases these may possibly be sub-units of larger crystals.

The interstitial areas, as in B1, were variable, with an interstitial glass bearing a calcic olivine being common, but other spaces are filled by a leucite-wustite cotectic. The main phase olivine locally shows a kirschsteinitic overgrowth and in turn locally overgrown rhönite, as small crystals fringing the glassy interstitial areas.

Sample C1
Context 86156
(Plate A8)

This sample shows some similarity to B2, but shows a lower porosity, a more general distribution of stout, small, wustite dendrites and is generally somewhat coarser-grained.

The olivine again forms equant crystals, but of up to about 600 µm; the arrangement of these suggests in some cases they are sub-units of larger complex crystals.

The main olivine grades out from Fa94 with 2% Ca and 0.4%Mn substitution to margins of Fa98 with 6%Ca and 0.4%Mn substitution. Olivine of this composition is then extensively intergrown with the leucite-wustite cotectic, leaving a final interstitial space filled by glass with a fine calcic olivine and rhönite.

Sample C2
Context 86156
(Plate A9)

Sample C2 is a rather coarse-grained tap slag. The primary phase is a small proportion of rather small, delicate, wustite dendrites. These are followed by an olivine, with an elongate form, up to 1mm in length and typically less than 30 µm in width. The olivine is slightly more calcic than in some other tapslags here, with cores of Fa92 with 4% Ca and 0.4%Mn substitution grading to margins of Fa98 with 13% Ca and 0.4% Mn substitution.

The interstitial spaces are filled with a glass rich in very fine grained olivine – apparently of a fairly calcic composition.

The sample is not well preserved, but lobe margins appear to be largely missing any substantial development of iron oxides, although a development of very fine wustite (and magnetite?) dendrites just inside the margin as observed. This may correlate with the observation the piece appears to have been tapped into or through charcoal.

Sample D1
Context 86165
(Plate A10)

Sample D1 is of a fine-grained, slightly vesicular slag, probably a tapslag, with a similar texture to samples A1 and A2, but with a markedly higher proportion of wustite (a reflection of its higher bulk iron content than those samples).

The main phase olivine reaches at least 1mm in length and 60 µm in width. The composition ranges from Fa95 with 3% Ca substitution to Fa98 with 7% Ca substitution on its margins, both with 0.3-0.4% manganese substitution.

The interstitial areas are dominantly glassy with fine olivine dendrites.

Sample D2
Context 86165
(Plates A11, A12)

This sample shows highly corroded iron particles, contained within a very iron-rich slag. The most likely interpretation of this sample is that it represents a small fragment detached from the margin of a bloom.

The iron is entirely corroded and nothing can be said about its former composition. Some relicts of texture are preserved. The broadly concentric structure of the weathering of the main iron particle (approximately 8mm across) probably reflects an original structure, with zones in which the iron appears to include an amalgamation of rounded bodies in close association with an area with rounded slag inclusions, locally up to several hundred microns across.

The associated slag shows a range of textures from areas dominated by coarse, rounded wustite ‘pseudodendrites’, through to glassy (or very finely fayalitic) areas with fine, delicate wustite dendrites. The same range of textures is seen in the external slag as in the probable slag inclusions within the iron.

Sample E1
Context 86174
(Plate A13)

Sample E1 shows considerable similarity to sample C1, although it is somewhat richer in wustite. The wustite forms stout dendrites with rounded arms, reaching up to about 1mm in size.

The main phase of olivine is elongate, reaching 3mm in length and 100 µm in width. The composition varies from Fa94 with 2% Ca and 0.4% Mn substitution in the cores to Fa98 with 6-10% Ca and 0.3%Mn substitution on the margins. The olivine is locally intergrown with a leucite-wustite cotectic. In these areas the olivine approaches Fa99 with 25%Ca and 0.4%Mn substitution (i.e. is approximately 50% kirschsteinite). In other areas the interstitial space is filled with glass bearing parallel late-stage olivine, with a composition up to Fa99 with 17% Ca and 0.6%Mn substitution.

Sample E2
Context 86174
(Plate A14)

Sample E2 is a dense tap slag, broadly comparable with other tap slags in the collection. It does not show clear evidence for well-marked oxide crusts on the flow lobes.

Primary wustite is present as fine delicate dendrites reaching about 500 µm across. The subsequent olivine is elongate, certainly reaching 2mm in length. The olivine composition ranges from Fa93 with 0.7% Ca and 0.6%Mn substitution out to Fa98 with 1.4% Ca and 0.5%Mn substitution. The interstitial areas are of glass with a late, fine, elongate olivine of around Fa98 with 1.8% Ca and 0.5%Mn substitution. The low calcium content of the olivines reflects a lower bulk concentration than in any of the other slags form the site, besides those attached to the bloom fragment (Sample D2).

Sample F1
Context 86196
(Plate A15, A16)

This sample is a somewhat unusual stack of flow lobes. The individual lobes are very thin and fine-textured. They are not typically well-bonded to each other, with significant inter-lobe porosity (possibly indicating they were non-wetting). They are also unusual in showing a relatively high degree of calcium enrichment, but little corresponding potassium enrichment.

Detailed observations of mineralogy were only made in one of the coarser lobes (still one of the finest textures observed from the site) because of the practical problems of obtaining reliable analyses from the finer textures.

Primary wustite was present in delicate dendrites. In some areas (Plate A15g) this showed a variable density on the BSEM image, suggesting that both wustite and possibly magnetite may be present.

The main olivine was very delicate and skeletal. The fine mixture of olivine with the glassy matrix meant that microanalysis of the olivine was not achievable, but it would appear to have been a fayalite with about 10% calcium substitution. The interstitial space is a glass bearing very fine crystals, probably also of olivine.

Sample F2
Context 86196
(Plate A17)

Sample F2 is texturally very similar to sample A2. Parts of the sample are very straightforward, chilled flow lobes (Plate A17c), but away from the most chilled area there appear to breaks in the oxide crusts and the olivine crystals pass through some boundaries (e.g. Plate A17a). Such textures do not necessarily indicate that the growth of the olivine was a continuous process, merely that growth was able to resume into the second lobe.

Analysis of olivine shows a core of Fa95 with 4% Ca and 0.3% Mn substitution grading out to Fa98 with 10-12%Ca and up to 0.4% Mn substitution, with a rather similar composition for late stage olivine within the interstitial spaces.

Sample G1
Context 86225
(Plate A18)

Sample G1 shows similarity with G2 and particularly with sample E1. Compared with E1, it shows a greater, if patchy, development of wustite. The wustite shows a wide distribution of rounded 'gaps' presumably early pores, some now filled by the fayalitic slag, others surviving as open pores. The olivine is typically very large, with dimensions greater than 1mm, and possibly of a relatively equant shape.

Rounded growths of leucite-wustite cotectic are associated with euhedral or subhedral leucite (Plate A18g). The leucite is clearly, at least locally, predating the enclosing olivine.

Remaining interstitial space is filled with complex, probably close to eutectic, growths of feathery dendritic olivine in glass.

The main olivine appears to grade between cores of Fa94 with 2% calcium substitution and margins of Fa98 with about 12% calcium and 0.4%manganese substitution. There seems to be localised late overgrowth of Fa99 with 34%calcium substitution (i.e. 68% kirschsteinite). The kirschsteinite is overlain in turn by a thin overgrowth and also by the late stage interstitial olivine – both with compositions around Fa99 with 17-19% Ca substitution.

Sample G2
Context 86225
(Plates A19, A20)

Sample G2 is a very porous slag, broadly similar to sample G1. The patchy primary wustite varies from agglomerations of large blebs to well-developed dendritic forms. The early gaps in the wustite coverage may be filled by later fayalite – sometimes in the form of otherwise isolated, large bridging crystals.

One margin of the sample (the right hand margin in Plate A19 and Plate A20a) shows indications of being a contact with hearth ceramic – but the orientation of the contact is not known. The contact zone includes localised coarse fayalite (without any wustite), zones of fine-grained iron oxides of uncertain origin, and zones of fine quench-textured fayalitic slag in association with what are probably weathered blebs, formerly of metallic iron.

Within the body of the piece, the voids are generally rimmed with leucite-rich zones, frequently multiple, and thin layers of olivine. The olivine in the body of the slag appears to be mainly somewhat elongate, up to 1mm by 0.5mm. Analyses suggest the cores of the large olivines are as low as Fa91, with under 2% calcium substitution and around 0.3% Mn substitution. The margins of these olivines reach about Fa97 with 5% Ca and 0.3% Mn substitution.

On the margins of the larger pores the leucite-rich zones include, as in G1, both areas of leucite-wustite cotectic and areas with euhedral to subhedral (just possibly resorbed) leucite (Plate A19g). As with other examples from this site, the olivine associated with the leucite is calcic and is mainly Fa99 to Fa100 with 12 to 36% Ca substitution.

Chemical composition of samples

The analyses of selected areas within the samples are presented in Table B2 and the averages of those areas for each sample are given in Table 4.

The general range exhibited by the averaged compositions for the slags is very small, with much of the variation simply be due to the variable levels of iron. Sodium, phosphorus, titanium and manganese are present in very low levels, with manganese rarely exceeding 1 wt% as an oxide. Potassium typically occurs at levels of 1-2% as an oxide; calcium is more variable , ranging from 1.4 to 5.9 wt% oxide. The Si:Al ratio is tightly constrained, with a mean of 4.5.

Various ternary diagrams have been employed to display, and to assist with the interpretation of, relationships in iron slag assemblages. The FeO-SiO_2-Al_2O_3 diagram is commonly employed, as is the CaO-FeO-SiO_2 diagram, but for the present material, in which the levels of CaO and Al_2O_3 are similar, the FeO-SiO_2- $CaAl_2Si_2O_8$ (anorthite) diagram (Levin *et al.* 1964, p. 288, fig. 869) is more appropriate. This diagram was first used for iron slags in the works of Morton & Wingrove (1969, 1972) in discussion of slags from this region of the UK. Morton & Wingrove appear, however, to have used an unusual methodology for calculating the position of data within this system and a revised methodology is adopted here, which discards excess components from analyses which lie outside the ternary plane.

The same diagram was used extensively to illustrate slag variation by Thomas (2000; with a corrected methodology).

The chemical analyses of individual areas are plotted on the FeO-SiO_2- $CaAl_2Si_2O_8$ (anorthite) diagram in Figures 3 and 4. Here they display a remarkably coherent pattern, which can be taken as indicative of a consistent process and technique.

The samples from tapslags form a very tight cluster of points. The analyses from tapslags D1 and parts of C2 lie at the iron rich end of the cluster; all others cluster below 75%FeO. At the iron-poor end of the spectrum the tapslag field is approximately bounded by the samples interpreted as furnace slags B2 and C1. Small, wustite-free zones with G1 and G2, samples interpreted as coming from the zone between the bloom and furnace wall, also plotted in this area.

The iron-rich tapslags of C2 and D1 plot in the same area of the diagram as the analyses from the slag rod (E1) and the majority of analyses from G1 and G2.

This cluster of analyses coincides with the relatively iron-poor slags associated with the bloom fragment, the more iron-rich of which lie at over 80%FeO within the wustite field. All other analyses plot within the fayalite field.

This distribution, tap slags forming a tight cluster in the centre of the more variable furnace slags, provides some support for the suggestion (Thomas & Young 1999a and 1999b) that tapslags from the moderately large slag-tapping furnaces of this area effectively sample the slags produced in the smelting reaction and may, therefore, be employed in mass balance discussions.

Interpretation

The low levels of abundance of many of the dominant elements in the chemical compositions of the slags are typical of slags generated during the smelting of the high-grade iron oxide ores of the Bristol Channel Orefield (*sensu* Young & Thomas 1998, 1999; Young 2000). Thomas (2000) described many of the features seen in the Plot 430 samples from material from other sites within the orefield.

Several separate databases of chemical analyses of smelting slags from the region exist:-

The first of these derives from work around the Severn Estuary by J.RL. Allen and co-workers from Reading (Allen 1988, 2009, 2010; Allen & Fulford 1986, 1987, 1990a, 1990b, 1992; Fulford & Allen 1992). These data provide a useful dataset, although the interpretation of the data raises some problems and, in particular, the differentiation of smelting and smithing slags is sometimes controversial.

The second database is that of work done in Cardiff, including the analyses made for the PhD thesis of Thomas (2000), together with various GeoArch projects (Young 2006a, 2010c, 2010d, 2012; Young & Thomas 1997) and the author's unpublished research on several sites in South Wales.

The third major source is the data compilation by Paynter (2006, 2007), which draws on both of the first two in part, but also includes other published sources and unpublished material from within English Heritage.

Comparison of these various regional data with the current analyses shows a high degree of coherence between the present suite and those previous analyses interpreted to be from the smelting of Forest of Dean ores.

The FeO-SiO_2- $CaAl_2Si_2O_8$ (anorthite) diagram is used to illustrate selected comparative analyses in Figure 6. The field containing the EDS analyses of samples from Plot 430 is shown in pale grey tone. A high degree of overlap is demonstrated with tapslags from the Severn Vale (Allen 1988), from the Chesters site at Woolaston (Fulford & Allen 1992) and from *Ariconium* (Thomas 2000; Young 2012). A lower degree of overlap is shown with materials from Worcester (McDonnell & Swiss 2004), Usk (Thomas 2000) and Frocester Court (Thomas 2000). Interestingly, it is those sites that are geographically closest to the Forest of Dean that provide the best comparisons, perhaps because of the highest degree of similarity of underlying geology.

The reasons for differences in the chemical compositions of slags from the region have been discussed on numerous occasions (Allen 1988, 2009; Paynter 2006, 2007; Thomas 2000). It seems clear, however, from the mass balance calculations (Thomas & Young 1999 a and b), that given the high-grade of the Forest of Dean ores, the influence of the composition of the furnace ceramic will be dominant on the concentration in the slag of those elements most involved in such discussions (e.g. Si, Al, Na, Mg, Ti; but also K and Ca which may also be strongly influenced by the fuel ash).The furnace ceramic contributes 25% - 30% of the mass of the slag according to the mass balance calculations of Thomas (2000). The clustering of data from this region may well thus be a reflection of the variation in the composition of available clays for furnace construction and therefore be a reflection on the local geology (possibly both bedrock and superficial in different cases).

In particular the data from samples from Plot 430 may be compared with analyses (Thomas 2000) of Roman materials from *Ariconium* – the major Roman smelting centre just 8km east of Plot 430 (Jackson 2012). The *Ariconium* site lies on very similar geology to Plot 430. Differences between the two suites of analyses are mainly seen in sodium and magnesium. Whilst this may be a genuine difference, it must be bore in mind that it is possible that analysing these two light elements at low concentrations may cause problems for the analytical techniques.

Discussion

Analyses of smelting residues from Plot 430 allow the confident provenancing of the ore employed to the Forest of Dean and close comparison may be made with residues from nearby *Ariconium*.

Rapid re-examination of the samples from the site suggests that the materials sampled are representative of the residue assemblage. It also suggests that the assemblage comprises dense tapped slags, porous/charcoal rich furnace slags, some slag 'runners' and rare examples of slag 'rods'. Such an assemblage is typical of many sites in the area. The significance of the 'rods' (= 'slag tubes' of McDonnell & Swiss 2004) is unclear. They occur widely on other sites of Roman age, not only in this area, but also in the Weald (e.g. Young 2011a). They appear distinct from the plano-convex 'runners' – which represent slag chilled in the tapping channels, and have usually been attributed to formation in blowholes or 'spy-holes' in the furnace wall. McDonnell & Swiss (2004) hint at an interpretation associated with a rather more exotic process. However, the abundance of the rods suggest that they are formed during the normal operation of a furnace. In the Weald, they may possibly be associated with dome furnaces (Young 2011a). The runners themselves are interesting, for they indicate the use of a channel to carry the slag through the tap arch area. They have been found at several other sites (e.g Miskin, Frocester, Caerleon) and are a characteristic component of the residue assemblage from these sites.

The assemblage does not include the thick, massive, dense, furnace slags, often with ore and roundwood charcoal inclusions, that are becoming recognised at some locations SW of the Forest of Dean (Caergwanaf, author's unpublished data; Cardiff, Young & Kearns 2011; Woolaston, Fulford & Allen 1992; possibly Alvington, Young 2009b; and within central Dean, Young 2011b). These sites include some that appear to have been 'official', in some cases possibly military, operations (e.g. Cardiff and Caergwanaf; Young forthcoming). These occurrences seem to indicate a significantly different smelting technology on these sites.

Unfortunately, very few furnaces have themselves been investigated in the region. The best known, but still with many questions attached, is the large furnace at the 'Chesters', Woolaston (Fulford & Allen 1992). Furnaces at *Ariconium* were dug by Bridgewater (1965), but appear to have been heavily truncated. Better examples at *Ariconium* were found in the unpublished 1967 excavations by Garrod and Moss. Although these have now been illustrated by Jackson (2012), they have not been described in detail. The evidence for the nature of the furnace structures in Plot 430 is therefore very important. Although simple slag-tapping, relatively low-shaft, furnaces are the most

likely class of furnace to produced the observed residue assemblage, other morphologies are possible.

Although not actually in the Forest of Dean, Plot 430 lies well within its hinterland – the area over which smelting sites are distributed with a fairly common occurrence. This hinterland extends at least 20km SE of Dean, into the margins of the Cotswolds, 20 km NW (into SW Herefordshire), but farther to NE and SW (35km NE up to Worcester and 35km SW to Caerleon) in which directions movement of ore may have been facilitated by movement on the Severn. The existence of the hinterland may be a response to the requirements for the production of large quantities of charcoal, which may not have been able to have been satisfied in the core area.

In summary, it appears that Plot 430 shows a similar style of iron smelting to other sites in the hinterland of the Forest of Dean, but a technology distinct from that of major, possibly military, centres of smelting. The ore was from Dean, but provenancing ore to particular sources within Dean requires data for elements not analysable under the SEM.

Plot 454

General nature of material

The residues from Plot 454 were re-examined to determine whether further inspection could clarify their origin and whether they would suitable for further investigation. The following list provides a revised catalogue of materials from this plot:

85000: small fragment of slag or clinker, two further certain clinker fragments, three pieces of sandy lining slags and six dense vesicular slag fragments, strictly indeterminate, but likely to be from smithing.

85029: blebby flow-slag penetrating between large charcoal moulds. Indeterminate as to origin in iron smelting or smithing.

85036: probable smithing slag piece, highly weathered, with adhering hammerscale.

85039: rather weathered probable smithing slag piece – surface accretion includes hammerscale.

85043: vitrified hearth lining, pale fine fabric and planar face very similar to material from 85103.

85082: four pieces of vesicular slag, some in poorly developed lobes -probably smithing slag, 1 tiny fragment of lining slag, 1 large piece(c.480g) probably representing a part of a rather prilly SHC of large size.

85088: bleb of convoluted lining slag (probably from iron working).

85101: three small fragments of iron slag attached to hearth/furnace wall

85103: vitrified hearth lining and several substantial pieces of iron slag. Most of the iron slag is probably from smithing - including one extremely coarse grained piece likely to be from bloomsmithing. Two pieces are indeterminate - either from smithing or from Iron Age style slagpit furnace smelting.

85106: three substantial pieces and one fragment of charcoal-rich flow slag, strictly indeterminate but probably smelting furnace slags (quite similar to Iron Age style slagpit furnace slags). One small fragment is probably tapped smelting slag with well-developed maroon haematised surface (i.e. not a morphological similar Iron Age non-slag tapping flow slag).

In summary, the residues from Plot 454 are probably mainly from smithing, probably particularly bloomsmithing, with just one tiny fragment of typical tapslag to indicate smelting nearby. Some of the charcoal-rich slag could just possibly be from Iron-Age smelting, but their evidence is not conclusive. Detailed analysis would not be capable of distinguish Iron Age furnace slags from their Roman equivalents. The assemblage is typical of a site involved in iron production at the period and further investigation would be unlikely to provide additional useful clarification. No further analysis was therefore pursued on the material from this plot.

Plot 496

General nature of material

The residues from Plot 496 were re-examined to determine whether further inspection could clarify their origin and whether they would suitable for further investigation. The following list provides a revised catalogue of materials from this plot:

90009: extremely dense iron slag, containing a high proportion of metallic iron.

90016: various prills, both horizontal (over charcoal) and vertical of dark surfaced slag. No superficial oxidation. one piece shows a planar non-wetted contact surface - possibly from stone or a tool.

90023: three unusual fragments of copper alloy waste - two are metal fragments that appear to have impregnated adjacent charcoal fragments, 1 is just an equivalent impregnated charcoal piece. The most likely interpretation, given the multiple charcoal fragments involved in the larger piece, is that they are the results of spills into a metalworking hearth.
There are also broken fragments from fine grained weathered slag with dimpled base -probably smithing slag, plus one long prill from slag flow through fuel, possibly associated with tapping.
There is also a large prilly SHC weighing 1080g. For the Roman period, such a large SHC is likely to be the result of bloomsmithing rather than blacksmithing.
There is also a bag of small indeterminate slag scraps of varying composition.

90025: lining slag bleb hanging on reduced fired lining

90029: 2 pieces of indurated material, probably out of a hearth floor, one shows a very dark prilly slag binding clay and stone fragments, the other has clay alone,

90038: 3 small blebs of dense iron slag, 2 small fragments of oxidised fired lining.

The residues from Plot 496 are somewhat similar to those from Plot 454, including large SHCs suggestive of bloomsmithing and some materials that just possibly might be from Iron Age smelting (although other interpretations are possible). The copper alloy materials are probably casting spills. It was an interesting facet of material from two sites in nearby Dymock (Dungworth 2007; Young & Kearns 2010b) that the residues there including iron smelting, bloomsmithing and copper alloy casting (including, specifically, the manufacture of brooches) along with possible silver reclamation/purifying (possibly for plating the brooches) - a very mixed range of metalworking activities taking place together .

In general, the iron slags are fairly unremarkable. They suggest (albeit on a very small sample) that this site may have been more involved with bloom processing than primary smelting. The well-flowed slags do not show surficial oxidation – and therefore accumulated with a fuel bed. This could happen with a slag-tapping smelting furnace, but in the absence of tapslag from this site it is probably more likely they are a flow slags from a non-slag tapping furnace, or are abnormal flows from within a smithing hearth. The assemblage is very small, as well as mixed, and in the absence of association with metallurgical features, detailed analytical investigation would be unlikely to be able to generate useful additional information or to differentiate between the possibilities suggested by the morphological investigation.

Analysis of the small amount of copper alloy residue would not be likely to generate useful data, since a wide range of copper alloys were used in the Roman period and were widely recycled.

No further analysis on material from this plot was therefore undertaken.

References

ALLEN, J.R.L. 1988. Chemical compositional patterns in Romano-British bloomery slags from the wetlands of the Severn Estuary. *Historical Metallurgy*, **22**, 81-86.

ALLEN, J.R.L. 2009. Romano-British iron-making on the Severn Estuary: towards a metallurgical landscape. *Archaeology in the Severn Estuary*, **19**, 73-79.

ALLEN, J.R.L. 2010. The alkali-metal ratio in Roman British bloomery slags. *Archaeology in Severn Estuary*, **20**, 41-45.

ALLEN, J. R. L. & FULFORD, M. G. 1986. The Wentlooge Level: A Romano-British Saltmarsh Reclamation in Southeast Wales. *Britannia*, **17**, 91-117.

ALLEN, J.R.L. & FULFORD, M.G. 1987. Romano-British settlement and industry on the wetlands of the Severn Estuary. *Antiquaries Journal,* **67**,237 -289.

ALLEN, J.R.L. & FULFORD, M.G. 1990a. Romano-British and later reclamations on the Severn salt marshes in the Elmore area, Gloucestershire. *Transactions of the Bristol and Gloucestershire Archaeological Society*, **108**, 17 -32.

ALLEN, J.R.L. & FULFORD, M.G. 1990b. Romano-British wetland reclamations at Longney, Gloucestershire, and the evidence for the early settlement of the inner Severn Estuary. *Antiquaries Journal*, **10**.288-326.

ALLEN, J.R.L. & FULFORD, M.G. 1992. Romano-British and later geoarchaeology at Oldbury Flats : reclamation and settlement on the changeable coast of the Severn Estuary, southwest Britain. *Archaeological Journal*, **149**, 82-123.

BARFORD, P.M. 1996. The metalworking debris from Bear Barn and the Bear Field. Pp. 205-209 *in:* J. Parkhouse & E. Evans, *Excavations in Cowbridge, South Glamorgan, 1977-88*. BAR, British Series, 245pp.

BRIDGEWATER, N.P. 1965. Romano-British iron working near Ariconium. *Transactions of the Woolhope Naturalists' Field Club*, **38**, 124-135.

CREW, P. 1987. Bryn y Castell Hillfort – a Late Prehistoric Iron Working settlement in north-west Wales. In: SCOTT, B.G. & CLEERE, H. (eds) The Crafts of the Blacksmith. 91-100.

CREW, P. 1989. Crawcwellt West excavations 1986-1989. A late prehistoric ironworking settlement. Archaeology in Wales, 29, 11-16.

CREW, P. 1998. Excavations at Crawcwellt West, Merioneth, 1990-98: A late prehistoric upland ironworking settlement. Archaeology in Wales, 38, 22-35.

CREW, P. 2003. Slags and other iron-working residues. pp. 333-340 *in:* H. James, *Roman Carmarthen: Excavations 1978-1993*. Britannia Monograph Series 20, Society for the Promotion of Roman Studies 2003.

DUNGWORTH, D. 2007. Slags and Moulds. *In: T.* Catchpole, 2007, Excavations at the Sewage Treatment Works, Dymock 1995, *Transactions of the Bristol and Gloucestershire Archaeological Society*, **125**, 183-186.

FULFORD, M.G. & ALLEN, J.R.L. 1992. Iron-making at the Chesters villa, Woolaston, Gloucestershire: survey and excavation 1987-91. *Britannia*, **23**, 159-215.

JACKSON, R. 2012*. Ariconium, Herefordshire: An Iron Age Settlement and Romano-British 'Small Town'*. Oxbow, 304pp.

LEVIN, E.M., ROBBINS, C.R. & McMURDIE, H.F., 1964. *Phase Diagrams for Ceramists*, Columbus, Ohio, American Ceramic Society.

McDONNELL, J.G. 1984. Interim Report. Slags, Risely Farm, Berkshire. *English Heritage Ancient Monuments Laboratory Report 4422*.

McDONNELL, J.G. & SWISS, A. 2004. Ironworking residues. pp. 368-378, in: H. Dalwood & R. Edwards *Excavations at Deansway, Worcester, 1988-89: Romano-British small town to late medieval city*. CBA Research Report 139.

McKENZIE, R. 2008. Appendix 10. Metallurgy Assessment. E77-E93 *In:* Network Archaeology 2010, Brecon To Tirley High Pressure Gas Pipeline, Assessment of Potential For Analysis. *Network Archaeology Report No. 413*.

MORTON, G.R. & WINGROVE, J. 1969. Constitution of bloomery slags: Part 1: Roman. *Journal of the Iron and Steel Institute*, **207**, 1556-1564.

MORTON, G.R. & WINGROVE, J. 1972.Constitution of bloomery slags: Part II: Medieval. *Journal of the Iron and Steel Institute*, **210**, 478–488.

PAYNTER, S., 2006. Regional variation in bloomery smelting slags of the Iron Age and Romano-British periods. *Archaeometry*, **48**, 271-292.

PAYNTER, S., 2007. Innovations in bloomery smelting in Iron Age and Romano-British England, pp. 202–210*, in:* S La Niece, D Hook and P Craddock (eds), *Metals and Mines. Studies in Archaeometallurgy* (London).

STARLEY, D. 2012. Ironworking debris from the Welsh Water pipeline. Pp. 161- 163 *in:* R. Jackson, *Ariconium, Herefordshire: An Iron Age Settlement and Romano-British 'Small Town'*. Oxbow, 304pp.

THOMAS, G., 2000. *A chemical and mineralogical investigation of bloomery iron-making in the Bristol Channel Orefield, UK*. Unpublished PhD thesis, Cardiff University.

THOMAS G.R. & YOUNG, T.P. 1999a. Bloomery furnace mass balance and efficiency. *In:* POLLARD, A.M. (ed) *Geoarchaeology: exploration, environments, resources*, Geological Society of London, Special Publication, 165, 155-164.

THOMAS, G.R. & YOUNG, T.P. 1999b. A graphical method to determine furnace efficiency and lining contribution to Romano-British bloomery iron-making slags (Bristol Channel Orefield, UK). *In:* YOUNG, S.M.M., BUDD, P.D., IXER, R.A. and POLLARD, A.M. (eds). *Metals in Antiquity*, British Archaeological Reports International Series, **792**, 223-226. Archaeopress, Oxford.

YOUNG, T.P. 2000. Chapter 10. The Paviland Ochres: characterisation and sourcing. *In*: Aldhouse- Green, S., *Paviland Cave and the 'Red Lady': a definitive report.* Western Academic and Specialist Press Limited, 205-225.

YOUNG, T.P. 2005. *Evaluation of metallurgical residues from Marsh Leys Farm*. GeoArch Report 2005/07.

YOUNG, T.P. 2006a. *Archaeometallurigcal residues from the Caerwent Forum-Basilica (provisional report).* GeoArch Report 2006/01. 33pp + 8 plates.

YOUNG, T.P. 2006b. *Archaeometallurgical residues from Coldfurrow, Lyonshall, Herefordshire.* GeoArch Report 2006/09. 12pp. & 2 plates.

YOUNG, T.P. 2008. *Archaeometallurgical residues from Richard Lander School (RLS04) and Truro College (TCF05)*. GeoArch Report 2007/22. 31pp. & 10 plates

YOUNG T.P. 2009a. *Archaeometallurgical residues from Crickhowell Road, Trowbridge, Cardiff*. GeoArch Report 2009/02. 11pp.

YOUNG, T.P. 2009b. *Evaluation of Archaeometallurgical residues from Alvington, Glos. (RCA08),* GeoArch Report 2009/14, 3 pp.

YOUNG, T.P. 2010a. Archaeometallurgical residues. 155-159. *In:* M. Brett, E. R. McSloy and N. Holbrook. A Roman enclosure at Crickhowell Road, Trowbridge, Cardiff. Evaluation and excavation 2005–06. *Archaeologicia Cambrensis*, **158**, 131-166.

YOUNG, T.P. 2010b. Caergwanaf. Pp. 214-216, *In:* B.C Burnham & J.L. Davies (eds) *The Roman Frontier in Wales and the Marches.* Royal Commission on the Ancient and Historical Monuments of Wales.380pp.

YOUNG, T.P. 2010c. *Analysis of archaeometallurgical residues from Brownslade, Pembrokeshire [NPRN 94225].* GeoArch Report 2010/07, 23 pp.

YOUNG, T.P. 2010d. *Archaeometallurgical residues from Robeston Wathen, Pembrokeshire. GeoArch Report 2010/09*, 13 pp.

YOUNG, T.P., 2011a. *Archaeometallurgical residues from Little Furnace Wood, Mayfield, East Sussex.* GeoArch Report 2011/21. 75 pp.

YOUNG, T.P. 2011b. *Evaluation of archaeometallurgical residues from the Forest of Dean Archaeological Survey, Stage 3B phase 2 (37920/37921/37923/37924).* GeoArch Report 2011/32. 13 pp.

YOUNG, T.P. 2011c. Metallurgical Residues, p. 112-114 and Appendix IV, p. 178-180 in: M. Luke & Preece, T. *Farm and Forge: late Iron Age/Romano-British farmsteads at Marsh Leys, Kempston, Bedfordshire*. East Anglian Archaeology, Report No. 138, 198 pp.

YOUNG, T.P. 2011d. *Assessment of the archaeometallurgical residues from the Milford Haven to Brecon High Pressure Gas Pipeline.* GeoArch Report 2011/40. 9 pp.

YOUNG T.P. 2012. Petrographic and chemical analysis. Pp. 163-164 *in:* R. Jackson, *Ariconium, Herefordshire: An Iron Age Settlement and Romano-British 'Small Town'*. Oxbow, 304pp.

YOUNG, T.P. *forthcoming*. Roman military control on ironmaking in South Wales. *In*: B. Cech, T. Rehren (Editors), *Ferrum Noricum – iron production and distribution 200 BC to AD 400, Proceedings of the conference on "Early Iron" in Hüttenberg, September 8th to 12th, 2008*.

YOUNG, T.P. & KEARNS, T. 2010a. *Evaluation of metallurgical residues from Caerleon Junior School (CA/JS/07)*. GeoArch Report 2010/17, 7pp.

YOUNG, T.P. & KEARNS, T. 2010b. *Evaluation of archaeometallurgical residues from Kyrleside, Dymock, Gloucestershire (32523 & 33787).* GeoArch Report 2010/19, 5pp.

YOUNG, T.P . & KEARNS, T. 2011. *Evaluation of metallurgical residues from the New Interpretation Centre, Cardiff Castle, Cardiff [ST181765].* GeoArch Report 2011/02, 27 pp.

YOUNG, T.P. & THOMAS, G.R. 1997. *Geochemistry of iron-making slags from Caerleon, Gwent.* Cardiff Earth Sciences Geoarchaeology Report 97/03. 7 pp.

YOUNG, T.P. & THOMAS, G.R. 1998. The cargo: iron ore analysis. pp. 105-111 *In:* Nayling, N. *The Magor Pill Medieval Wreck*, CBA Research Report 115, Council for British Archaeology.

YOUNG, T.P. & THOMAS G.R. 1999. Provenancing iron ore from the Bristol Channel Orefield: the cargo of the Magor Pill Boat. *In:* POLLARD, A.M. (ed) *Geoarchaeology: exploration, environments, resources*, Geological Society of London, Special Publication 165, 103-121.

Glossary

Bleb: a small rounded particle or textural component, often a droplet or prill

Blacksmithing: The working of iron for the creation or repair of artefacts.

Bloom: The raw block of iron produced during smelting in the bloomery process. Blooms require further compaction and reworking (bloomsmithing or bloom-refining) in order to remove voids, charcoal and most of the slag entrained in the raw bloom. The remaining slag forms elongate inclusions in the iron, which gives bloomery iron its toughness. Many of the objects described as blooms have undergone at least some compaction. Fully compacted blooms (but not yet worked down to usable bar iron) are termed billets.

Bloomery: a furnace for smelting iron from ore in which iron is produced as a solid material. The bloomery process was employed mainly prior to the introduction of the later blast furnace from the late 15th century.

Bloom-refining: Usually taken as an alternative term for bloomsmithing, but may encompass techniques other than physical working (such as re-melting).

Bloomsmithing: The process of reworking a raw bloom, through repeated reheating and hammering, to reduce its content of slag, to remove unwanted inclusions and to draw out the remaining slag into elongate inclusions. The end product may be a bar or billet. Usually taken as an alternative term for *bloom-refining.*

Blowhole: A hole through a furnace or hearth wall through which air is blown.

Bog Iron Ore: hydrated iron oxide ores formed in superficial sediments (including, but not limited to bogs) through the oxidation of iron-bearing groundwaters.

Cotectic: crystallisation of a liquid to produce two phases at the same time.

Dendrite: a branched crystal form, often associated with rapid growth.

End-member: The limits of solid solution in a mineral system. Used in cases where all the possible sites which a particular element can occupy in a crystal are occupied by atoms of the element. An example would be fayalite, Fe_2SiO_4 being the iron end-member of the olivine group, whereas forsterite, Mg_2SiO_4 is the magnesium end-member.

Euhedral: a crystal shape in which the crystal has developed its faces, indicating its growth was unobstructed by previously formed phases.

Fayalite: the iron-rich end member of the olivine group, Fe_2SiO_4.

Forging: the process of hot-forming a metal by beating it.

Forsterite: the magnesium-rich end member of the olivine group, Mg_2SiO_4.

Goethite: a hydrated iron III oxide, FeO.OH.

Hematite: an iron III oxide Fe_2O_3

Hercynite: an iron-aluminium member of the spinel group of minerals: $FeAl_2O_4$

Interstitial space or *interstice*: the space between the main generation of crystals in a material. On cooling the main phase of crystals will solidify whilst the interstitial spaces are still occupied by molten material, which will solidify at a lower temperature.

Iscorite: the informal name for a phase (artificial mineral) to date only observed in metallurgical slags. The chemical composition is $Fe^{2+}{}_5Fe^{3+}{}_2SiO_{10}$. The mineral is typically encountered in contexts where wustite is oxidised in the presence of fayalite.

Kaolinite: a hydrous alumina-silicate clay mineral, the major component of china clay, $Al_2Si_2O_5(OH)_4$

Kirschsteinite: the calcium/iron-rich end member of the olivine group, $FeCaSiO_4$.

Leucite: a potassium-bearing mineral $KAlSi_2O_6$

Magnetite: an iron oxide member of the spinel group, Fe_3O_4.

Olivine: a group of silicate minerals of the form $(M^{2+})_2SiO_4$ where M can commonly be iron, magnesium, calcium (up to half the M^{2+} ions) or manganese. Includes the end-members fayalite (Fe_2SiO_4), forsterite (Mg_2SiO_4), tephroite (Mn_2SiO_4), kirschsteinite ($CaFeSiO_4$) and monticellite ($CaMgSiO_4$). The complex substitutions are described in this report by using the convention of describing the Fe-Mg as the fayalite-forsterite proportion (for instance Fa95Fo5, where Mg is 5% of the total of Mg+Fe) and then describing the Ca and Mn concentrations as percentage substitutions of the forsterite-fayalite.

Prill: a small aggregate of a material, either a spheroidal droplet or a runnel, formed from a melted liquid and either occurring as a discrete particle or as an inclusion within another material.

Quench: to cool rapidly from high temperature.

Rhönite: An aenigmatite group mineral with a formula of $Ca_2(Mg,Fe^{2+},Fe^{3+},Ti)_6(Si,Al)_6O_{20}$.

Shaft furnace: A furnace that is taller than wide. The shaft furnace permits the reaction of the charge, which descends as the fuel burns, with rising carbon monoxide. Many bloomery furnaces are shaft furnaces, as are blast furnaces.

SHB: Abbreviation for smithing hearth base. This is a synonym of *smithing hearth cake* (*SHC*), which has more general use because the slag cake does not typically form in the bottom of the hearth.

SHC: Abbreviation for smithing hearth cake. A slag cake, typically plano-convex, that forms just below the air inlet in a smithing hearth.

Slagpit Furnace: a variety of bloomery iron smelting furnace in which much of the slag formed during the smelt drains into a pit below the shaft (rather than being tapped outside the furnace).

Smithing: the activity involved in forming a metal object, including, but not limited to, forging metal and joining metal by welding.

Smithing hearth: a hearth used for the heating of metals for smithing.

Smithing hearth cake: a cake of slag formed in the smithing hearth below the level of the air blast. They typically have a rounded convex base, with an upper surface that may be concave, planar or convex depending on the amount of slag that accumulates (abbreviated to *SHC*).

Spinel: a mineral group with the general formula $X^{2+}Y^{3+}{}_2O_4$, which includes, amongst many others, the minerals hercynite and magnetite.

Subhedral: a form of crystal growth which is impeded by some pre-existing phases to permit only some of a crystals faces to be developed.

Tap slag (or *tapped slag*, sometimes *tapslag*): slag that has been *tapped* from a furnace as a liquid to solidify outside the furnace.

Tapping: the process or act of allowing a liquid to flow from a furnace. In the bloomery process it is the slag that may be tapped; in a blast furnace both slag and iron are tapped.

Valency: a measure of the number of bonds formed by an atom of a given element

Vesicle: a void or pore, usually rounded and formed as a preserved gas bubble in a solidified melt.

Wustite: an iron II oxide FeO.

Illustration Captions

Plate 1:
Backscattered Electron Photomicrographs of selected specimens of smithing slags from Plot 331

a. Sample K: montage of images (SOI8-11) showing a section through the lower (?) part of the SHC. The lower part of the section shows a large inclusion formed of inwardly-growing large magnetite dendrites. The zone above shows dendrites and angular skeletal grains of magnetite (pale grey) overgrown by wustite (bright) and followed by elongate fayalite (mid-grey). This is bounded by a scale-like margin (see (c) for detail), above which magnetite is subordinate to wustite.

Scale bar 1mm.

b. Sample H (SOI 5): typical area of sample showing wustite (pale) in rounded blebs and poorly-developed dendrites. The wustite is followed by fayalite (mid grey), which forms the filling of much of the pore on the upper margin, leaving surviving open vesicles (black).

Scale bar 1mm.

c. Sample K (SOI12): detail of a scale-like inclusion associated with dendrites with cores of magnetite (pale grey), overgrown by wustite (bright, rounded margins) and iscorite (bright elongate, thin). The matrix is formed of very finely grained fayalite (mid grey) in glass (dark grey).

Scale bar 200µm.

d. Sample L (SOI9): partially-reacted flake hammerscale fragment, formed of wustite, overgrown by new-formed wustite (bright). The matrix includes elongate fayalite (mid grey) with interstitial phase mainly a leucite-wustite cotectic (black with white specks).

Scale bar 200µm.

e. Sample L (SOI2): detail of zone around a bleb of glass derived from the hearth lining (mid-grey, lower right). The complex reaction zone is dominated by calcic olivine (pale grey) and leucite (dark). For detail see (f).

Scale bar 200µm.

f. Sample L (SOI3): detail of (e). Calcium poor fayalite is overgrown by intergrowths calcium-rich olivine and leucite. The remaining interstitial space is filled with a glass (mid-dark grey) containing hollow crystals of rhönite (slightly paler).

Scale bar 200µm.

Plate 2:
Backscattered Electron Photomicrographs of selected specimens of smelting slags from Plot 430

a. Sample A1 (SOI2): detail of a typical oxidised flow lobe margin from a tapslag. Pale phase in the margin and as fine dendrites is wustite. The mid-grey crystals are fayalite, which has an interstitial matrix of glass with very fine late-stage olivine (dark).

Scale bar 200µm

b. Sample B1 (SOI1): lobe margin in a tap slag, lacking a oxidised crust. The arcuate margin has acted a point for nucleation of the elongate (pale grey) fayalite, which are secondary to very delicate wustite dendrites (bright).

Scale bar 1mm

c. Sample B1 (SOI7):detail of an interstitial space between wustite dendrites (pale) and olivine crystals (mid grey) filled with glass (dark), bearing very fine dendrites of a secondary olivine.

Scale bar 80µm

d. Sample B1 (SOI 3): detail of an interstitial space between wustite dendrites (pale) and olivine crystals (mid grey) filled with a kirschsteinitic olivine (slightly darker than the main phase fayalite) and rounded mass of a leucite-wustite cotectic (leucite dark, wustite bright).

Scale bar 80µm

e. Sample C2 (SOI4): typical microstructure of a tap slag with a moderate wustite (bright) content. Elongate olivine crystals (mid-grey) with an interstitial space filled by glass (dark) bearing fine-grained dendrites of olivine.

Scale bar 60µm

f. Sample E1 (SOI3): microstructure within the slag 'rod' in which the two interstitial fill types (see (c) and (d)) occur together. The glass occurs on the left, in a quench structure between parallel fine olivine crystals; the calcic olivine plus leucite-wustite cotectic occur to the right.

Scale bar 50µm

g. Sample B2 (SOI4): a pore margin in a wustite-poor furnace slag. Much of the interstitial space between the olivines is here occupied by large leucite-wustite cotectic intergrowths (speckled), and locally leucite (dark) on its own.

Scale bar 600µm

h. Sample G2 (SOI42): detail of a wustite-rich furnace slag, showing the wustite developing a framework around 'pores', some of which are entirely filled by fayalitic slag, some bridge by isolated fayalite crystals and others surviving as open vesicles (with margins rich in leucite).

Scale bar 1mm

Figure 1:
Plots of individual area analyses from samples from Plot 331, plotted on the FeO-SiO_2- $CaAl_2Si_2O_8$ (anorthite) diagram.

Figure 2:
Composite of all area analyses from samples from Plot 331, plotted on the FeO-SiO_2- $CaAl_2Si_2O_8$ (anorthite) diagram.

Figure 3:
Plot of area analyses from Plot 331 averaged for each sample (red points), with the field of all area analyses (grey tone), compared with bulk chemical analyses of

smithing slags from other localities (see text for discussion of the origin of these comparative data).

Figure 4:
Plots of individual area analyses from samples from Plot 430, plotted on the FeO-SiO_2- $CaAl_2Si_2O_8$ (anorthite) diagram.

Figure 5:
Composite of all area analyses from samples from Plot 430, plotted on the FeO-SiO_2- $CaAl_2Si_2O_8$ (anorthite) diagram.

Figure 6:
Plot of the field of all area analyses from Plot 430 (grey tone), compared with bulk chemical analyses of smelting slags from other localities (see text for discussion of the origin of these comparative data).

Table 1: Details of samples from Plot 331.

sample	*context*	*original note from assessment*	*surviving sample*	*mounted sample*
H	3021	classic SHB	small fragment from SHC; dense, rusted top, dished, some vesicles, particularly just above weathered base	probably section from top (vesicular, fayalitic) to middle (wustite-rich) of cake
I	3021	classic SHB	[from same piece as above?]	lobate base of cake, passing up towards dense wustite zone
J	3021	dense slag (poss. SHB or furnace?)	rather strongly-curved fragment - probably pale slag on top - so probably an SHC burr	shows gradation from heterogeneous slag (wustite- and ceramic- rich zones) into more uniformly dense material (below?)
K	3050	dense slag (poss. SHB or furnace?)	only tiny chips remaining from preparation; these are very dense slags with internal lobes picked out by lines of vesicles. Presumed original block 854g remaining in separate box. SHC, dense internally slightly lobate, deep, bun shaped, 110x110x40mm.	Unusual slag, apparent lobe margins or scale with iscorite, and a dense zone with coarse magnetite dendrites
L	3052	Dense SHB slag	tiny fragment remaining - show small and large pores as well as dense area - could be SHC	Vesicular slag with well-developed vesicle margin minerals, including rhönite and leucite. Some included flake hammerscale.

Table 2: average chemical composition of samples from Plot 331. Analyses presented as wt% oxides, calculated stoichiometrically from the average of the normalised EDS analyses of representative areas within each sample.

	Na_2O	MgO	Al_2O_3	SiO_2	P_2O_5	S	Cl	K_2O	CaO	TiO_2	MnO	FeO
H	0.53	0.77	2.86	18.21	0.43	0.08	0.01	1.94	4.32	0.04	0.12	70.69
I	0.34	0.79	5.69	19.18	0.30	0.03	0.00	0.89	2.53	0.19	0.00	70.07
J	0.66	0.75	6.34	28.16	0.29	0.02	0.03	2.75	4.75	0.15	0.03	56.06
K	0.43	0.64	3.95	18.59	0.12	0.00	0.00	1.95	2.90	0.07	0.09	71.27
L	1.76	1.16	7.52	32.06	0.19	0.01	0.00	2.76	2.89	0.23	0.08	51.34

Table 3: Details of samples from Plot 430.

sample	*context*	*original note from assessment*	*surviving sample*	*mounted sample*
A1	86104	tap	dense tap slag in narrow lobes	fine-grained tap slag in lobes
A2	86001	tap	large block of tap slag with sandy base, part of side is raised and may be a down-flow or just possibly (from shape of base) a hot deformed bend	coarse grained tap slag with possible remelted (or not initially solid) internal lobe margins
B1	86131	tap	dense tap slag in broad lobes,	coarse tap slag, no oxide on lobe margins, abundant leucite
B2	86131	furnace	from small broken piece of charcoal rich vesicular slag	coarse charcoal bearing slag with leucite and rhönite
C1	86156	furnace	[none]	coarse slag with irregular voids and leucite
C2	86156	tap	rather porous conventional tap slag as part of small flow on/through charcoal	fine grained tap slag
D1	86165	tap	[none]	fine vesicular slag with abundant wustite
D2	86165	furnace	rusted and accreted fragment with some signs of exploding	bloom fragment
E1	86174	porous tap	20x30mm slag rod	vesicular slag - probably from slag rod fragment, well developed vesicle margins
E2	86174	tap	very dense tap slag with strong radial crystals in upper flow; one piece has 'sandy' base, other very reflective with ore fragments	dense tap slag lobe with more abundant fine vesicles in upper part
F1	86196	dense furnace	[none]	tap slag in very thin lobes
F2	86196	dense furnace	[none]	fine grained tap slag
G1	86225	possible SHC	[none] (possible source – 2 concavo-convex blocks with large pore spaces, and rusty concave surfaces	coarsely vesicular ?burr material from smelting furnace
G2	86225	possible SHC	[none] (as above)	coarsely vesicular ?burr material from smelting furnace

Table 4*: average chemical composition of samples from Plot 430. Analyses presented as wt% oxides, calculated stoichiometrically from the average of the normalised EDS analyses of representative areas within each sample.*

	Na_2O	MgO	Al_2O_3	SiO_2	P_2O_5	S	Cl	K_2O	CaO	TiO_2	MnO	FeO
A1 (tap)	0.41	0.65	4.29	25.83	0.27	0.00	0.00	1.77	3.22	0.05	0.12	63.39
A2 (tap)	0.39	0.71	4.27	24.98	0.13	0.00	0.00	1.70	3.63	0.09	0.24	63.88
B1 (tap)	0.24	0.90	6.17	27.80	0.14	0.00	0.00	2.24	3.12	0.20	0.08	59.11
B2 (furnace)	0.17	1.35	6.38	29.36	0.34	0.02	0.00	1.70	3.20	0.22	0.13	57.12
C1 (furnace)	0.11	0.62	7.31	27.16	0.18	0.03	0.00	1.94	3.73	0.29	0.23	58.42
C2 (tap)	0.06	1.13	4.34	24.94	0.30	0.00	0.00	1.21	3.79	0.15	0.17	63.91
D1 (tap)	0.17	0.79	3.92	20.71	0.26	0.02	0.00	1.40	2.87	0.05	0.04	69.77
D2 (bloom)	0.07	0.89	3.31	15.02	0.19	0.01	0.13	0.90	1.44	0.06	0.20	77.76
E1 (rod)	0.16	0.83	3.92	18.74	0.00	0.02	0.00	1.25	2.36	0.04	0.18	72.50
E2 (tap)	0.37	0.97	6.49	25.26	0.00	0.05	0.00	1.90	1.69	0.12	0.31	62.85
F1 (tap)	0.27	0.85	4.21	24.06	0.11	0.01	0.00	1.57	5.88	0.07	0.08	62.90
F2 (tap)	0.28	0.70	4.66	23.79	0.20	0.01	0.02	1.59	4.64	0.09	0.06	63.96
G1 (furnace)	0.38	0.84	3.27	20.63	0.38	0.03	0.02	1.15	2.58	0.00	0.06	70.65
G2 (furnace)	0.19	0.83	3.95	21.17	0.35	0.00	0.00	1.40	2.41	0.00	0.05	69.65
Average tapslag	0.26	0.84	4.70	24.01	0.16	0.01	0.00	1.63	3.47	0.09	0.14	64.69
Average furnace slag	0.18	0.90	4.85	22.67	0.29	0.02	0.03	1.42	2.67	0.11	0.14	66.72
Overall average	0.23	0.86	4.75	23.53	0.20	0.02	0.01	1.55	3.18	0.10	0.14	65.42

Table 5: Comparison of the weight of SHCs from Plot 331 with those of other comparative sites

Site				Statistics of SHC weight distribution where known					
Name	**Reference**	**Age**	**Comment**	**Number**	**Minimum wt.**	**Maximum wt.**	**Mean wt.**	**% <500g**	**%>1000g**
Carmarthen	Crew 2003	RB		136	100	820	227	94%	0%
Cowbridge	Barford 1996	RB		?	175	700	403	?	0%
Marsh Leys Farm	Young 2005, 2011c	RB		30	?	824	333	77%	0%
Caerleon Endowed Schools Field	Young & Kearns 2010a	RB		6	58	284	172	100%	0%
Trowbridge, Cardiff	Young 2009a, 2010a	RB		3	144	290	225	100%	0%
Lyonshall	Young 2006b	RB		14	176	2077	564	64%	14%
Dymock	Young & Kearns 2010b	RB C2?		10	112	3885	1032	60%	14%
Cardiff Castle	Young & Kearns 2011	RB C2-3		5	193	1090	626	40%	20%
Miskin School Road	Author's unpub data	RB C3-4?	SHCs mainly 1-2kg, some over 2kg			>2000			
Ariconium	Starley 2012	RB	Small SHCs average 200g, one was 2740g	8		2740			13%
Crawcwellt	Crew 1998	M-L IA	SHCs mainly either 100-150g (secondary) or 300-400g (primary)						
Plot 331		LIA - RB		15	230	1035	565	47%	7%

a

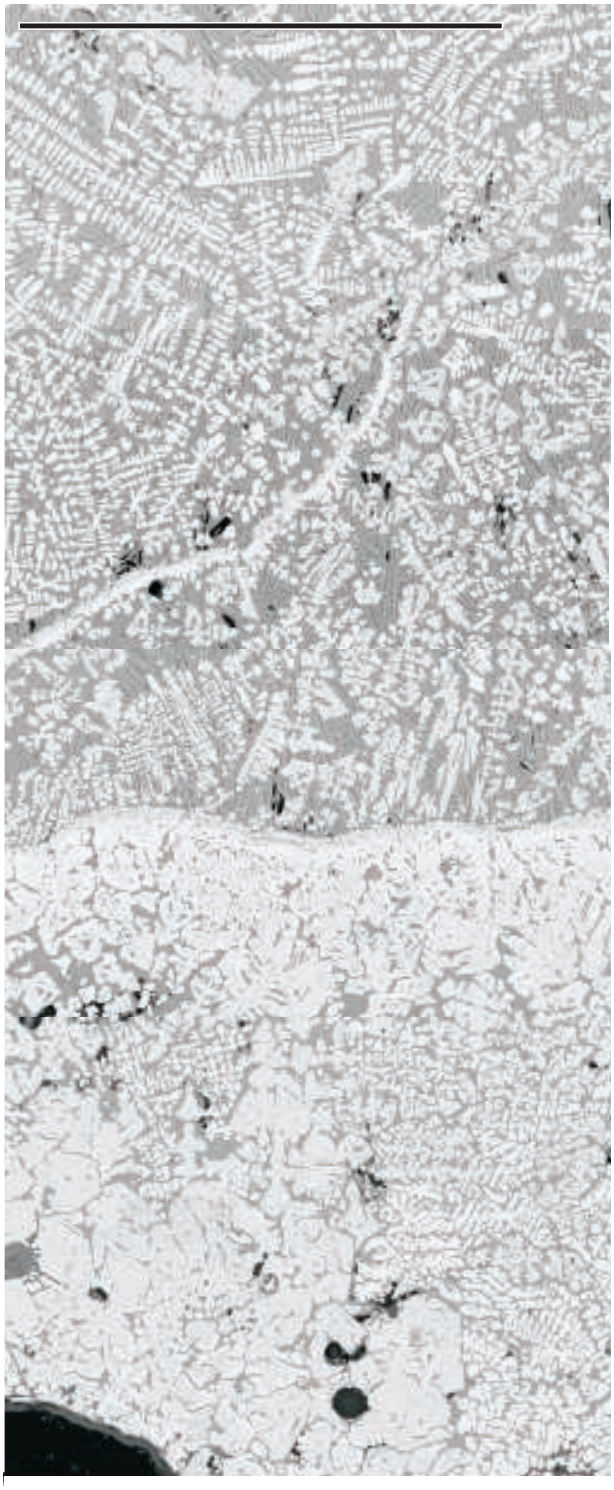

b

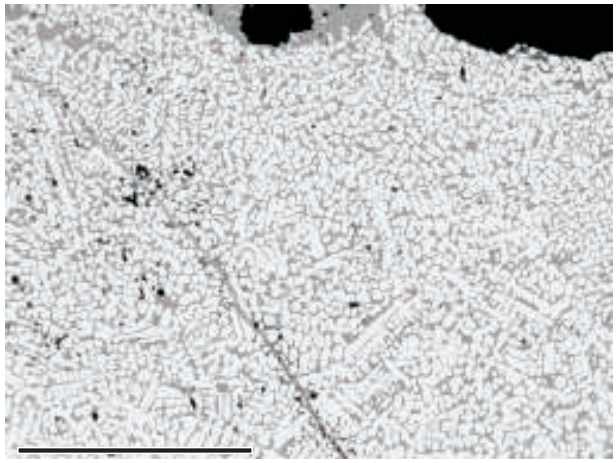

c

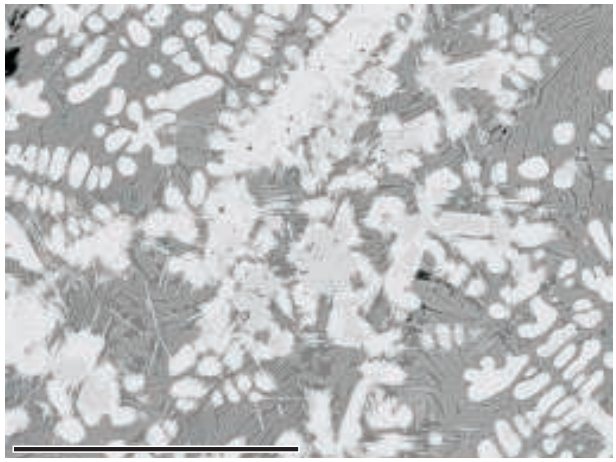

d

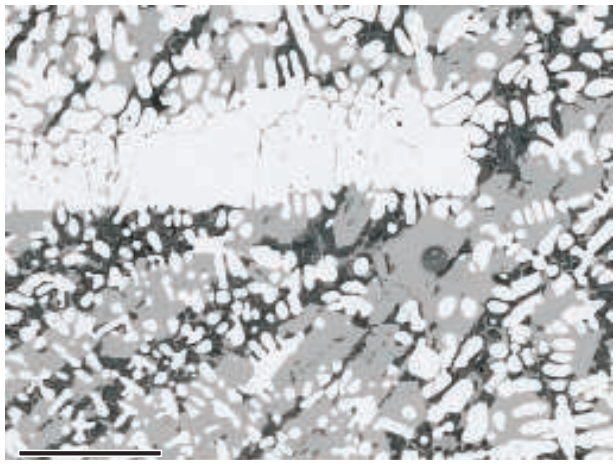

e

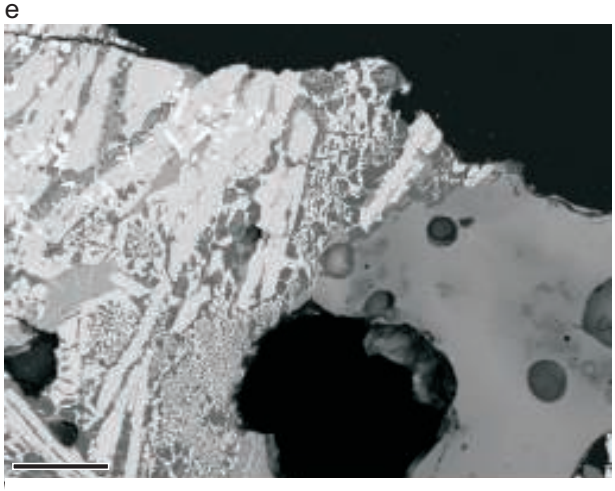

f

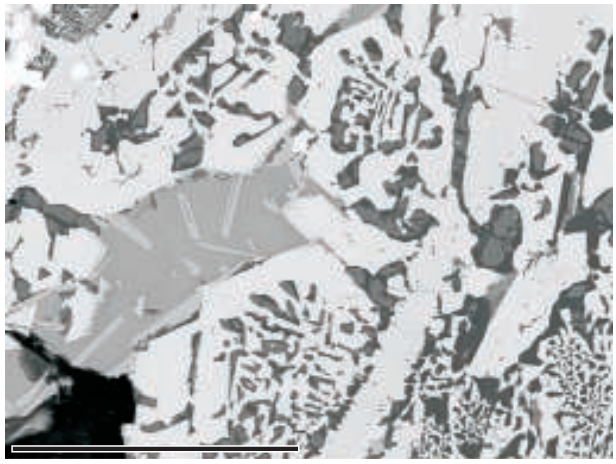

a

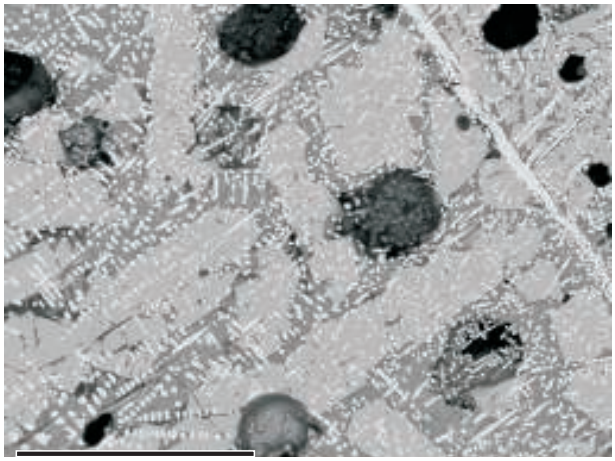

b

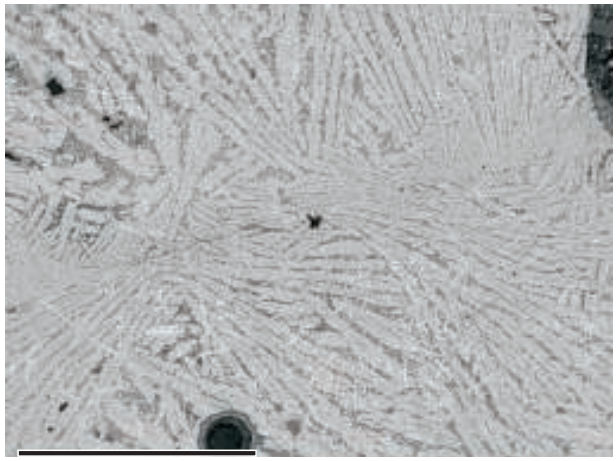

c

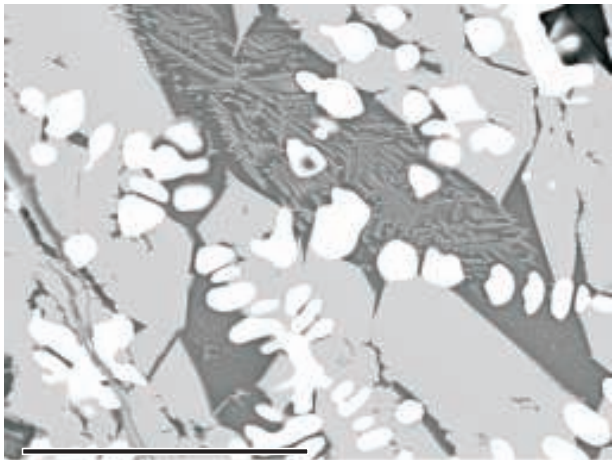

d

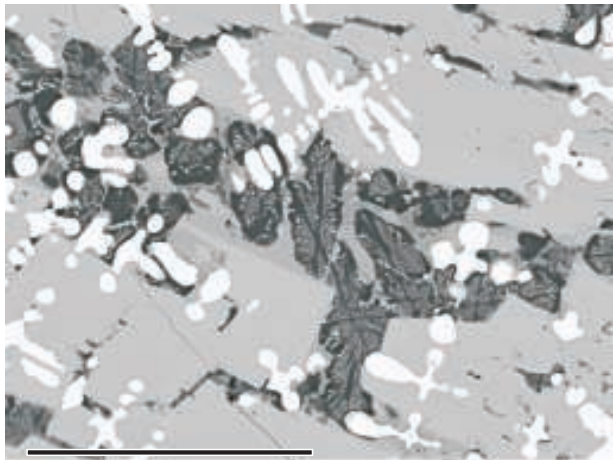

e

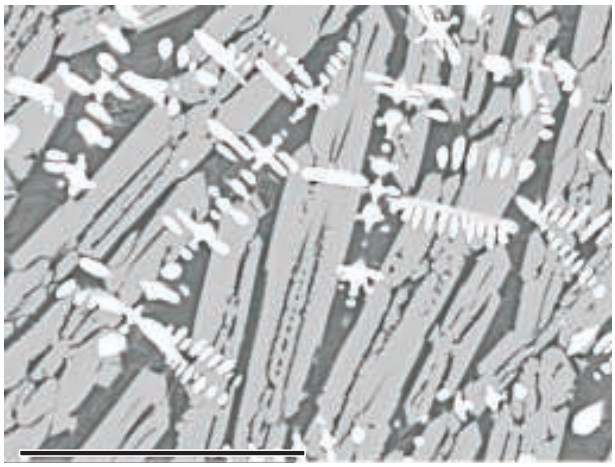

f

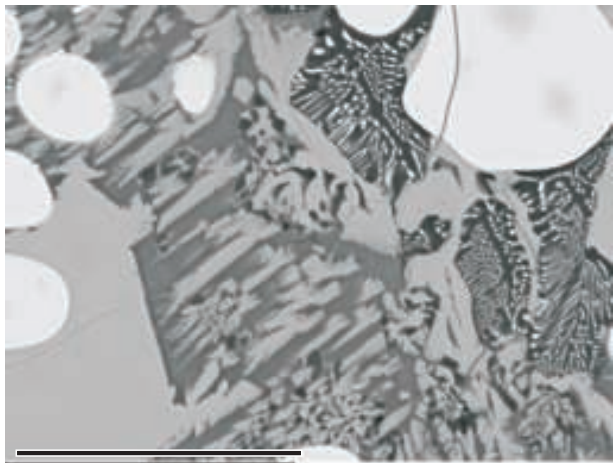

g

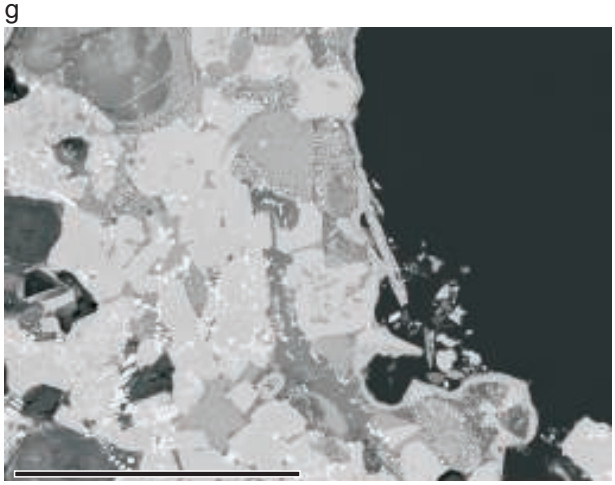

h

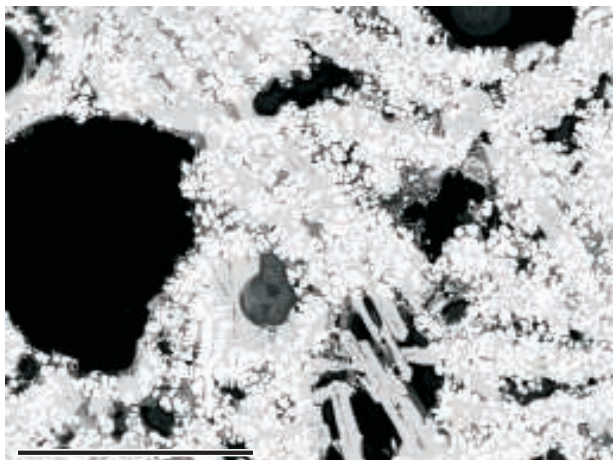

Figure 1

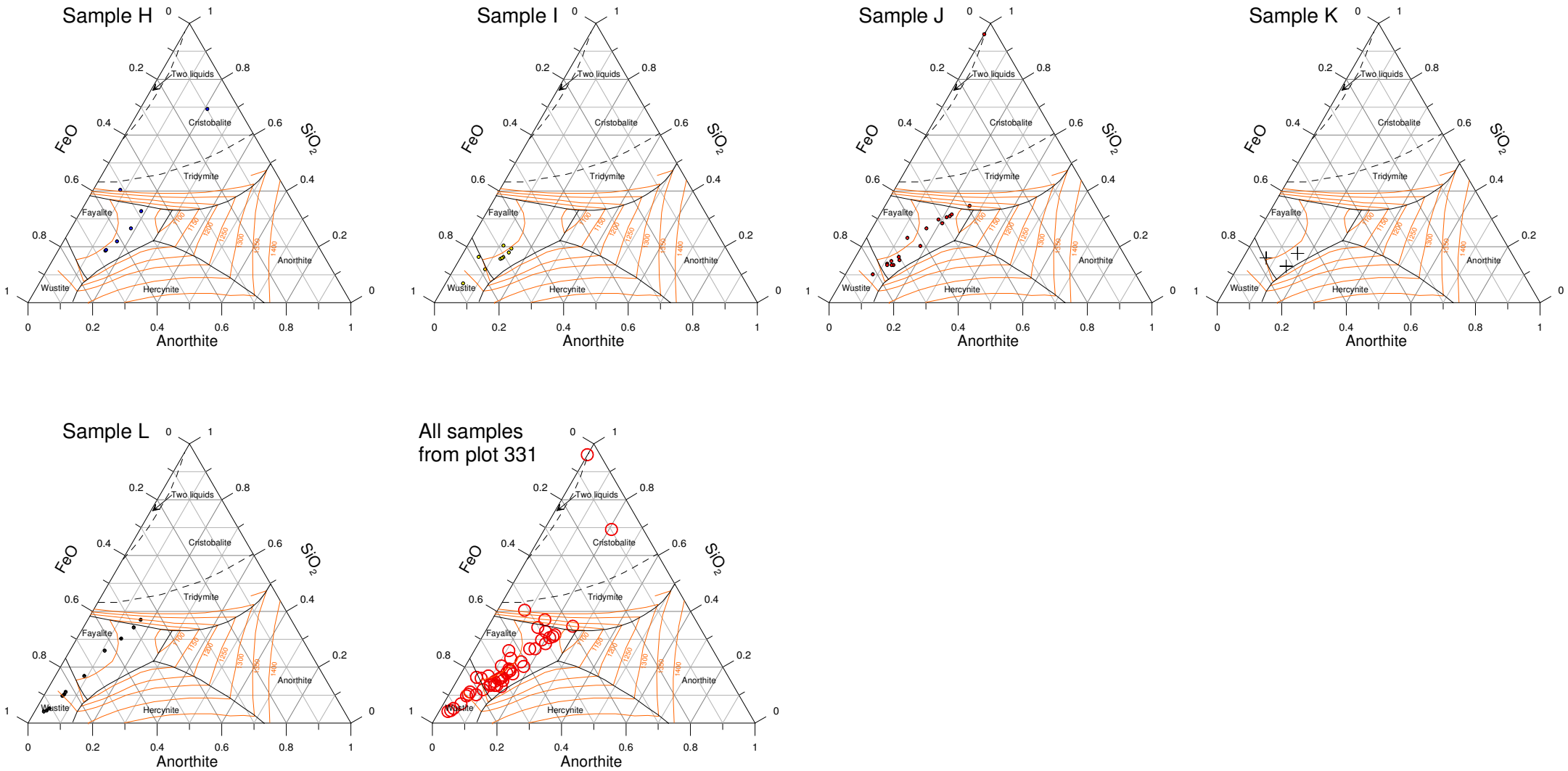
Sample H
Sample I
Sample J
Sample K
Sample L
All samples
from plot 331
Two liquids
Cristobalite
Tridymite
Fayalite
Wustite
Hercynite
Anorthite
FeO
SiO2
Anorthite

Figure 2

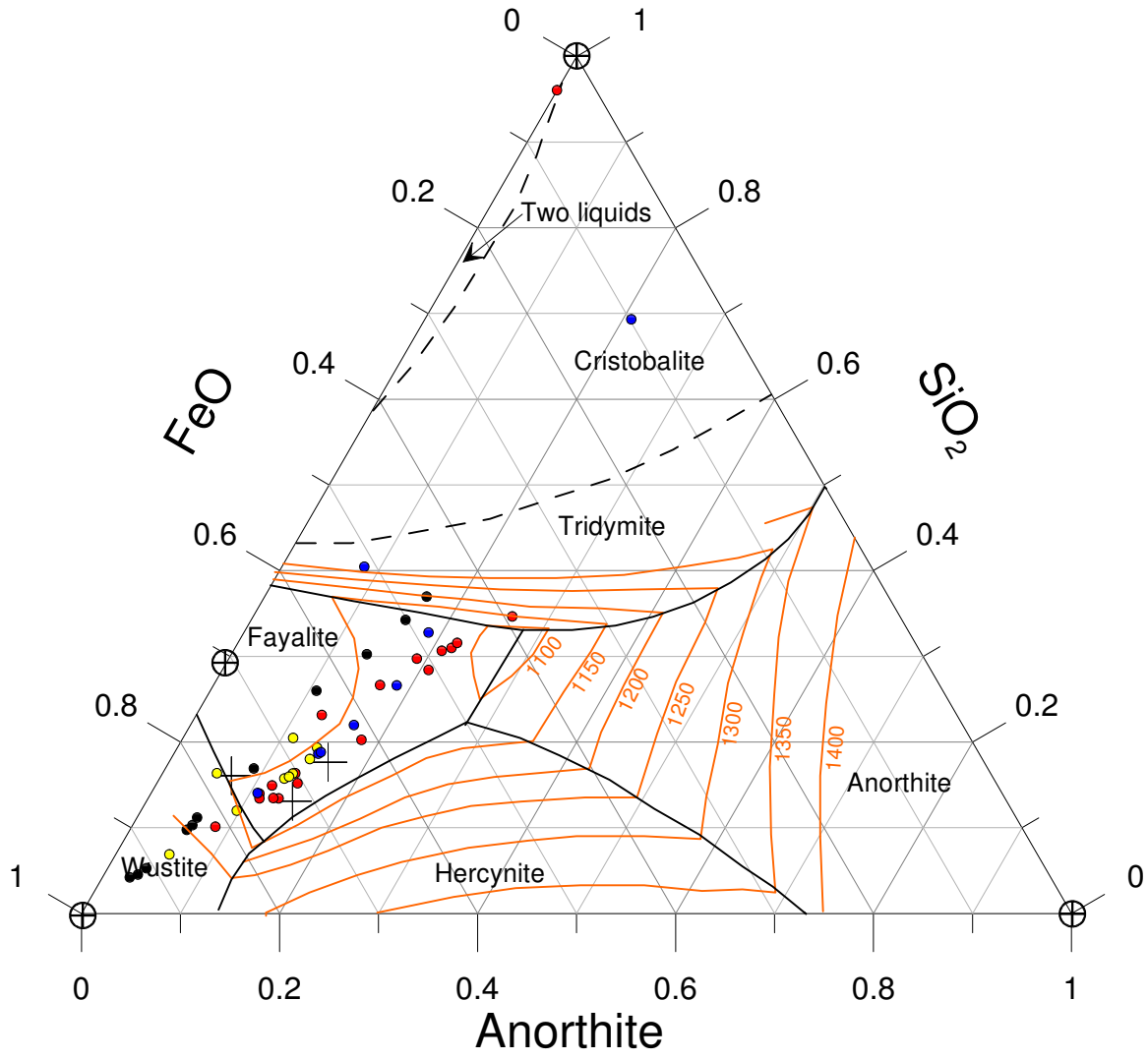

Sample from Plot 331 - area EDS analyses

- H: 3021 SHC upper
- I: 3021 SHC lower
- J: 3021 small SHC upper
- K: 3050 large SHC
- L: 3052 SHC

Figure 3

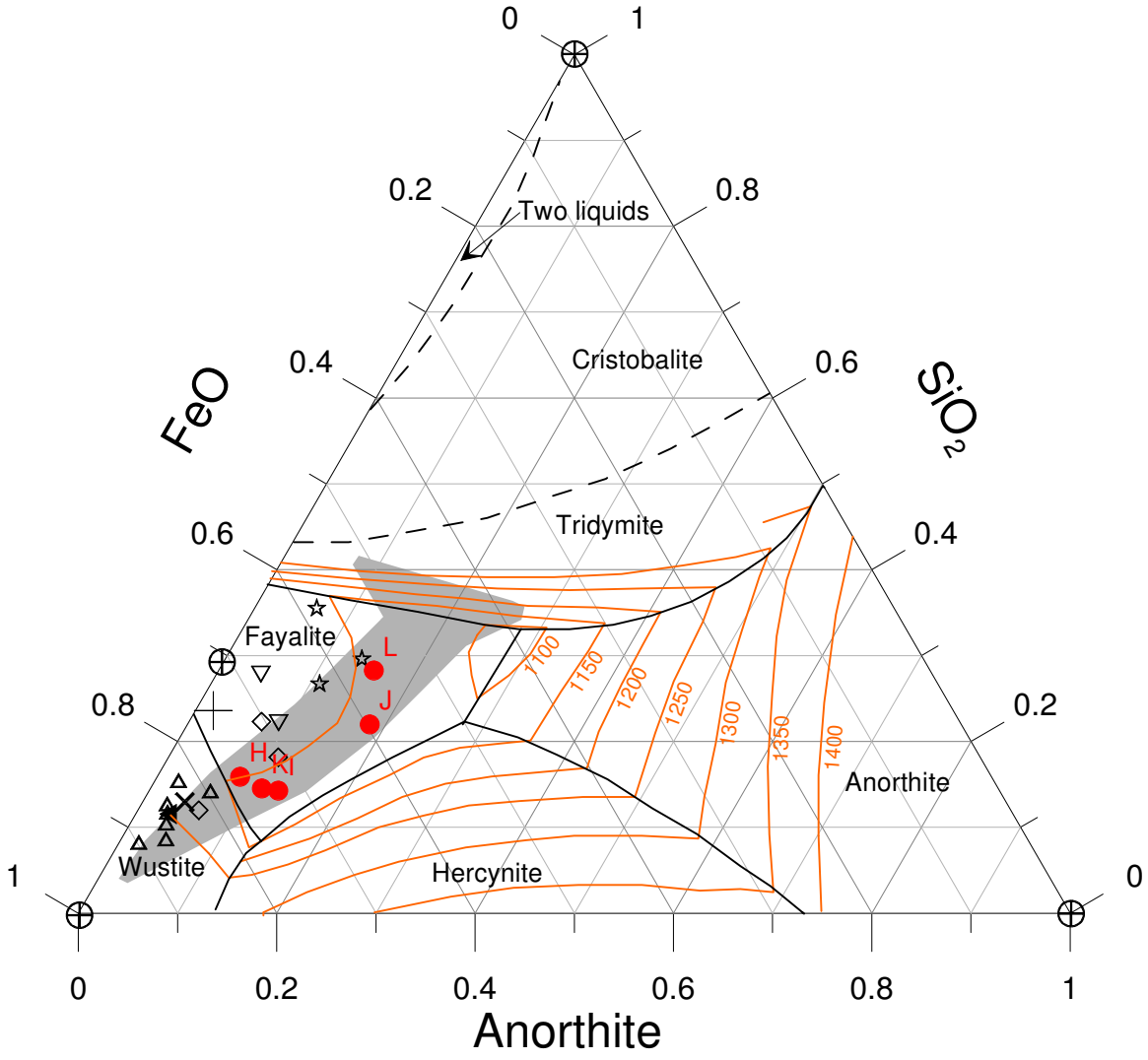

Plot 331 smple averages and comparative analyses

- Lyonshall smithing
- Trowbridge smithing
- Trellech smithing
- Frocester smithing
- Porth y Rhaw smithing
- Usk Smithing
- Caerwent smithing
- Plot 331 averages

Figure 4

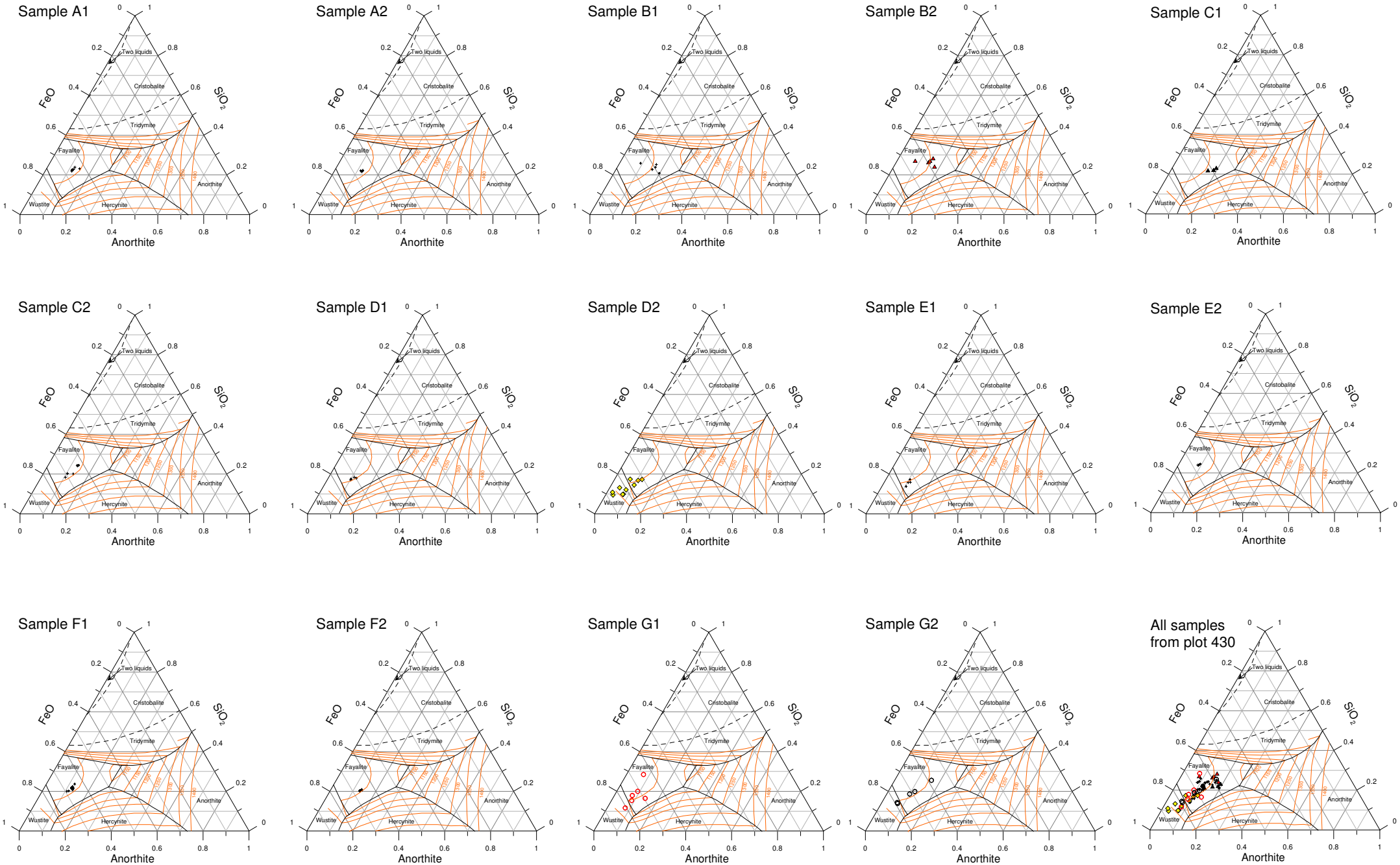
Sample A1
Sample A2
Sample B1
Sample B2
Sample C1
Sample C2
Sample D1
Sample D2
Sample E1
Sample E2
Sample F1
Sample F2
Sample G1
Sample G2
All samples from plot 430
FeO
SiO2
Anorthite
Two liquids
Cristobalite
Tridymite
Fayalite
Wustite
Hercynite
Anorthite

Figure 5

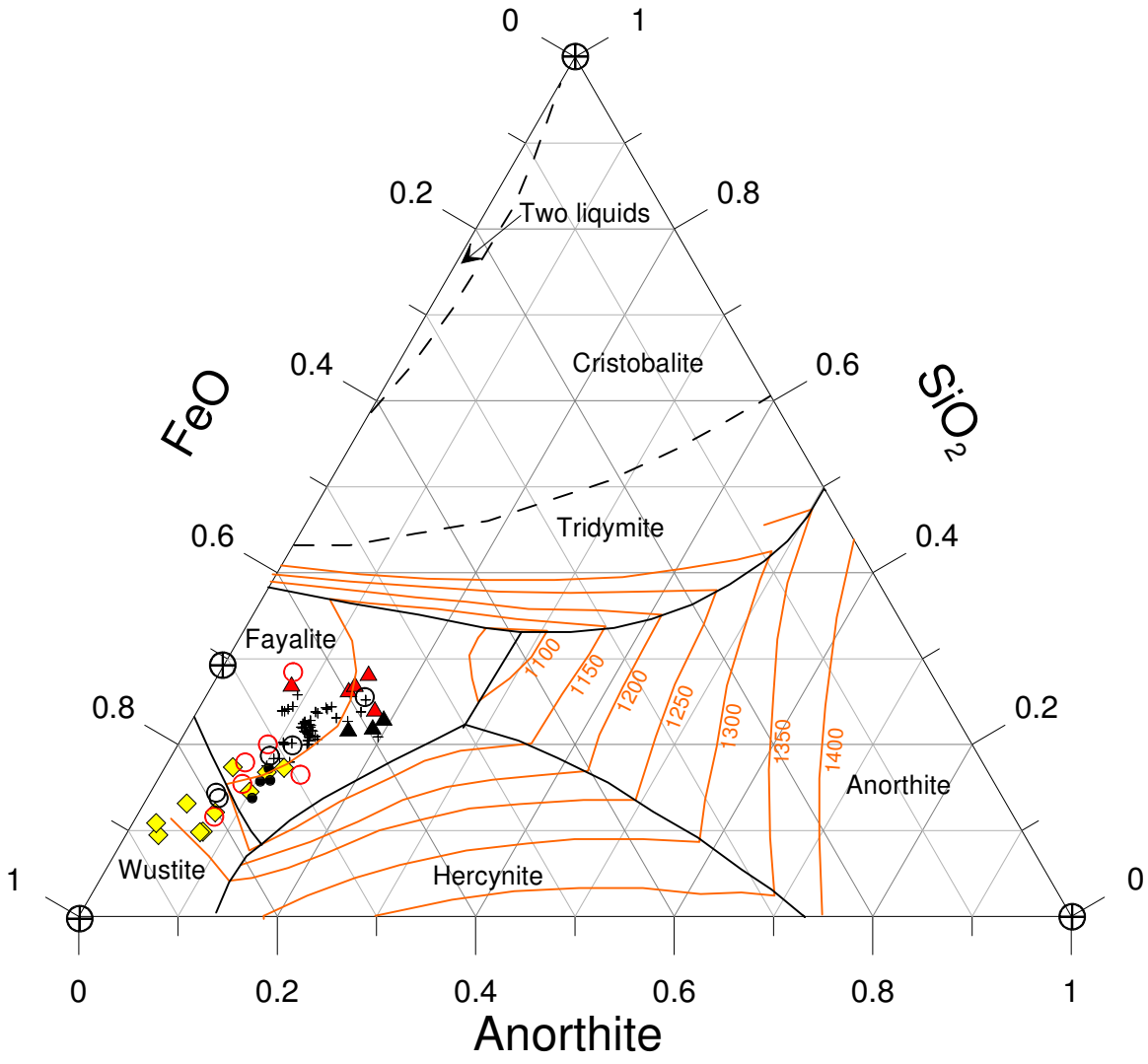

Plot 430 smelting residues

- A1: 86104 tapslag
- A2: 86001 tapslag
- B1: 86131 tapslag
- B2: 86131 furnace slag
- C1: 86156 furnace slag
- C2: 86156 tapslag
- D1: 86165 tapslag
- D2: 86165 bloom fragment
- E1: 86174 slag rod?
- E2: 86174 tapslag
- F1: 86196 thin tapslag
- F2: 86196 tapslag
- G1: 86225 burr?
- G2: 86225 burr?

Figure 6

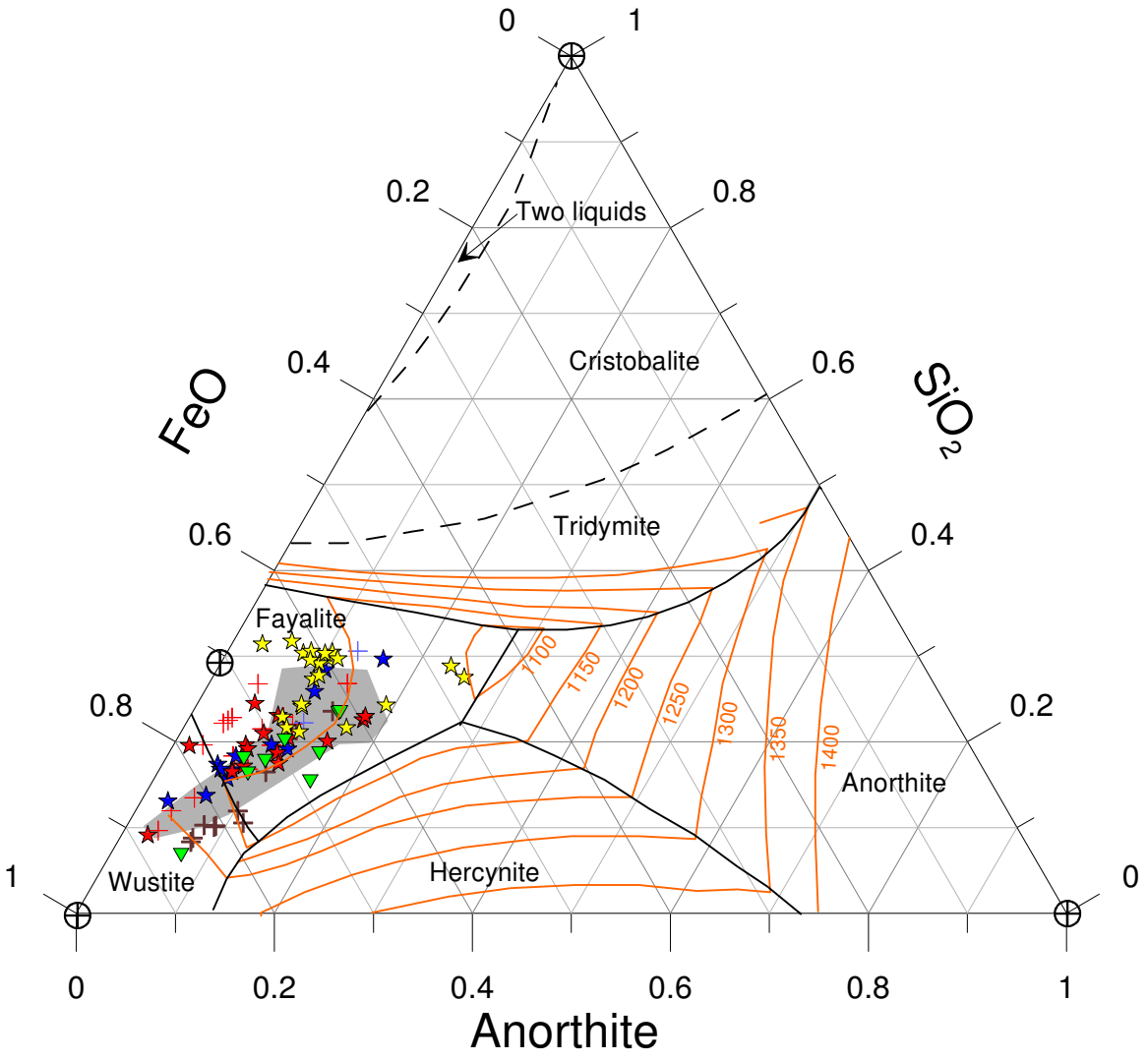

Comparative analyses of smelting slags

- Frocester smelting (Thomas 2000)
- Ariconium smelting (Thomas 2000)
- Usk smelting (Thomas 2000)
- Caerleon (Young & Thomas 1997)
- Caerwent (Young 2006)
- Severn Vale (Allen 1988)
- Chesters (Fulford & Allen 1992)
- Worcester (McDonnell & Swiss 2004)

APPENDIX A
IMAGE ARCHIVE

Archive plates

Plate A1: Sample A1
a) SOI1. Scale bar 2mm .
b) SOI2. Scale bar 200µm.
c) SOI3. Scale bar 1mm.
d) SOI4. Scale bar 1mm.
e) SOI5. Scale bar 1mm.
f) SOI6. Scale bar 1mm.
g) SOI7. Scale bar 1mm.
h) SOI8. Scale bar 70 µm.

Plate A2: Sample A1
a) SOI9. Scale bar 1mm.
b) SOI10. Scale bar 1mm.
c) SOI11. Scale bar 1mm.
d) SOI12. Scale bar 1mm.

Plate A3: Sample A1
Montage of SOI 3 – SOI7 and 9-12. Scale bar 10mm.

Plate A4: Sample A2
a) SOI1. Scale bar 1mm.
b) SOI2. Scale bar 1mm.
c) SOI3. Scale bar 1mm.
d) SOI4. Scale bar 1mm.
e) SOI5. Scale bar 1mm.
f) SOI6. Scale bar 100µm.

Plate A5: Sample B1
a) SOI1. Scale bar 1mm.
b) SOI2. Scale bar 200µm.
c) SOI3. Scale bar 80µm.
d) SOI4. Scale bar 1mm.
e) SOI5. Scale bar 80µm.
f) SOI6. Scale bar 80µm.
g) SOI7. Scale bar 80µm.

Plate A6: Sample B2
a) SOI2. Scale bar 100µm.
b) SOI2. Scale bar 100µm.
c) SOI2. Area as (a). Elemental density map: Al
d) SOI2. Area as (a). Elemental density map: Ca
e) SOI2. Area as (a). Elemental density map: Fe
f) SOI2. Area as (a). Elemental density map: K
g) SOI2. Area as (a). Elemental density map: Si
h) SOI2. Area as (a). Elemental density map: Ti

Plate A7: Sample B2
a) SOI1. Scale bar 200µm.
b) SOI3. Scale bar 600µm.
c) SOI4. Scale bar 600µm.
d) SOI5. Scale bar 100µm.
e) SOI6. Scale bar 600µm.

Plate A8: Sample C1
a) SOI1. Scale bar 2mm.
b) SOI2. Scale bar 600µm.
c) SOI3. Scale bar 600µm.
d) SOI4. Scale bar 200µm..

Plate A9: Sample C2
a) SOI1. Scale bar 600µm.
b) SOI2. Scale bar 600µm.
c) SOI3. Scale bar 600µm.
d) SOI4. Scale bar 60µm.
e) SOI5. Scale bar 600µm.
f) SOI6. Scale bar 600µm.
g) SOI7. Scale bar 600µm.
h) SOI8. Scale bar 60µm.

Plate A10: Sample D1
a) SOI1. Scale bar 600µm.
b) SOI2. Scale bar 600µm.
c) SOI3. Scale bar 60µm.
d) SOI4. Scale bar 600µm.
e) SOI5. Scale bar 600µm.
f) SOI6. Scale bar 60µm.

Plate A11: Sample D2
Montage of SOI 1 – SOI38. Scale bar 5mm.

Plate A12: Sample D2
a) SOI39. Scale bar 600µm..
b) SOI40. Scale bar 70µm.
c) SOI41. Scale bar 400µm.
d) SOI42. Scale bar 100µm.
e) SOI43. Scale bar 1mm.
f) SOI44. Scale bar 600µm.
g) SOI45. Scale bar 800µm.

Plate A13: Sample E1
a) SOI1. Scale bar 1mm.
b) SOI2. Scale bar 100µm.
c) SOI3. Scale bar 50µm.
d) SOI4. Scale bar 600µm.
e) SOI5. Scale bar 600µm.
f) SOI6. Scale bar 600µm.
g) SOI7. Scale bar 100µm.

Plate A14: Sample E2
a) SOI1. Scale bar 1mm.
b) SOI2. Scale bar 1mm.
c) SOI3. Scale bar 70µm.
d) SOI4. Scale bar 1mm.
e) SOI5. Scale bar 1mm.

Plate A15: Sample F1
a) SOI3. Scale bar 1mm.
b) SOI4. Scale bar 1mm.
c) SOI5. Scale bar 1mm.
d) SOI6. Scale bar 1mm.
e) SOI7. Scale bar 1mm.
f) SOI8. Scale bar 1mm.
g) SOI9. Scale bar 60µm.

Plate A16: Sample F1
Montage of SOI3-SOI8
Scale bar 5mm.

Plate A17: Sample F2
a) SOI1. Scale bar 1mm.
b) SOI2. Scale bar 1mm.
c) SOI3. Scale bar 1mm.
d) SOI4. Scale bar 1mm.
e) SOI5. Scale bar 100µm.

Plate A18: Sample G1
a) SOI1. Scale bar 1mm.
b) SOI2. Scale bar 1mm.
c) SOI3. Scale bar 1mm.
d) SOI4. Scale bar 400µm.
e) SOI5. Scale bar 60µm.
f) SOI6. Scale bar 1mm.
g) SOI7. Scale bar 100µm.
h) SOI8. Scale bar 600µm.

Plate A19: Sample G2
Montage of SOI1-SOI65.
Scale bar 5mm.

Plate A20: Sample G2
a) SOI66. Scale bar 1mm.
b) SOI67. Scale bar 400µm.
c) SOI68. Scale bar 200µm.
d) SOI69. Scale bar 1mm.
e) SOI70. Scale bar 500µm.
f) SOI71. Scale bar 1mm.
g) SOI72. Scale bar 300µm.

Plate A21: Sample H
Montage of SOI1-SOI13.
Scale bar 5mm.
Image inverted to correct orientation.

Plate A22: Sample H
a) SOI14. Scale bar 700µm.
b) SOI15. Scale bar 1mm.
c) SOI16. Scale bar 60µm.
d) SOI17. Scale bar 400µm.
e) SOI18. Scale bar 1mm.
f) SOI19. Scale bar 1mm.
g) SOI20. Scale bar 200µm.
h) SOI21. Scale bar 100µm.

Plate A23: Sample I
a) Montage of SOI1-SOI6. Scale bar .
b) SOI7. Scale bar 600µm (not as stated on image).
c) SOI8. Scale bar 120µm (not as stated on image).

Plate A24: Sample I
a) SOI9. Scale bar 600µm (not as stated on image).
b) SOI10. Scale bar 280µm (not as stated on image).
c) SOI12. Scale bar 3mm (not as stated on image).
d) SOI13. Scale bar 600µm (not as stated on image).
e) SOI14. Scale bar 240µm (not as stated on image)..

Plate A25: Sample J
a) SOI1. Scale bar 1.2mm (not as stated on image).
b) SOI2. Scale bar 240µm (not as stated on image).
c) SOI3. Scale bar 1.2mm (not as stated on image).
d) SOI4. Scale bar 600µm (not as stated on image).
e) SOI5. Scale bar 1.2mm (not as stated on image).
f) SOI6. Scale bar 1.2mm (not as stated on image).
g) SOI7. Scale bar 1.2mm (not as stated on image).
h) SOI8. Scale bar 1.2mm (not as stated on image).

Plate A26: Sample J
a) SOI9. Scale bar 4mm.

Plate A27: Sample K
a) SOI1. Scale bar 600µm (not as stated on image).
b) SOI2. Scale bar 600µm (not as stated on image).
c) SOI3. Scale bar 120µm (not as stated on image).
d) SOI4. Scale bar 600µm (not as stated on image).
e) SOI5. Scale bar 600µm (not as stated on image).
f) SOI6. Scale bar 600µm (not as stated on image).
g) SOI7. Scale bar 600µm (not as stated on image).
h) SOI8. Scale bar 600µm (not as stated on image).

Plate A28: Sample K
a) SOI9. Scale bar 600µm (not as stated on image).
b) SOI10. Scale bar 600µm (not as stated on image).
c) SOI11. Scale bar 600µm (not as stated on image).
d) SOI12. Scale bar 200µm (not as stated on image).
e) SOI13. Scale bar 60µm (not as stated on image).
f) SOI14. Scale bar 600µm (not as stated on image).

Plate A29: Sample K
Montage of SOI8-SOI11.
Scale bar 1mm.

Plate A30: Sample L
a) SOI2. Scale bar 600µm (not as stated on image).
b) SOI3. Scale bar 200µm (not as stated on image).
c) SOI4. Scale bar 600µm (not as stated on image).
d) SOI5. Scale bar 600µm (not as stated on image).
e) SOI6. Scale bar 600µm (not as stated on image).
f) SOI7. Scale bar 600µm (not as stated on image).
g) SOI8. Scale bar 600µm (not as stated on image).
h) SOI9. Scale bar 400µm (not as stated on image).

Plate A31: Sample L
a) SOI10. Scale bar 200µm (not as stated on image).

a

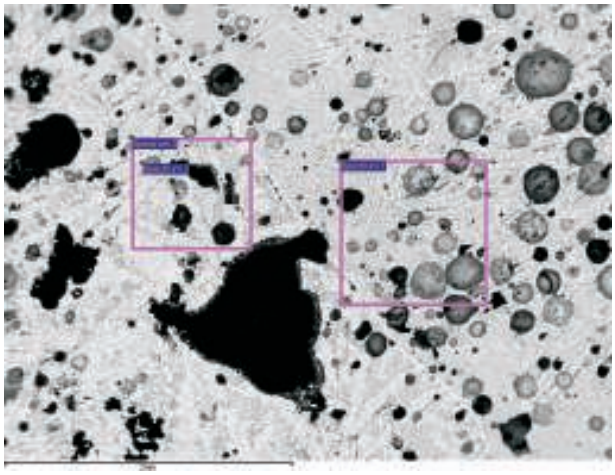

b

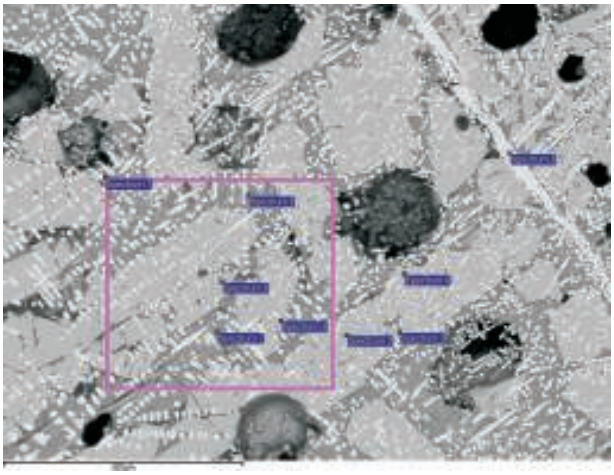

c

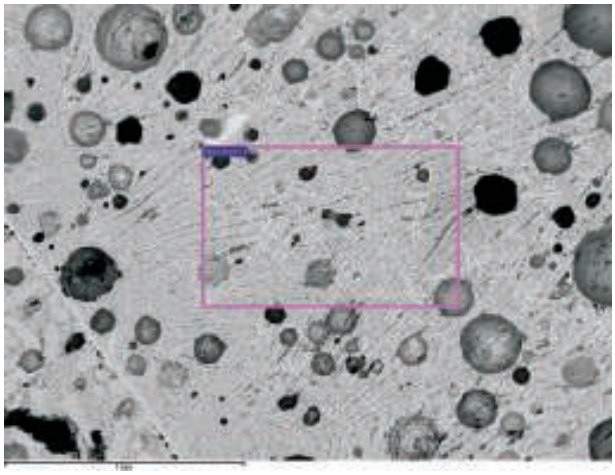

d

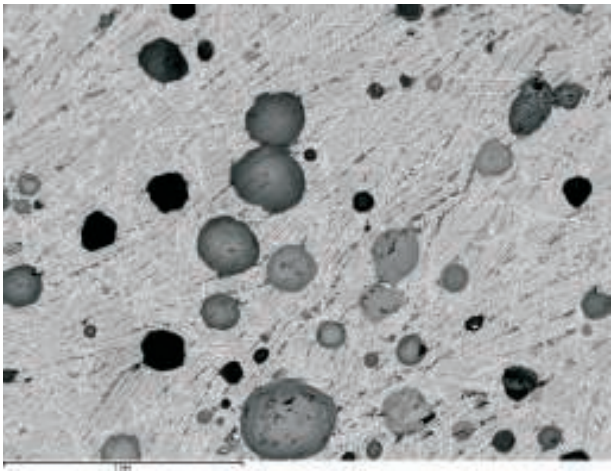

e

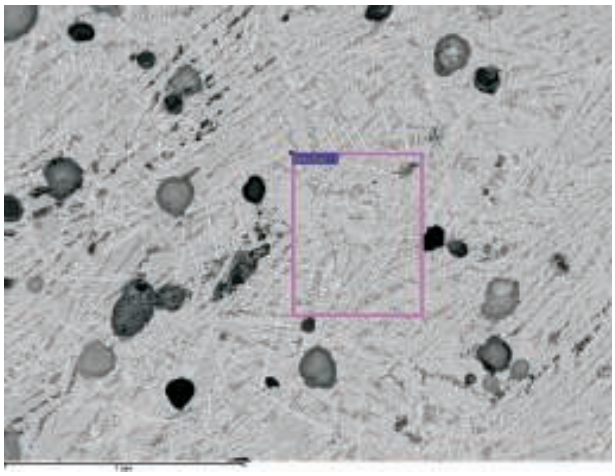

f

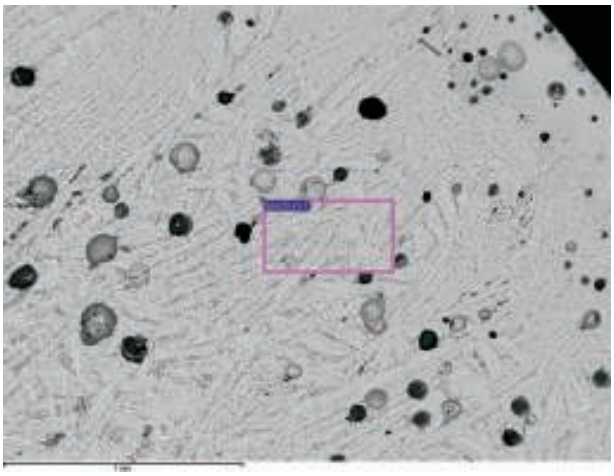

g

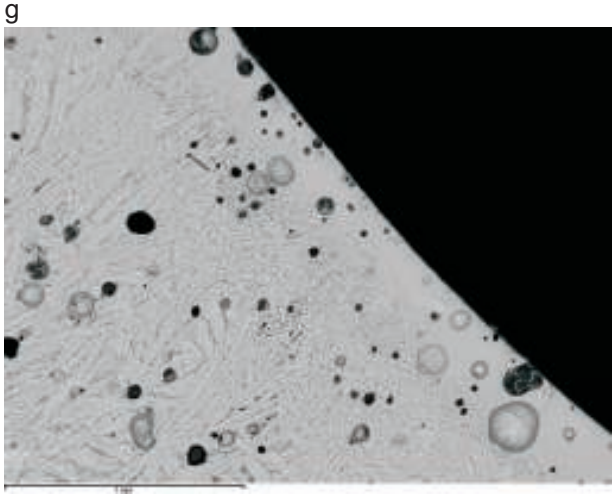

h

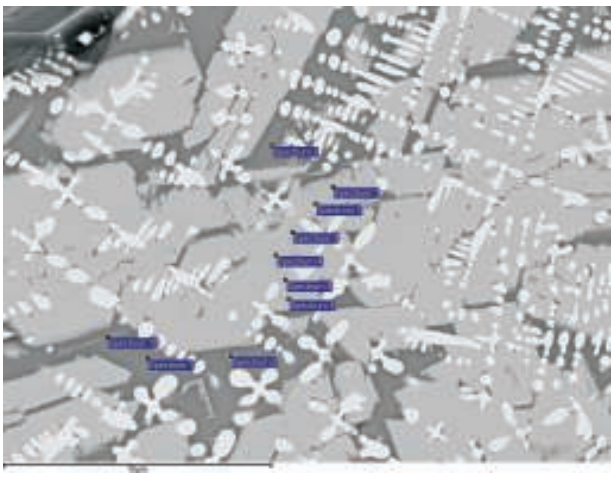

a

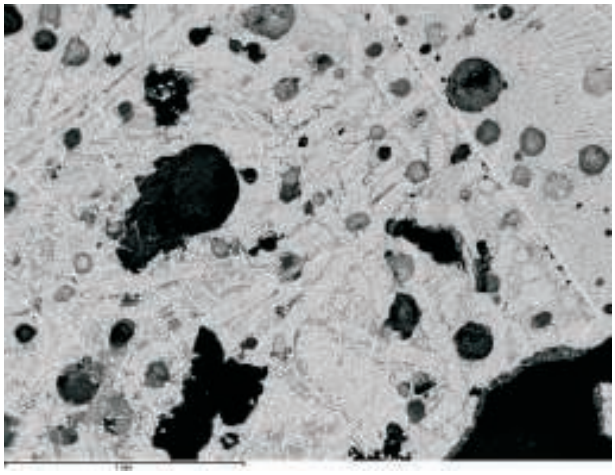

b

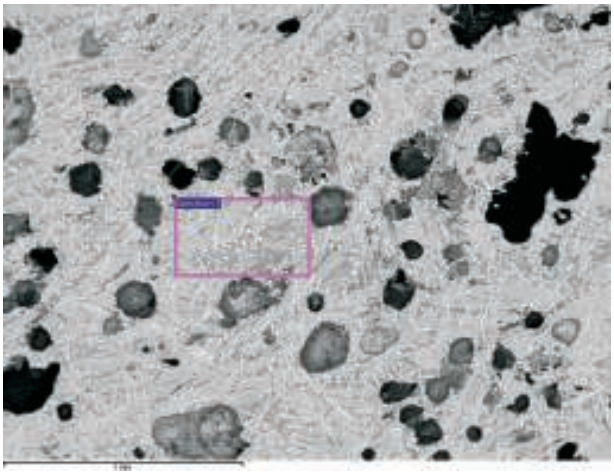

c

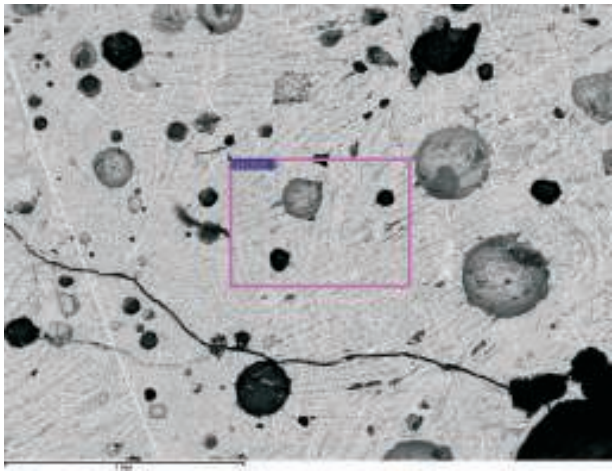

d

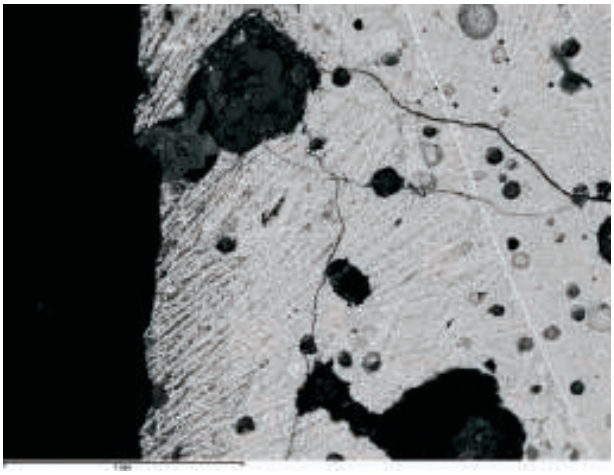

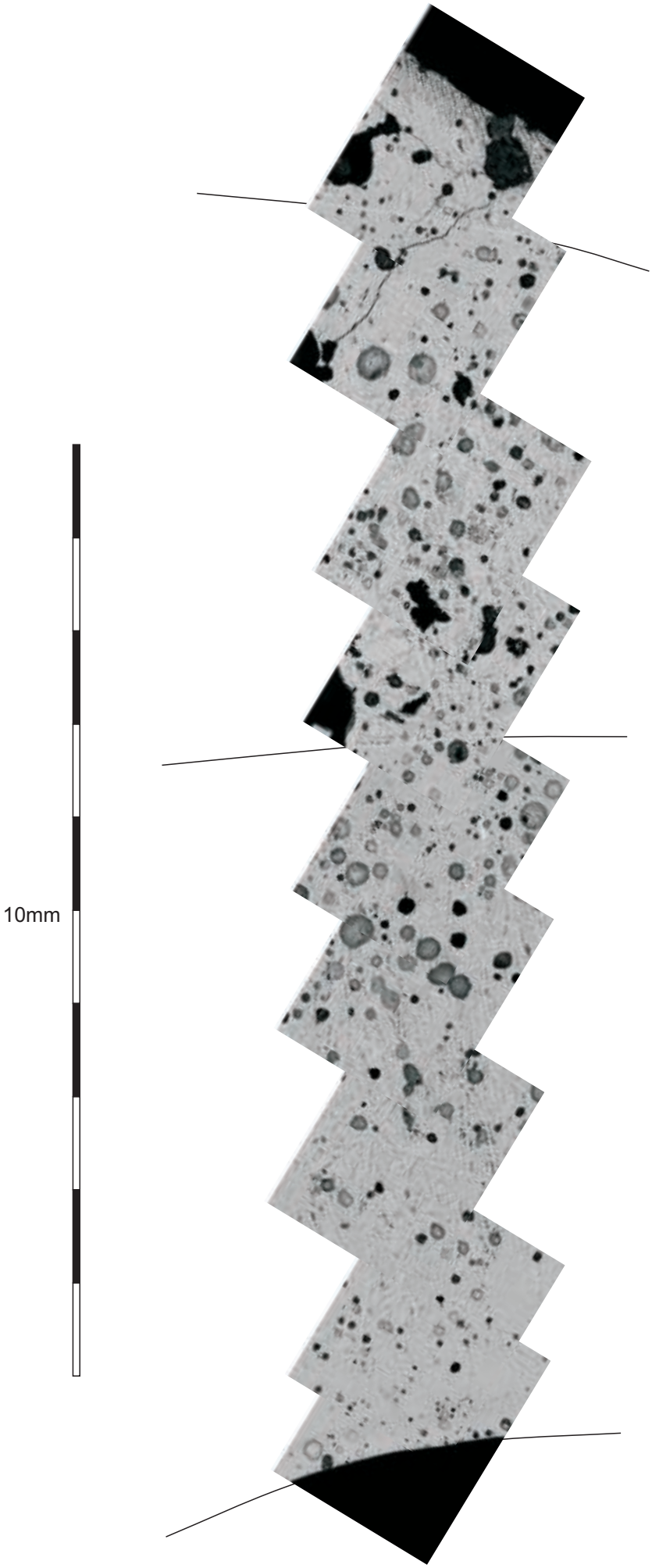
10mm

a

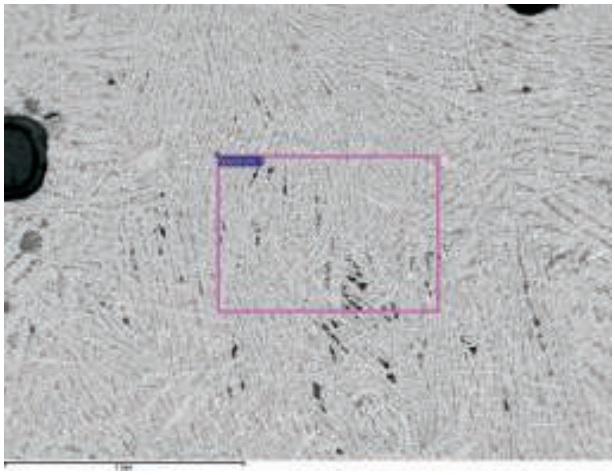

b

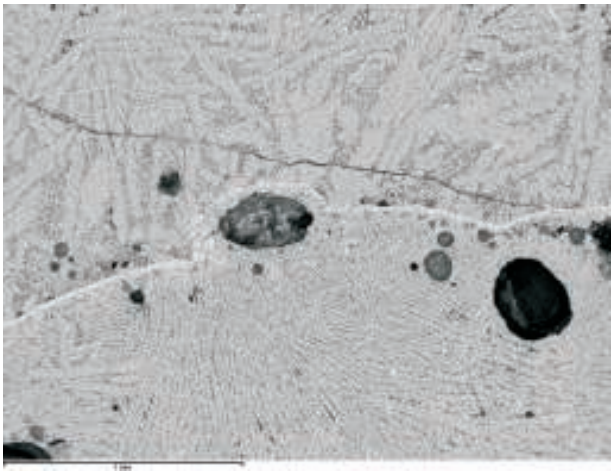

c

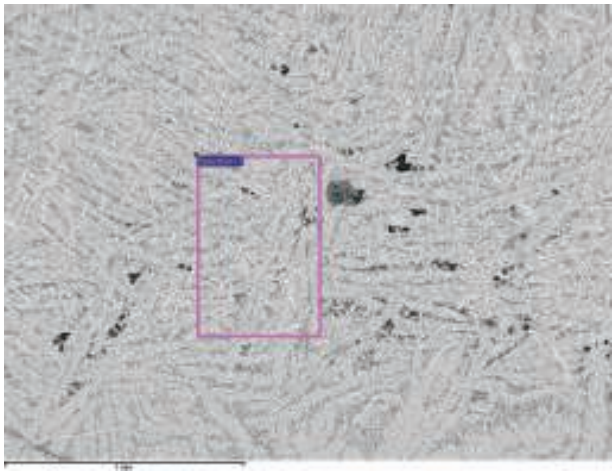

d

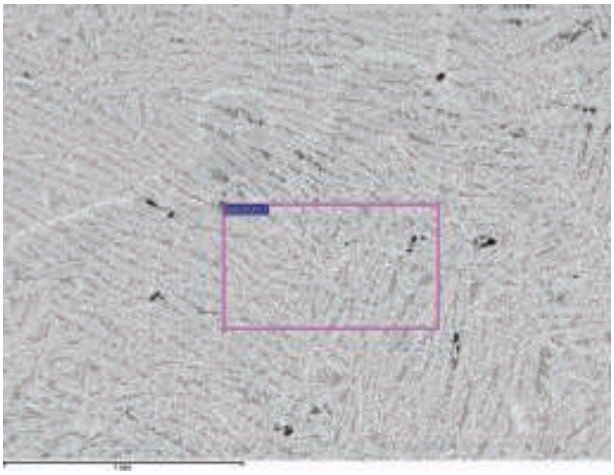

e

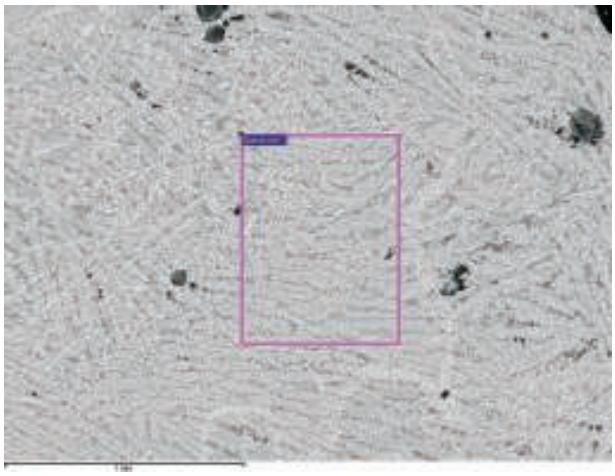

f

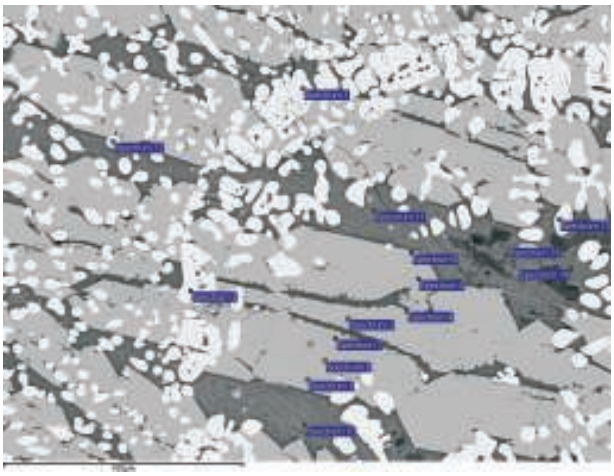

a

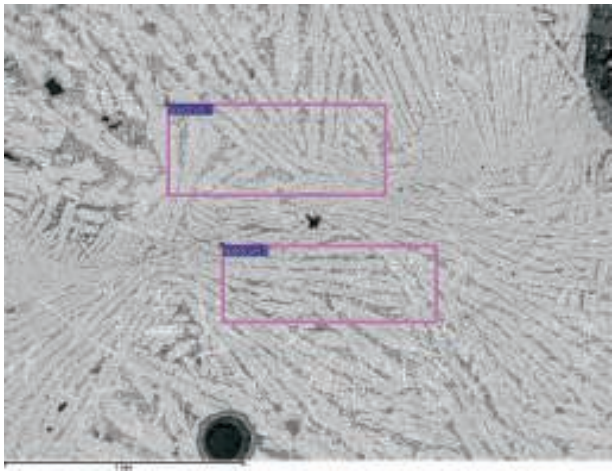

b

c

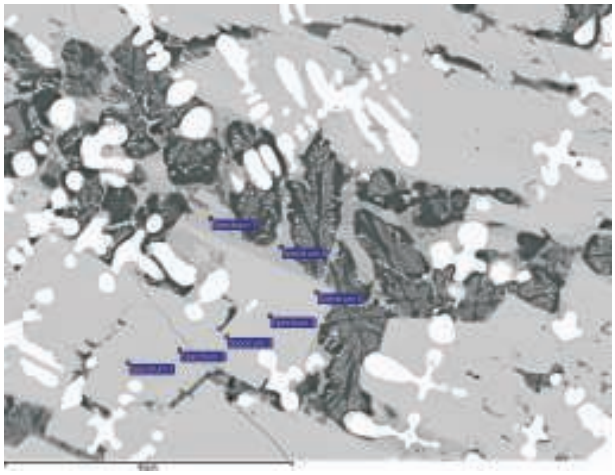

d

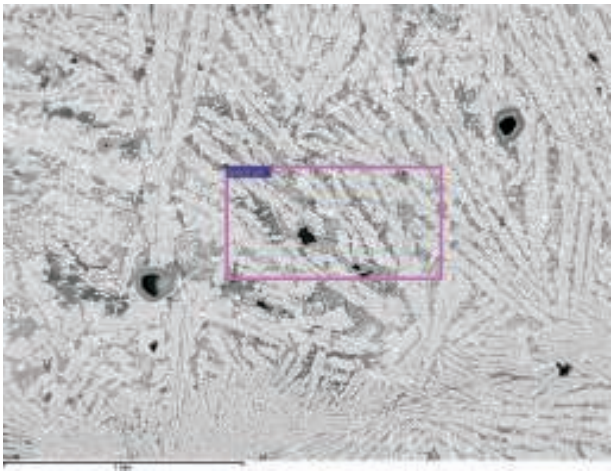

e

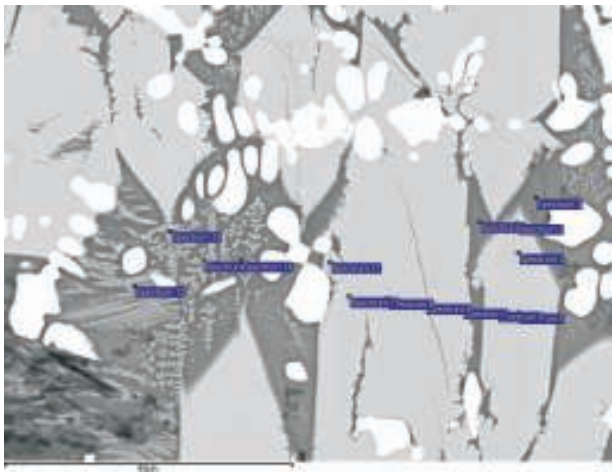

f

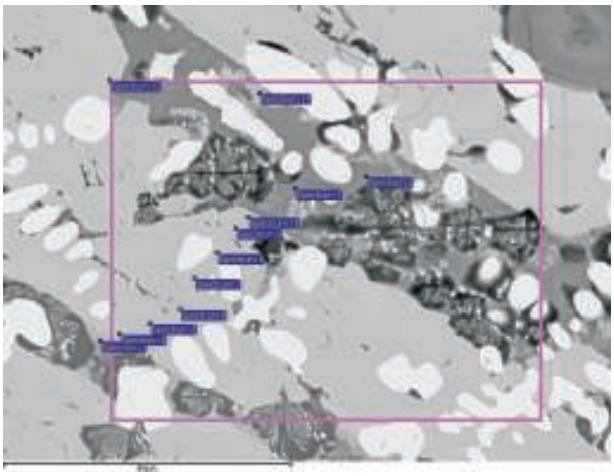

g

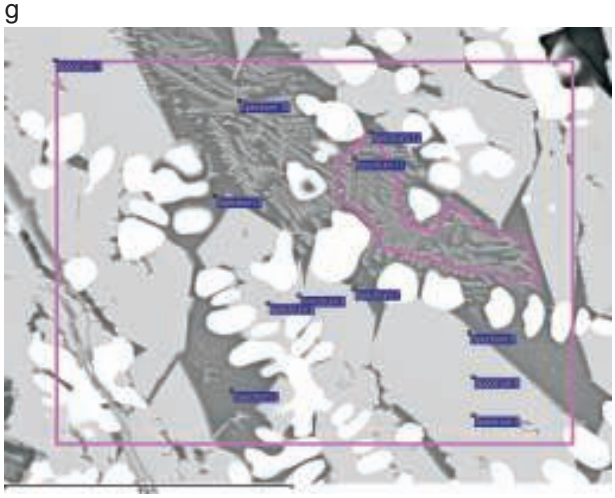

a

b

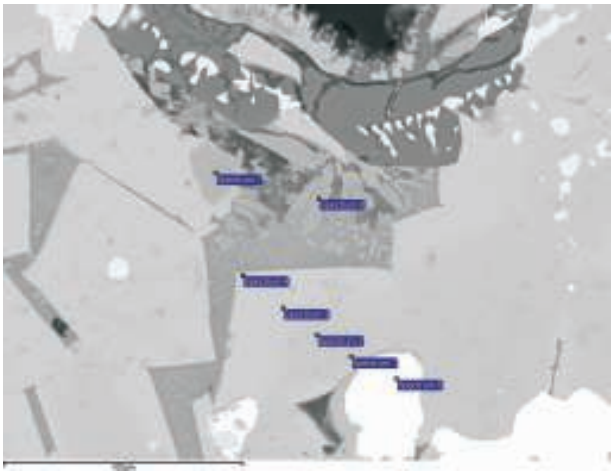

c

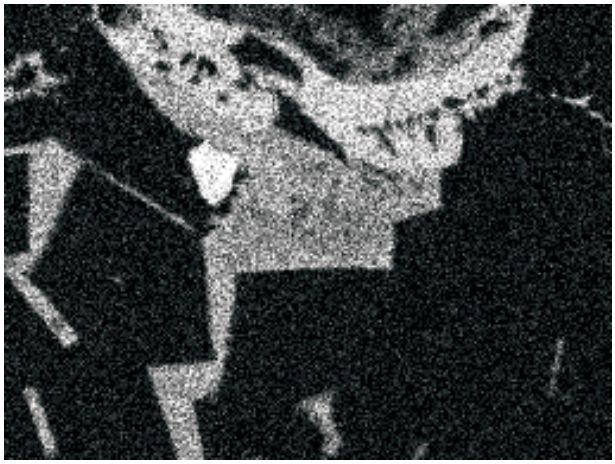

d

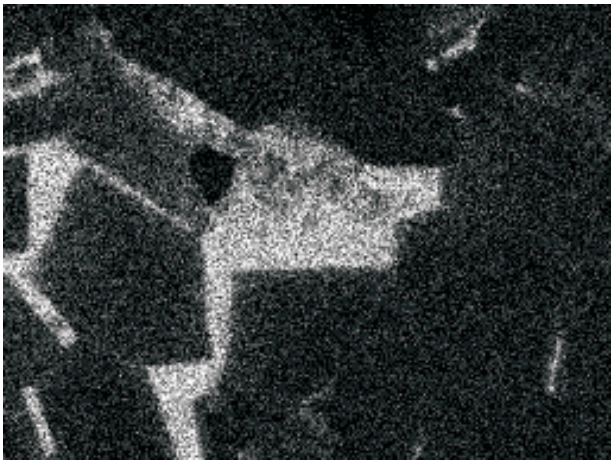

e

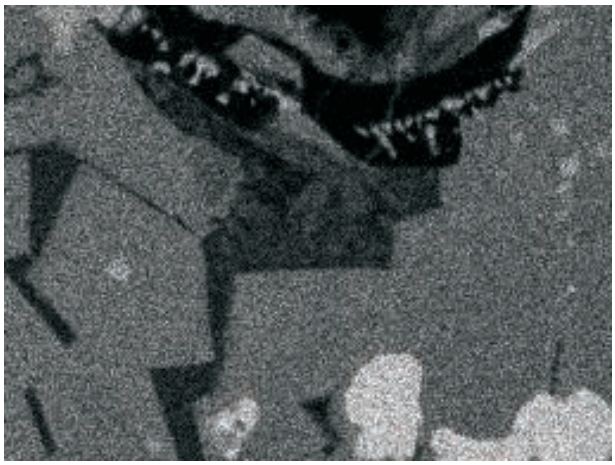

f

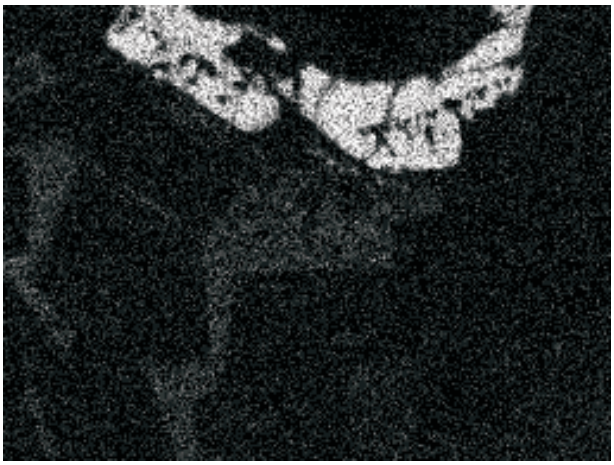

g

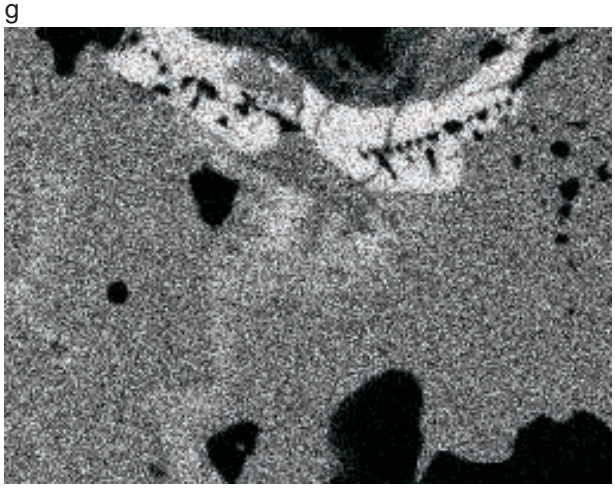

h

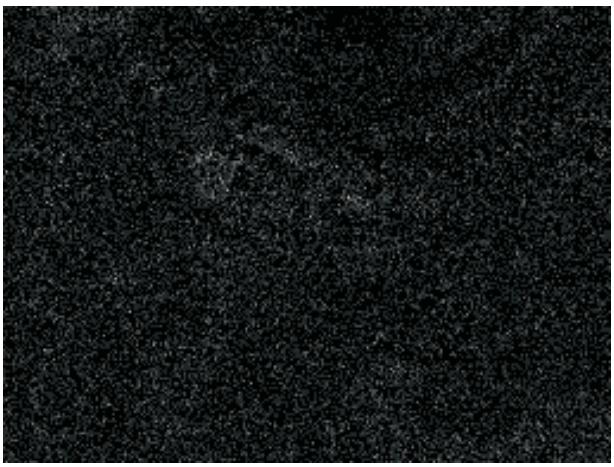

a

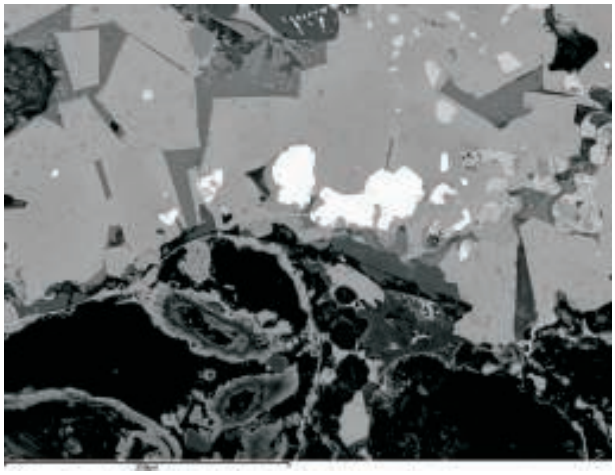

b

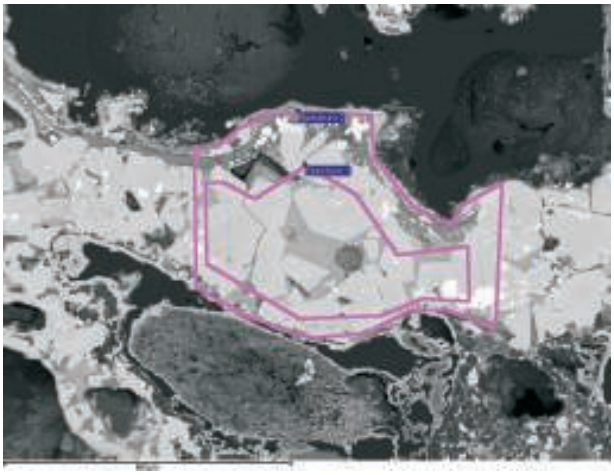

c

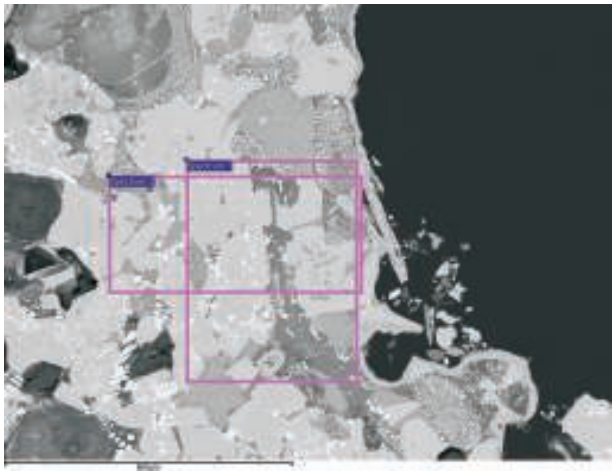

d

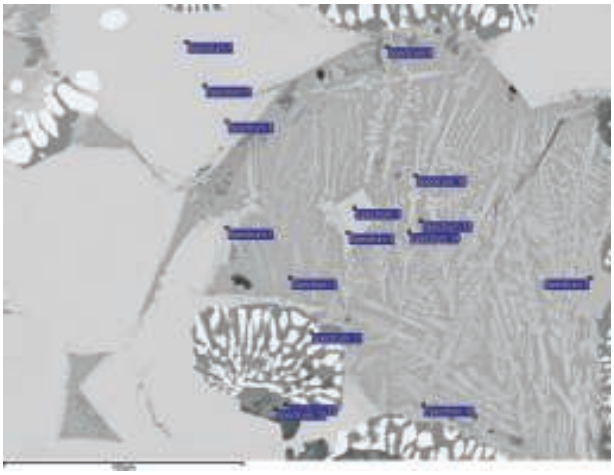

e

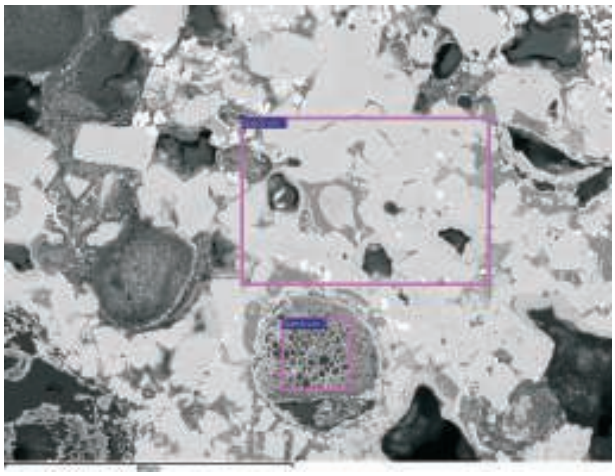

a

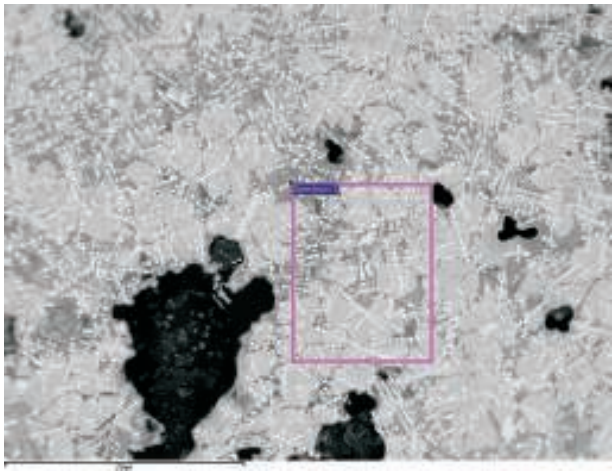

b

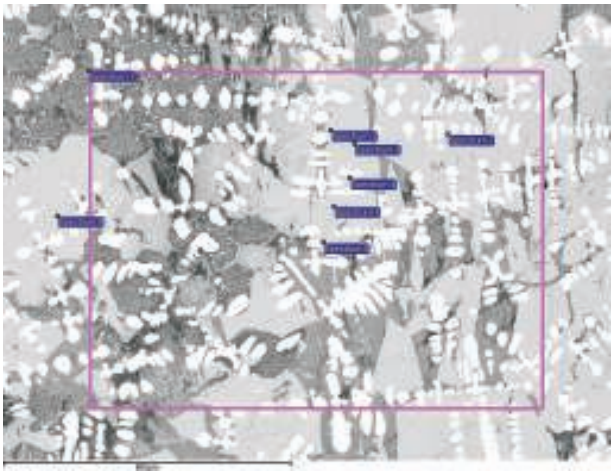

c

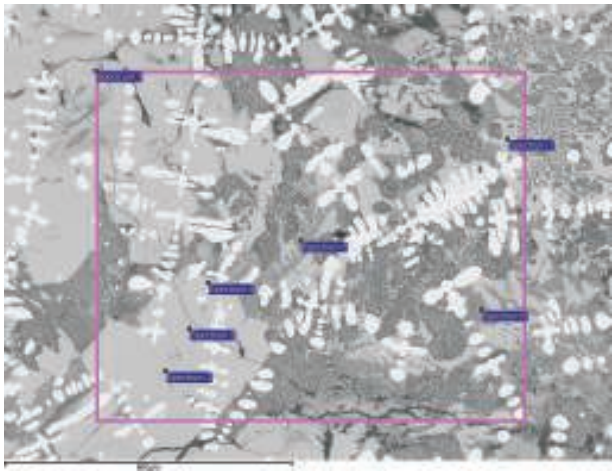

d

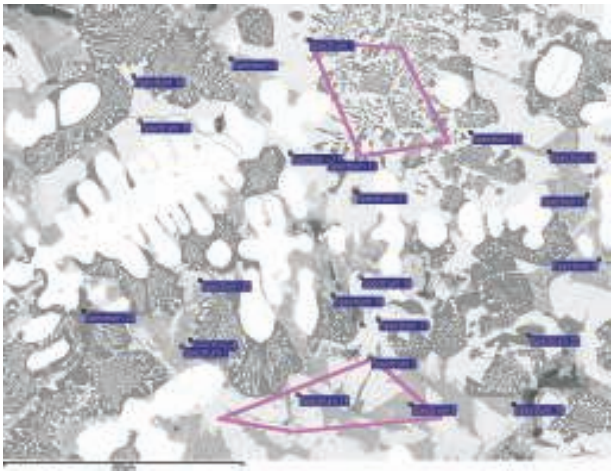

a

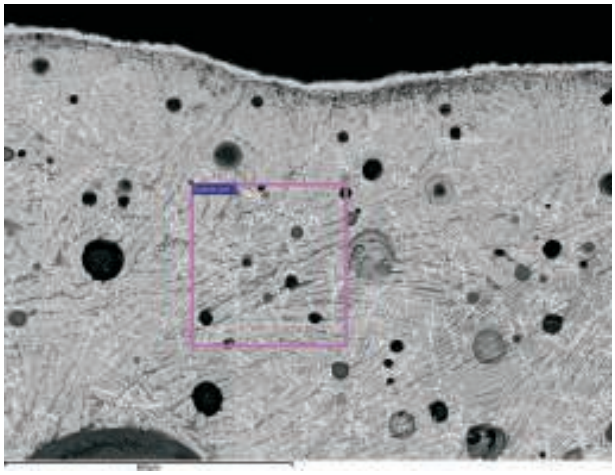

b

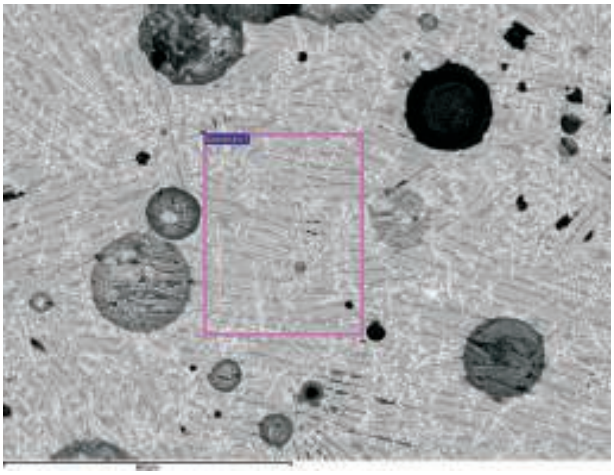

c

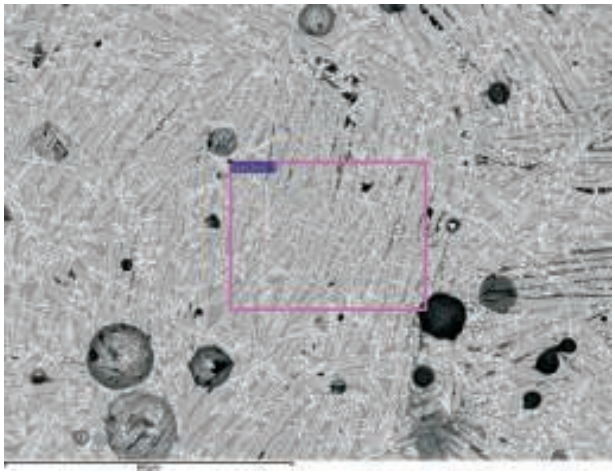

d

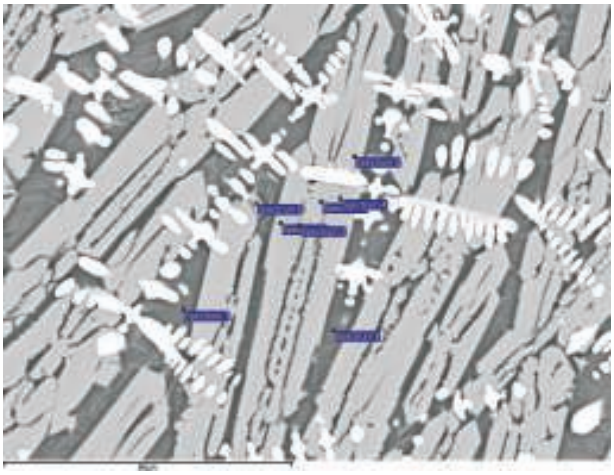

e

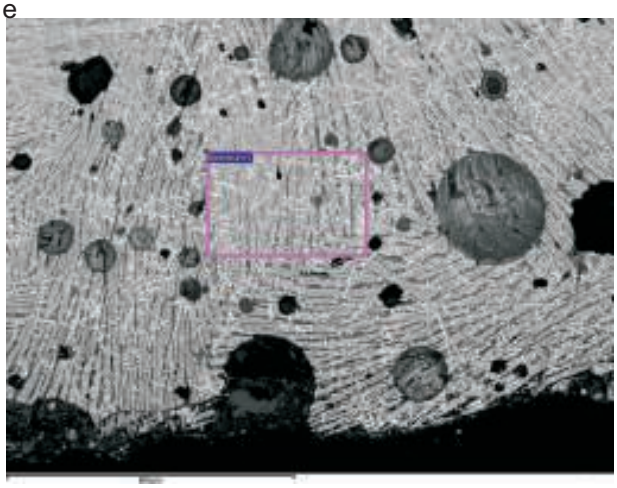

f

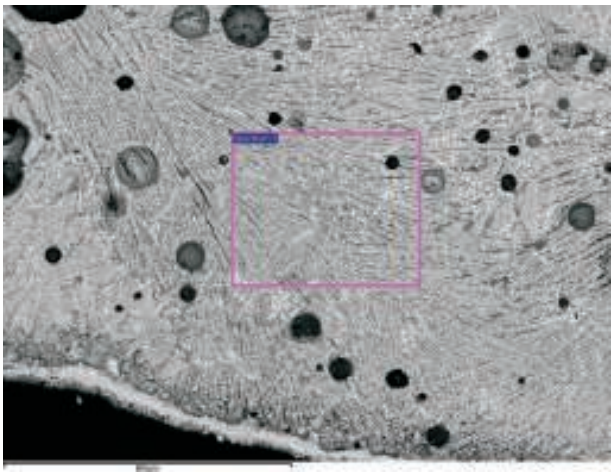

g

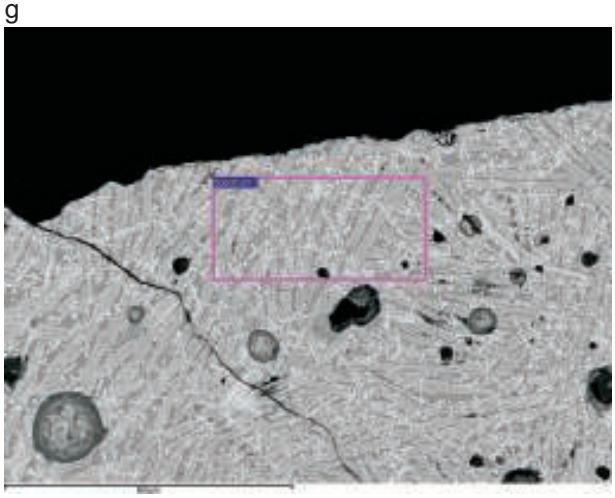

h

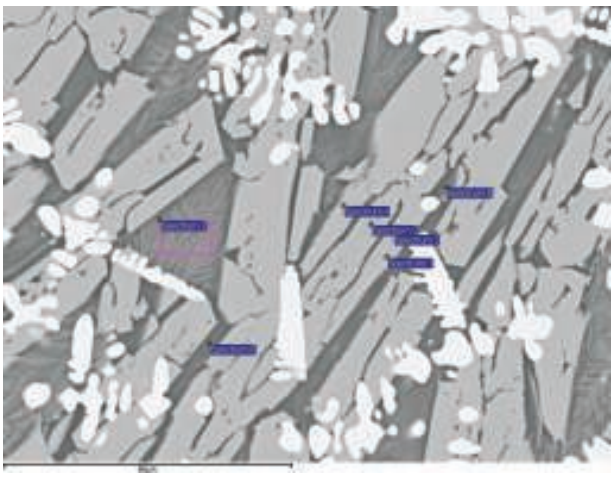

a

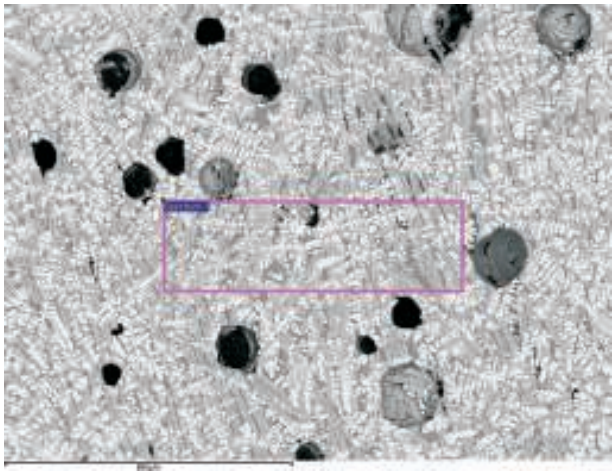

b

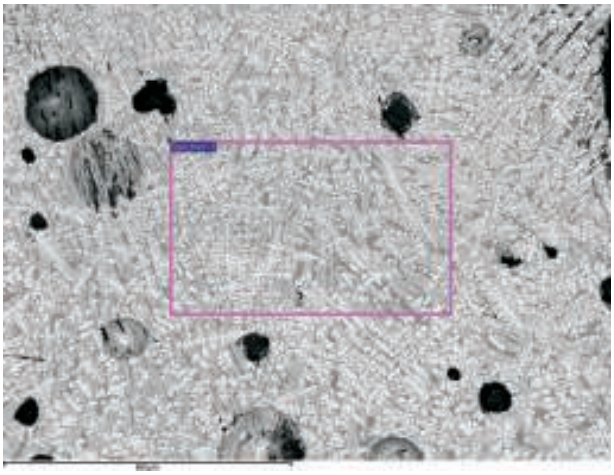

c

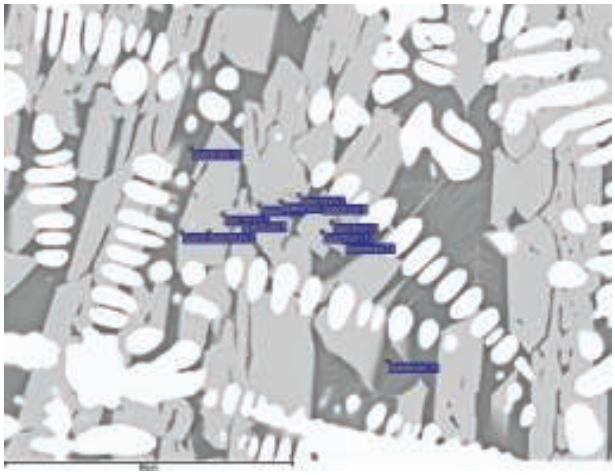

d

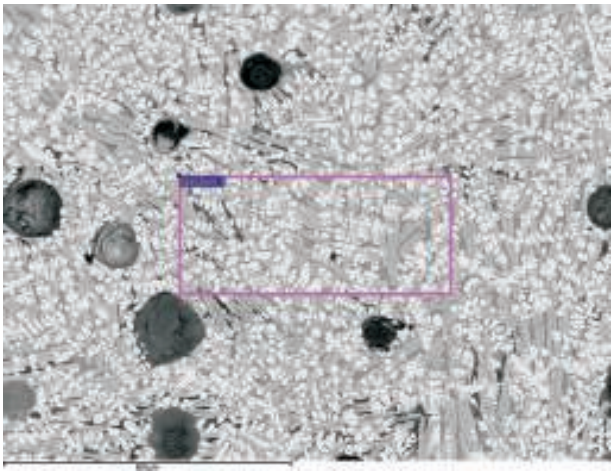

e

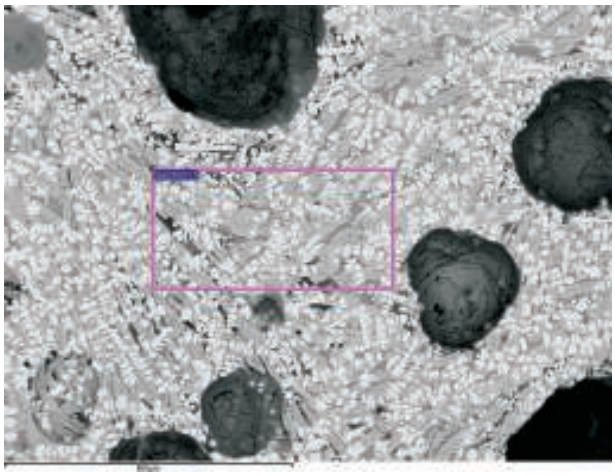

f

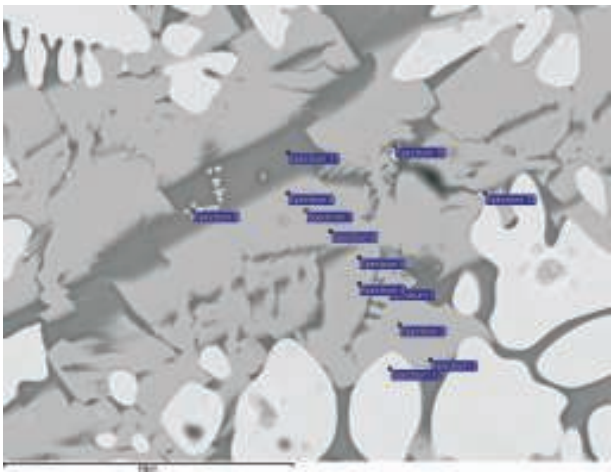

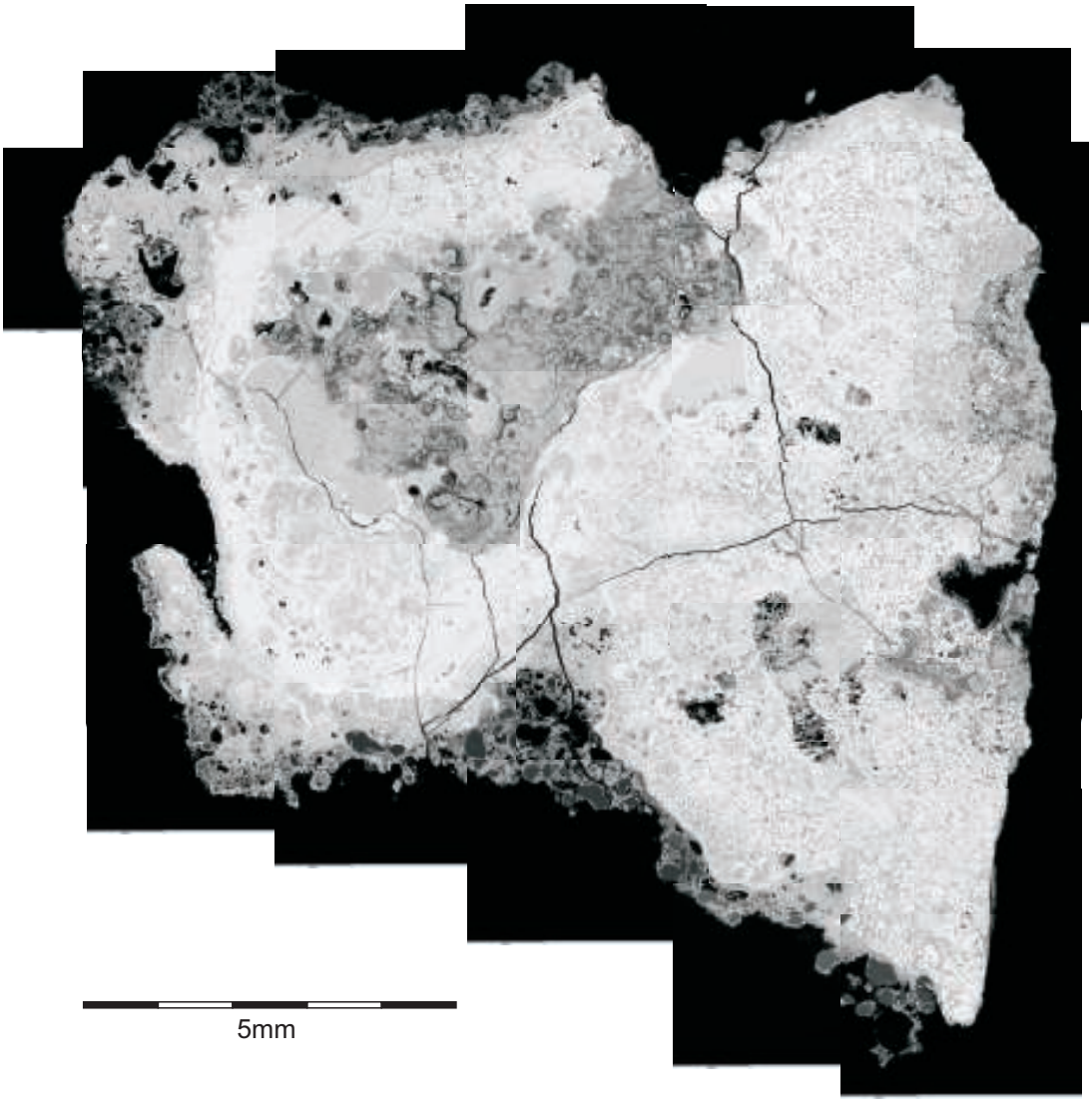
5mm

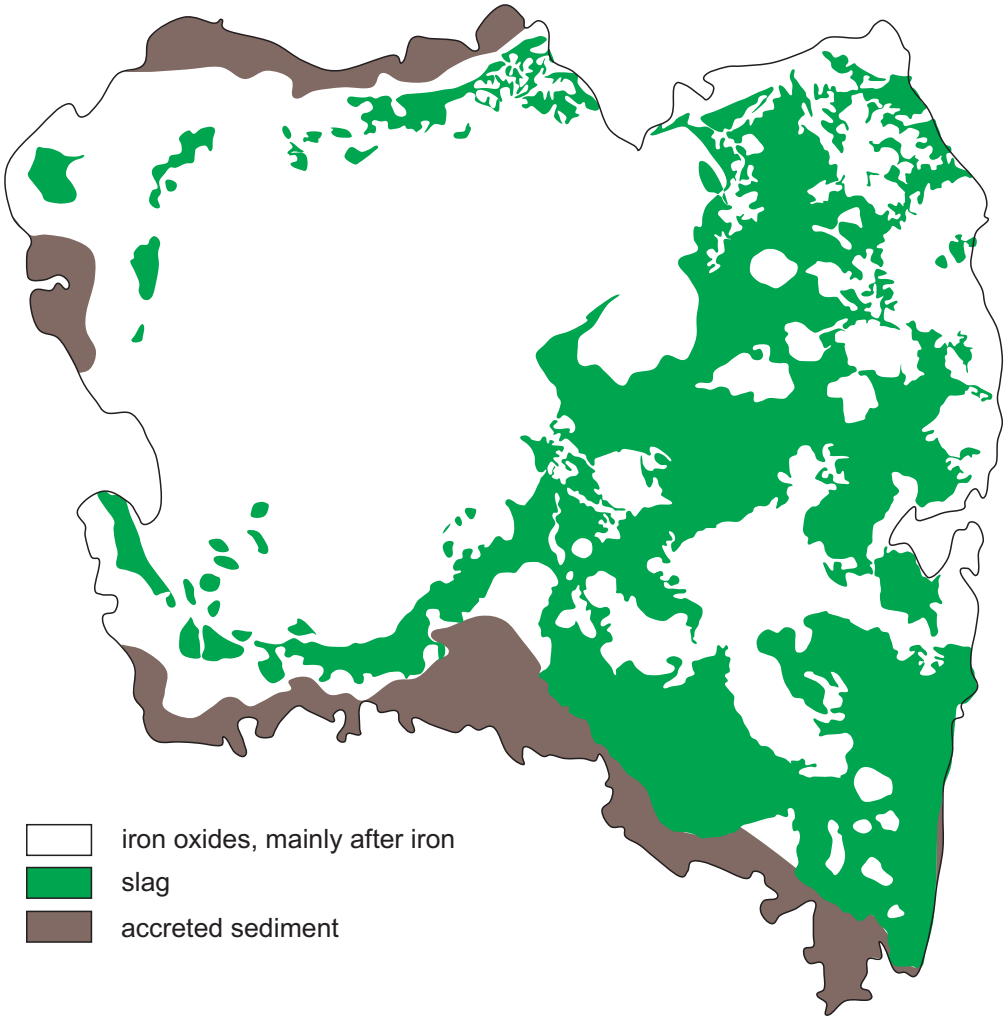
iron oxides, mainly after iron
slag
accreted sediment

a

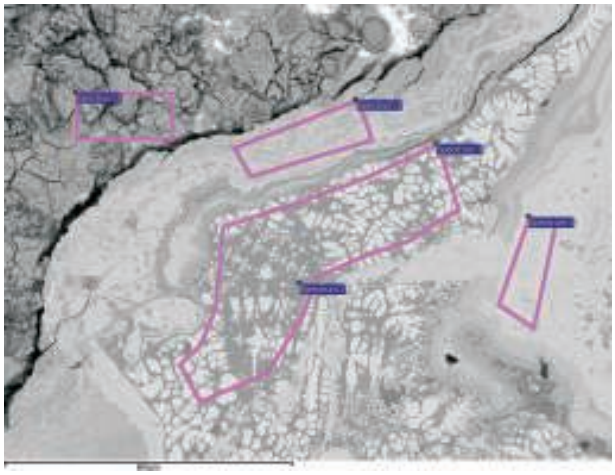

b

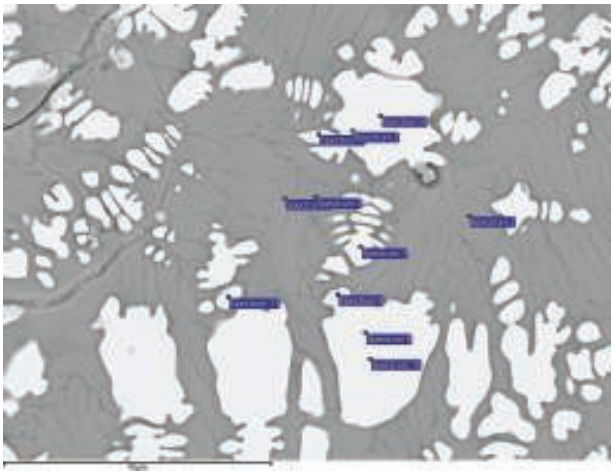

c

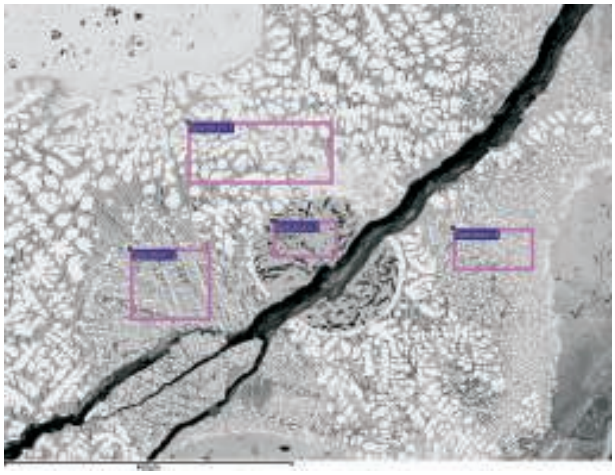

d

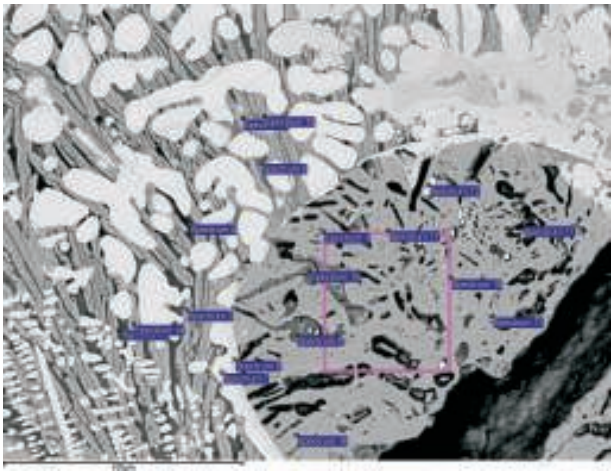

e

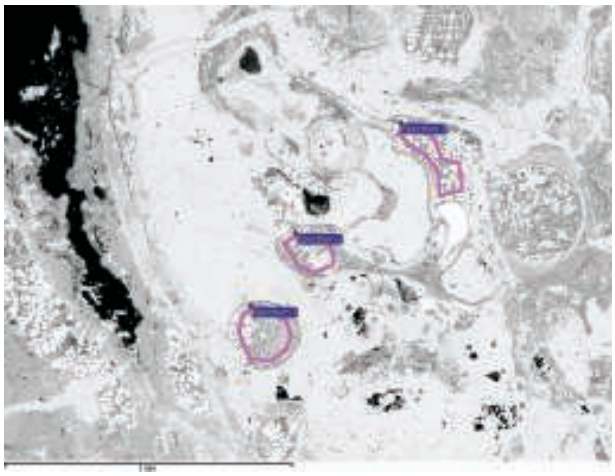

f

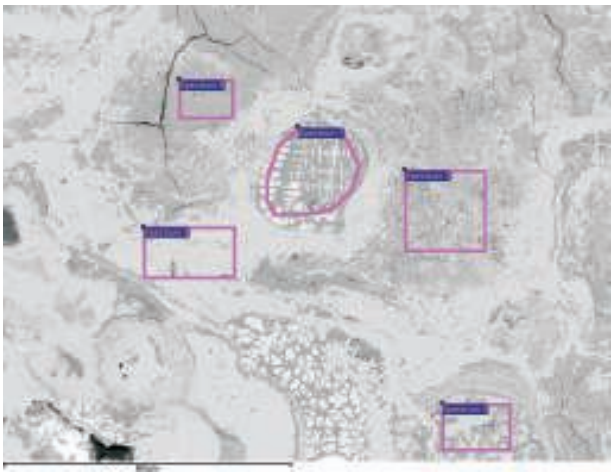

g

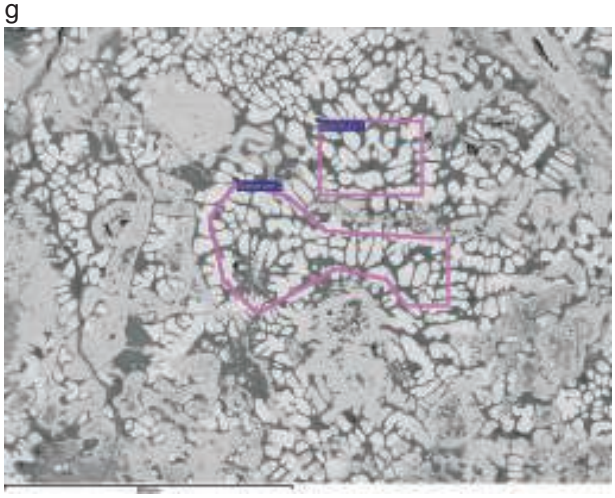

a

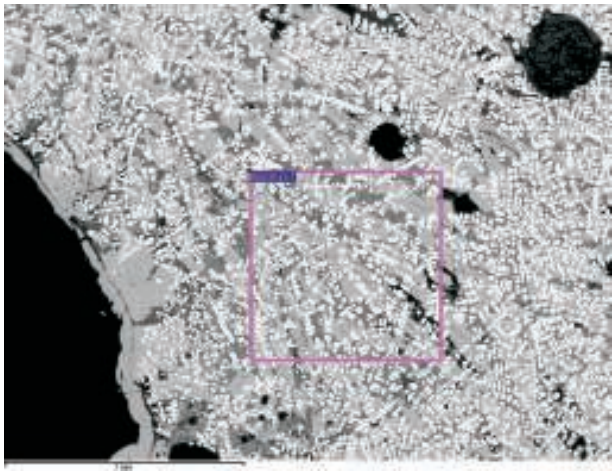

b

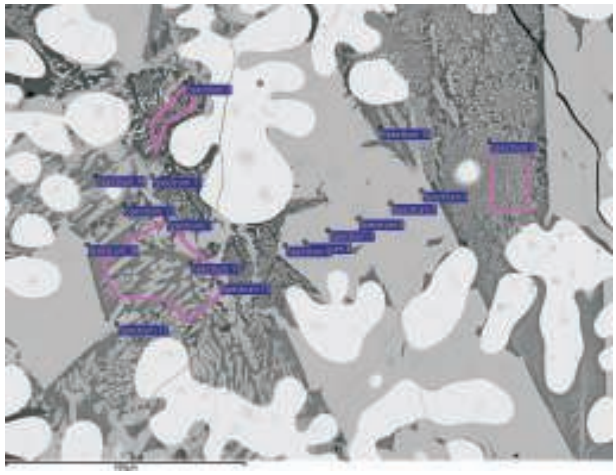

c

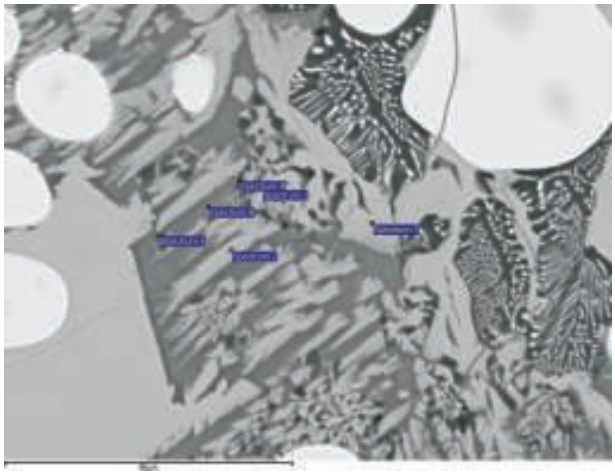

d

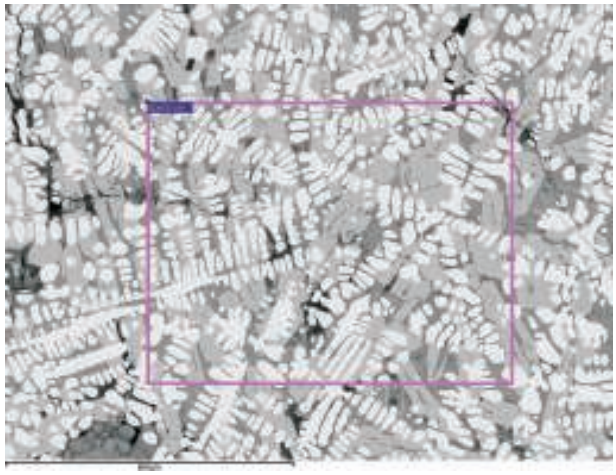

e

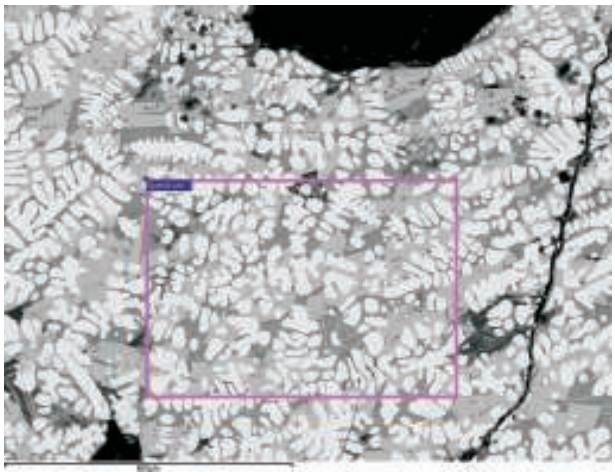

f

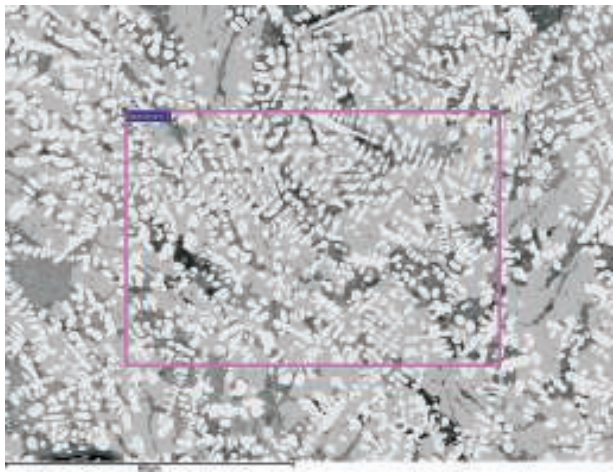

g

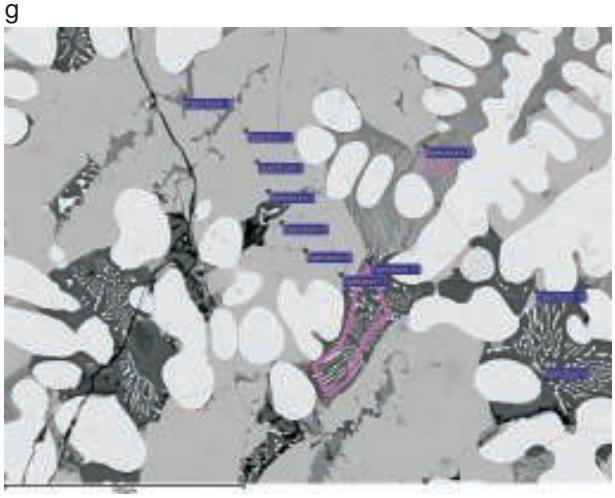

a

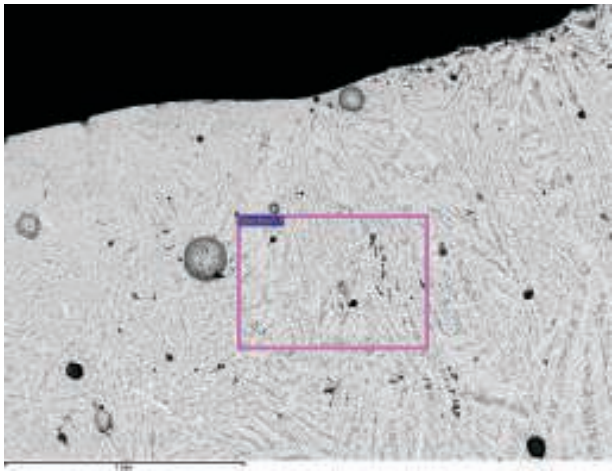

b

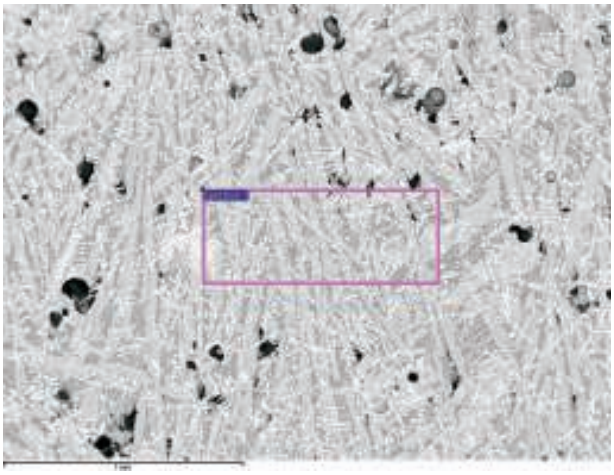

c

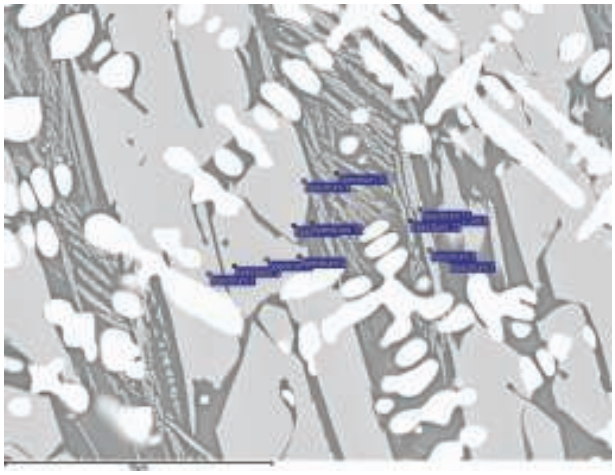

d

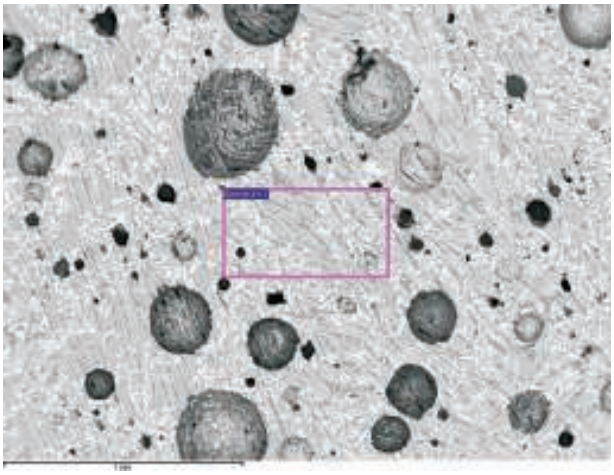

e

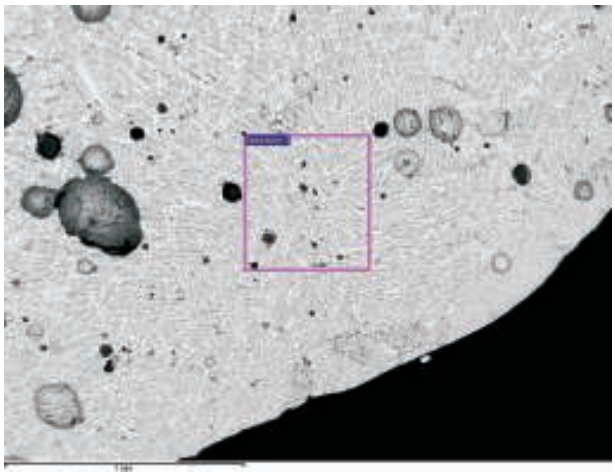

a

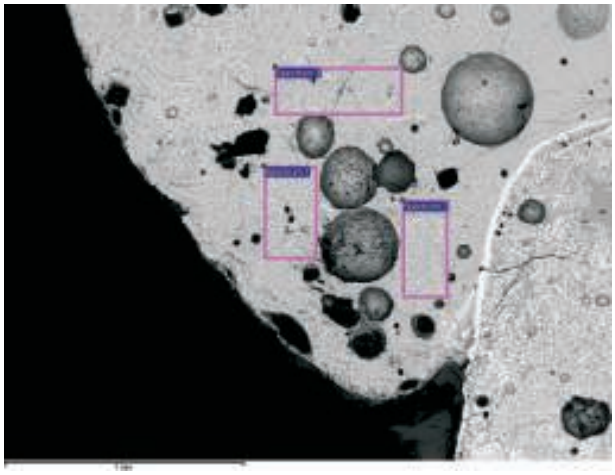

b

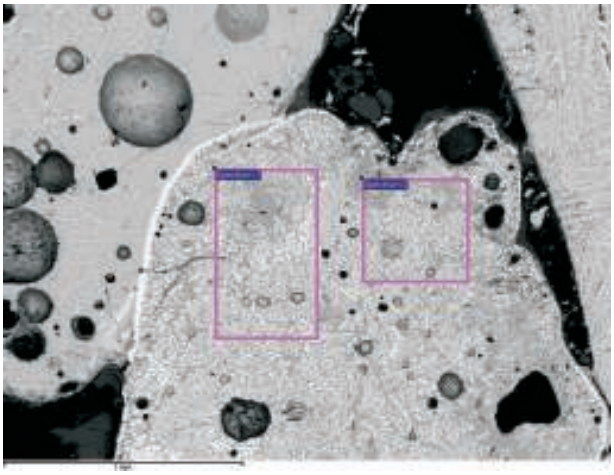

c

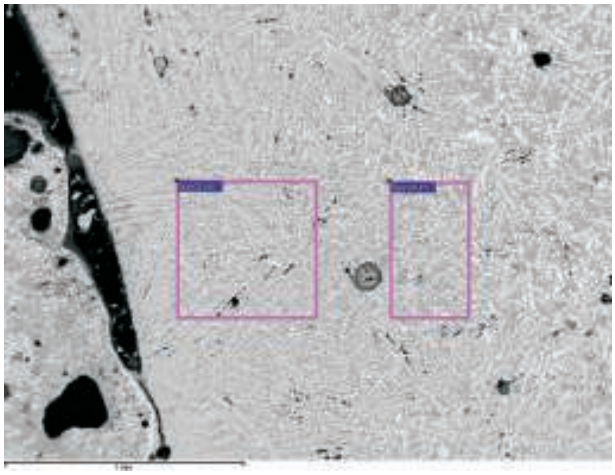

d

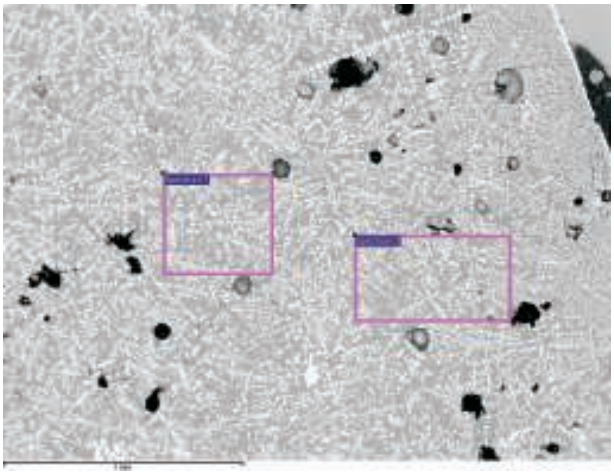

e

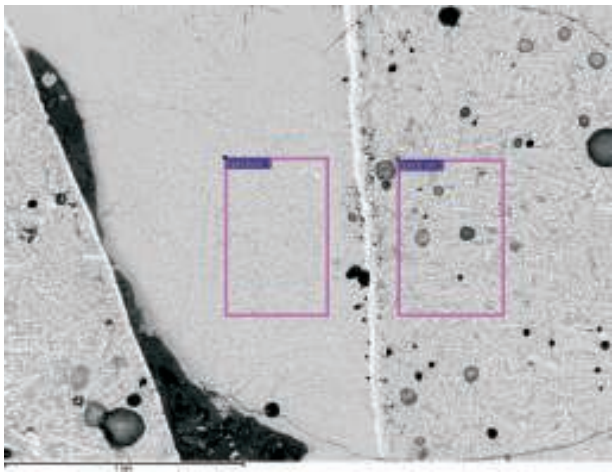

f

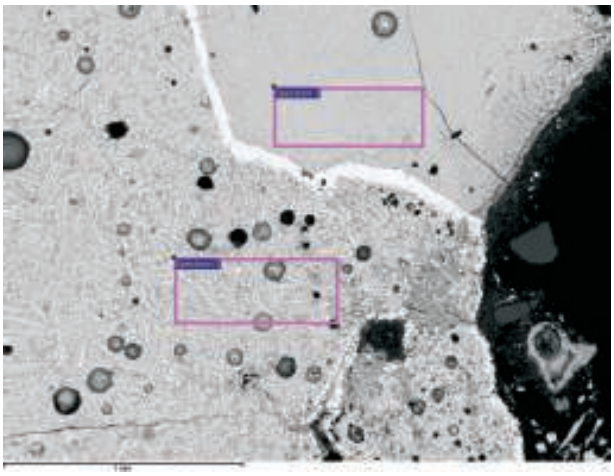

g

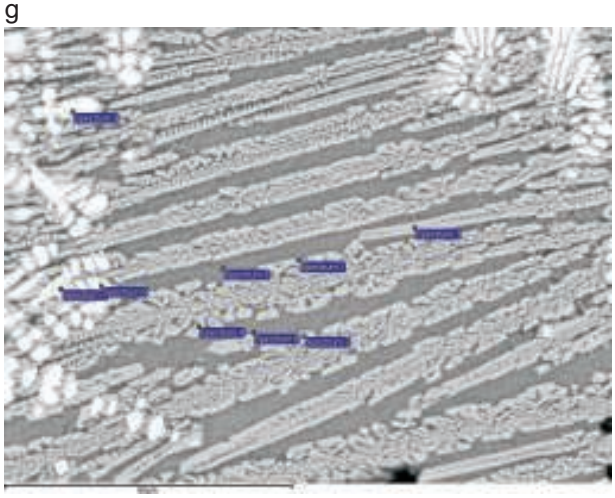

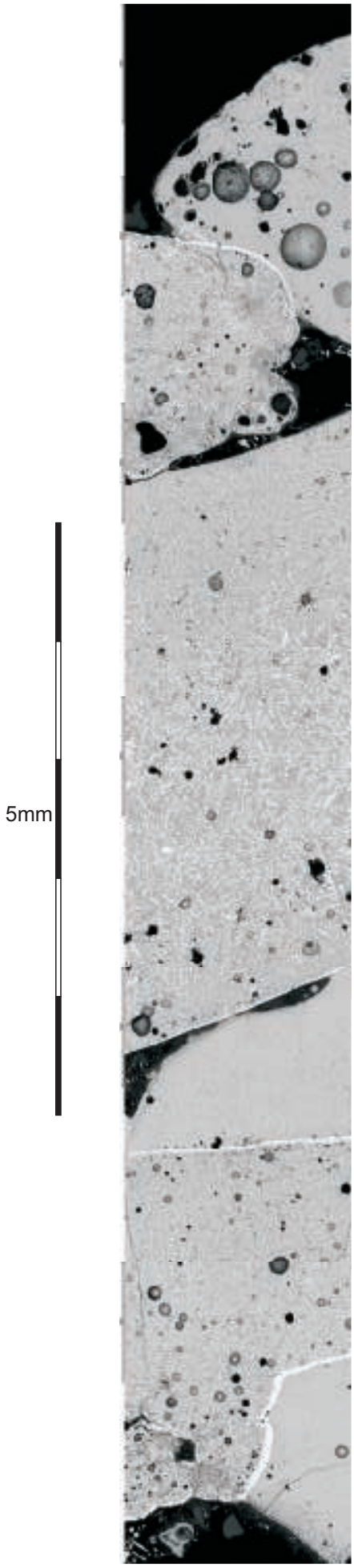
5mm

a

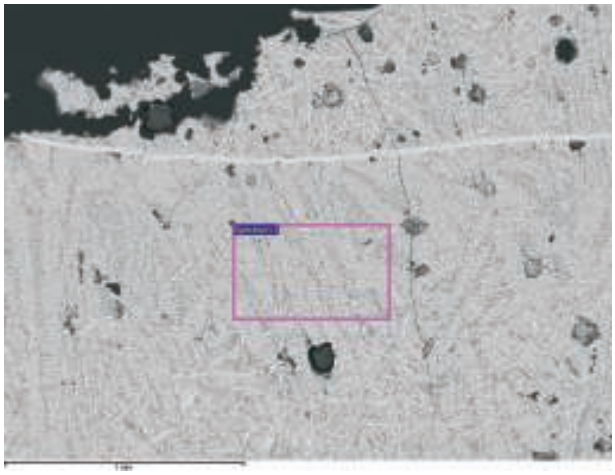

b

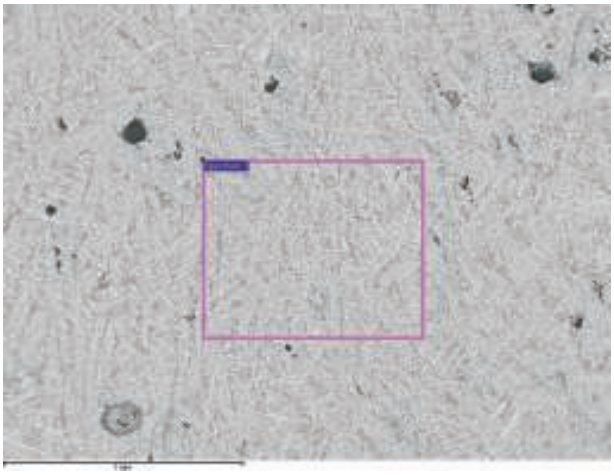

c

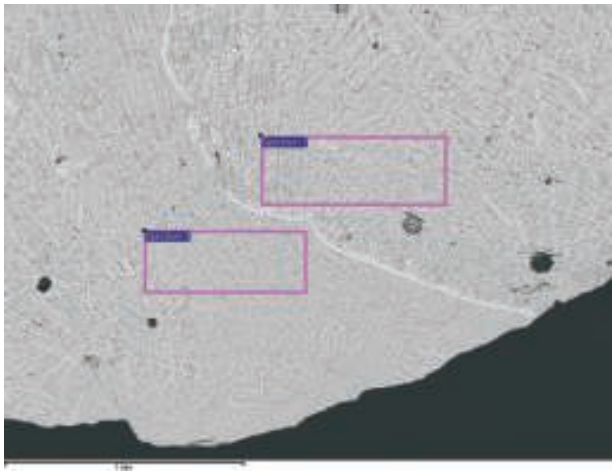

d

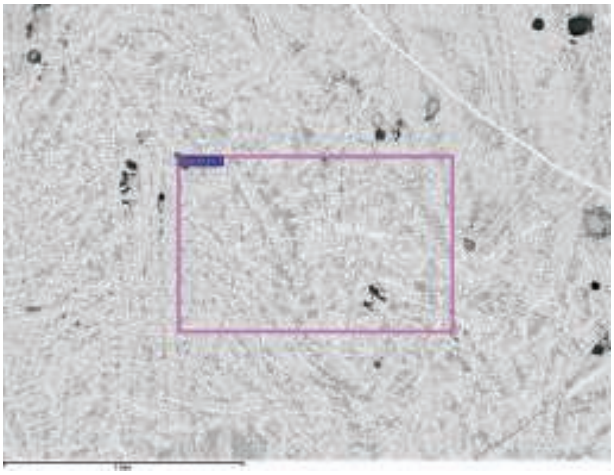

e

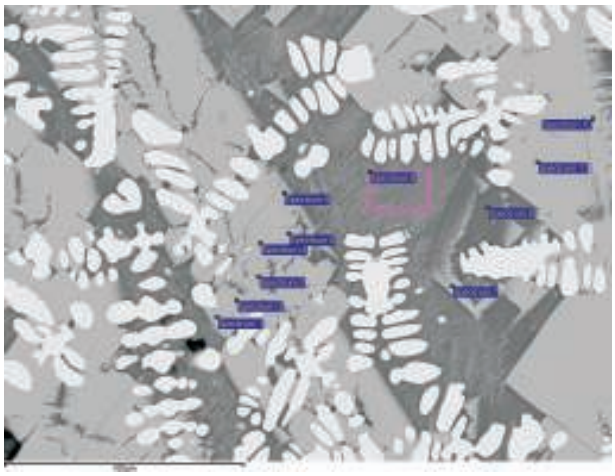

a

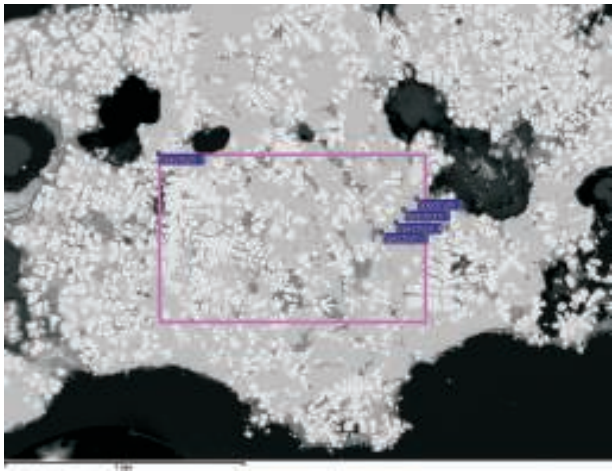

b

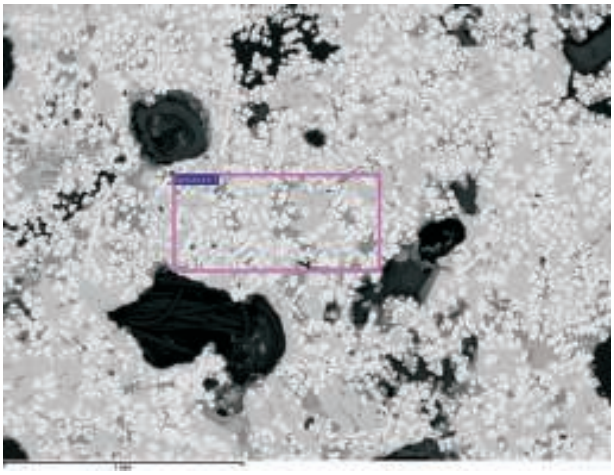

c

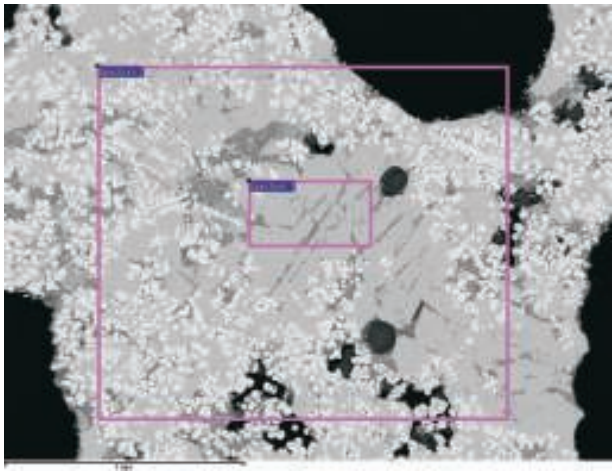

d

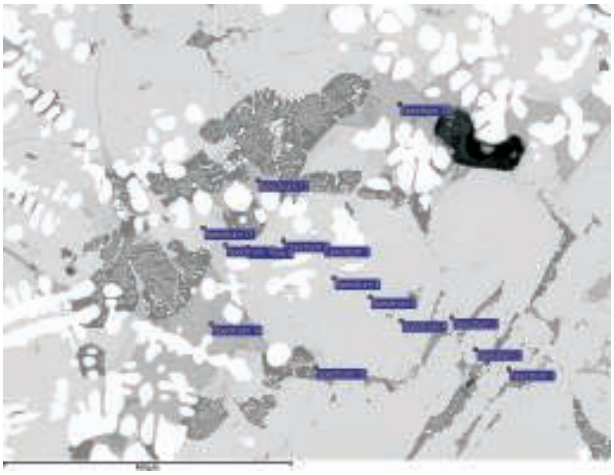

e

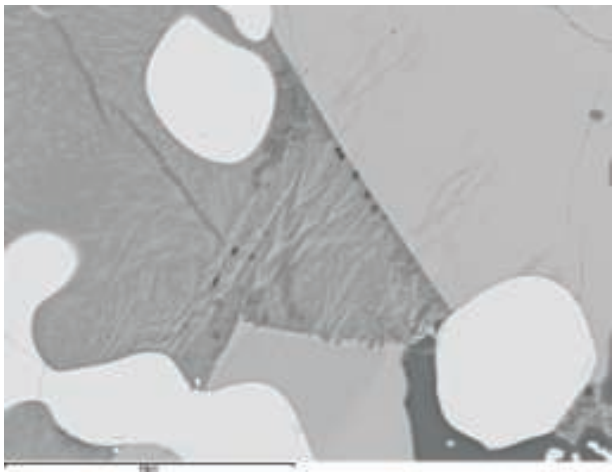

f

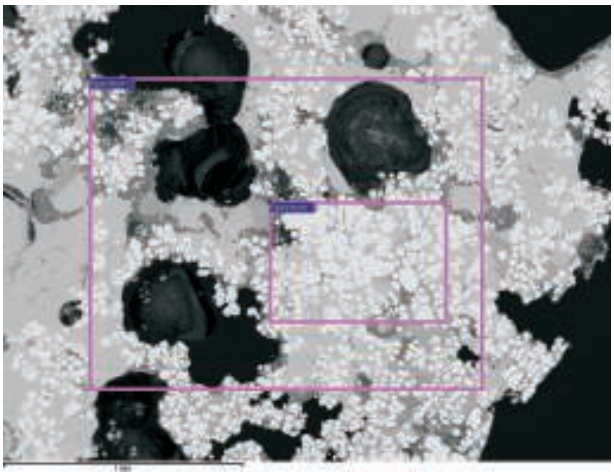

g

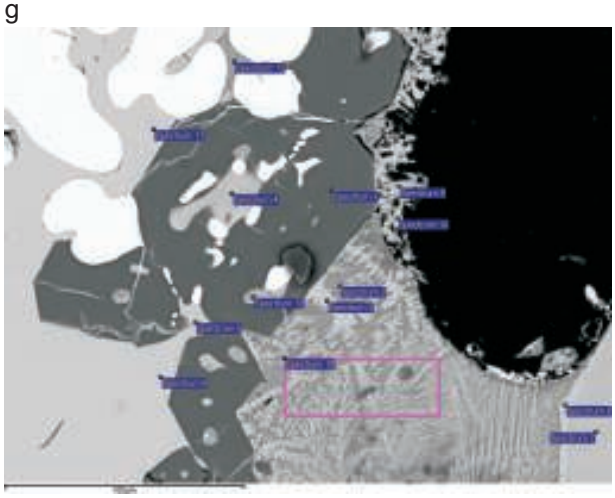

h

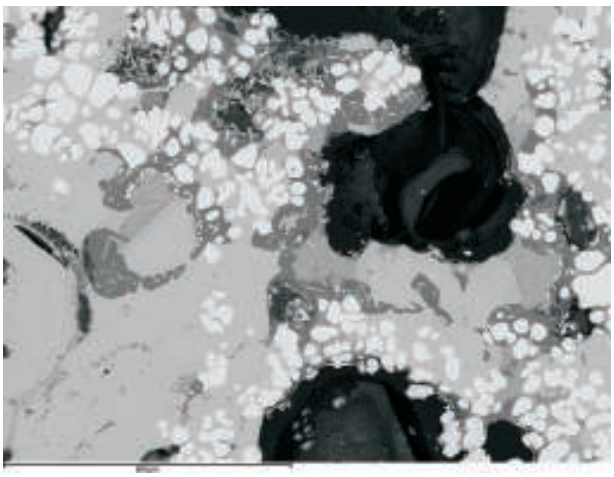

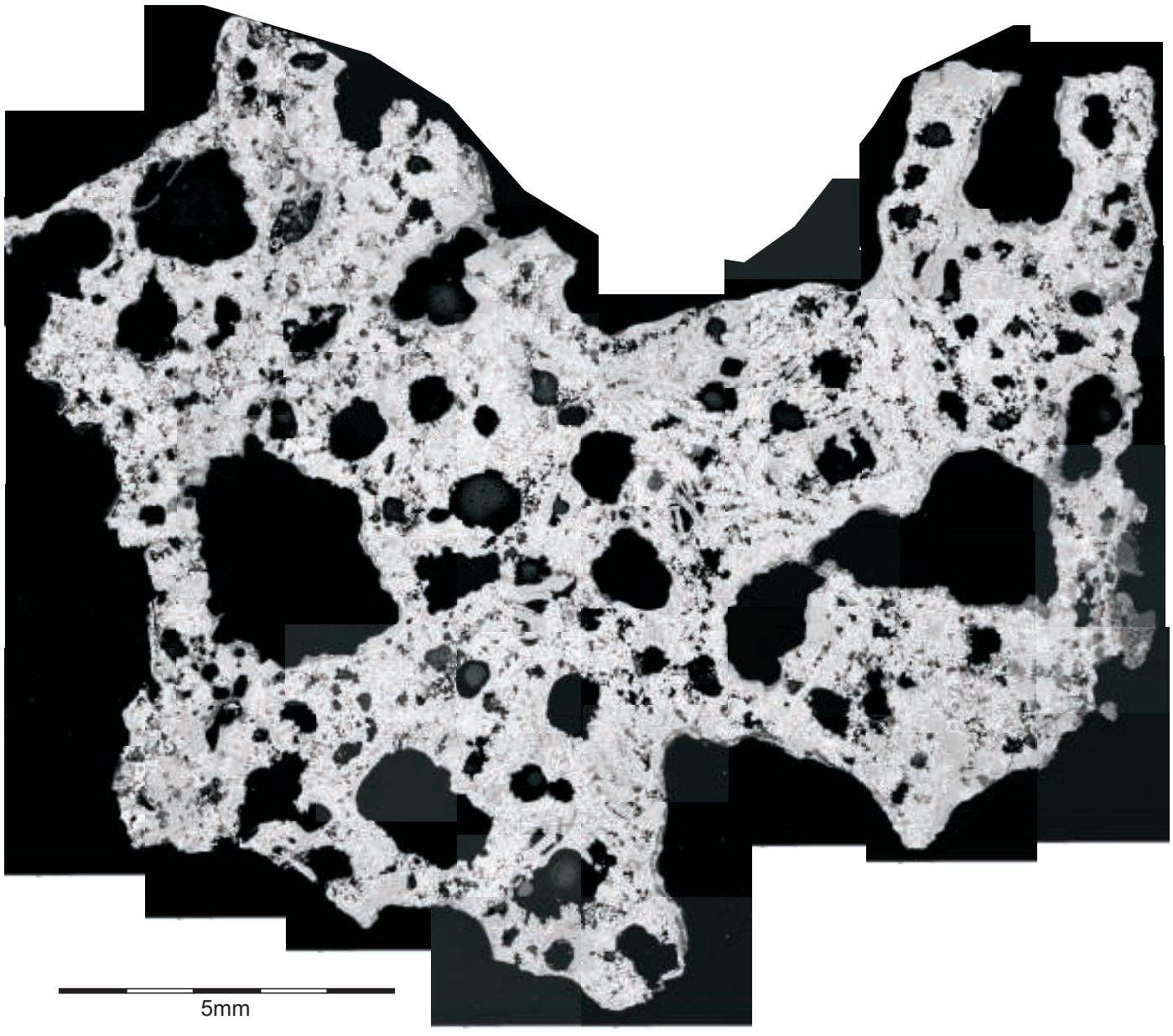
5mm

a

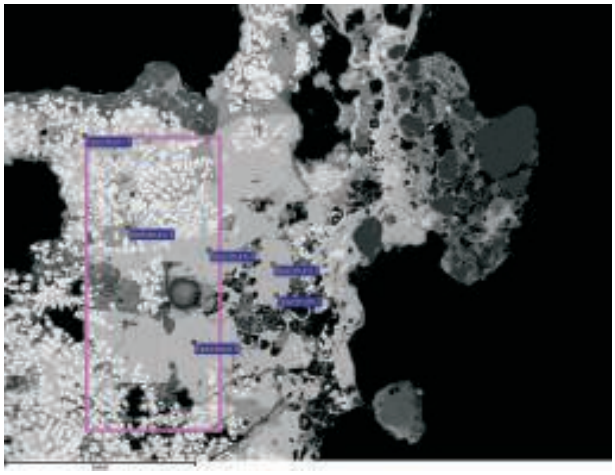

b

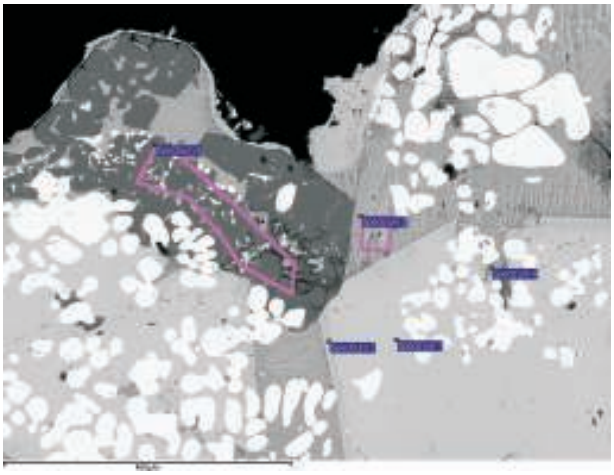

c

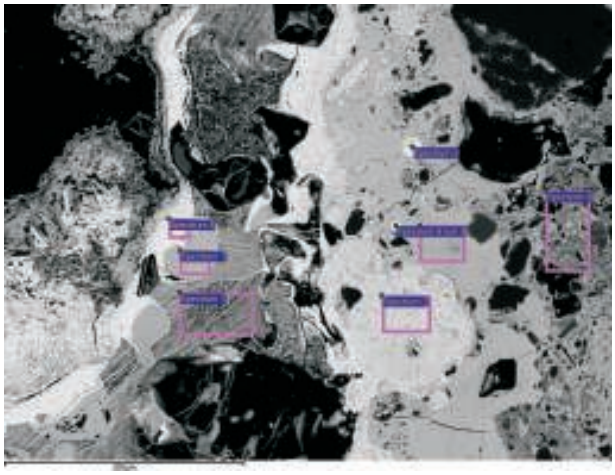

d

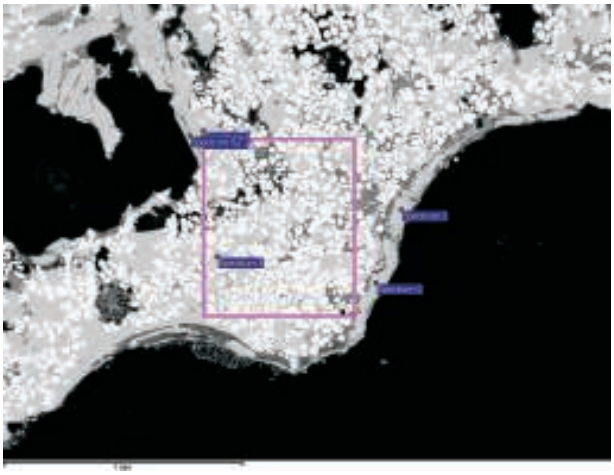

e

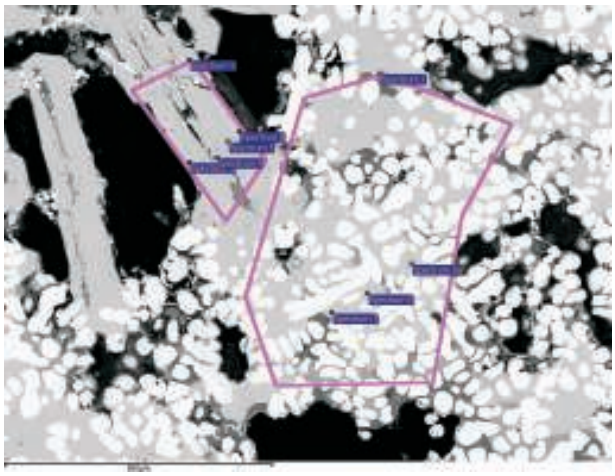

f

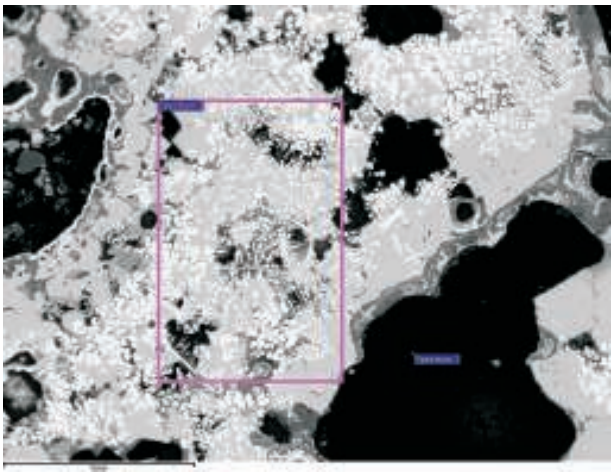

g

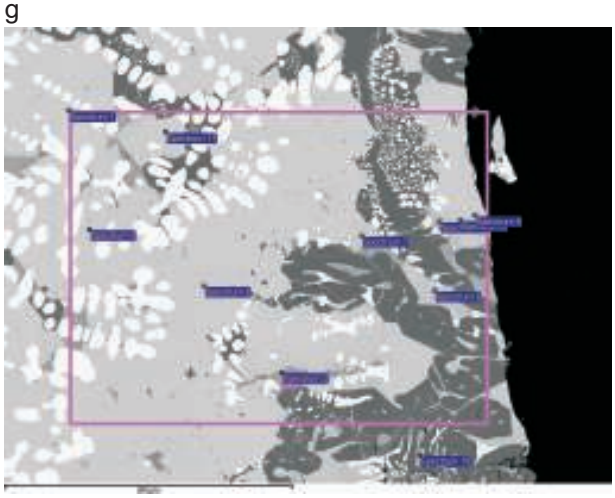

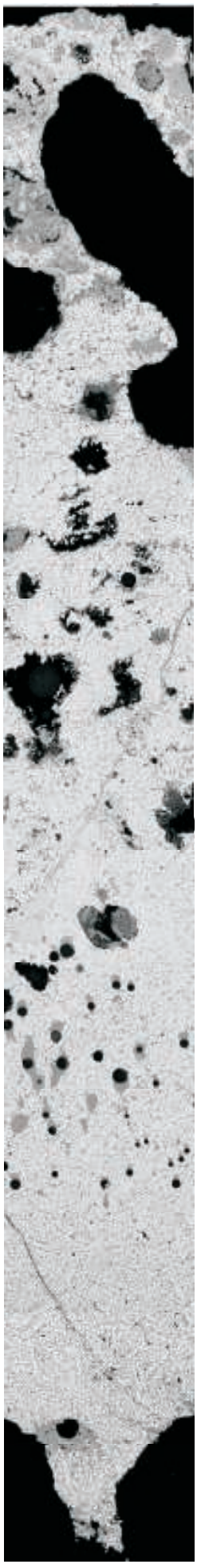

5mm

a

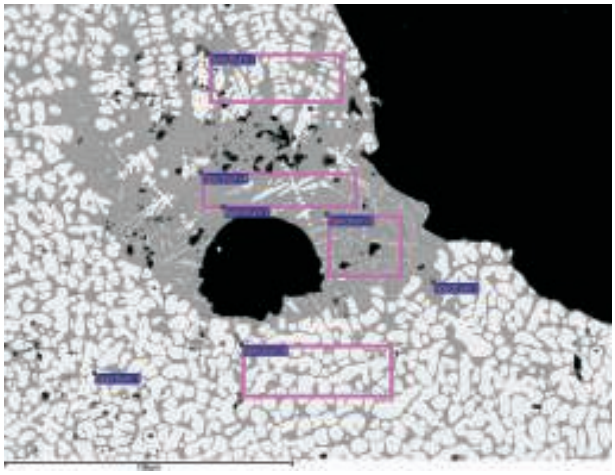

b

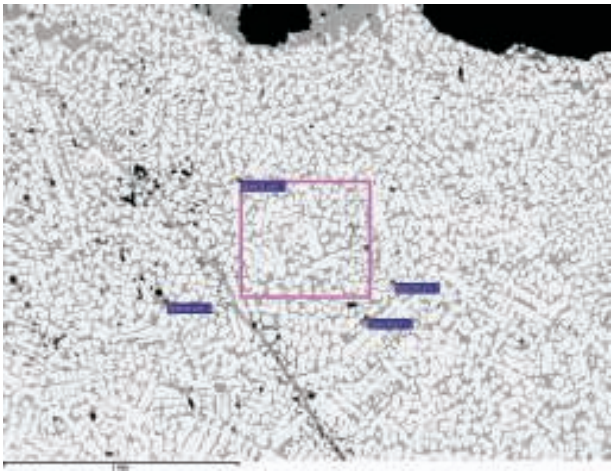

c

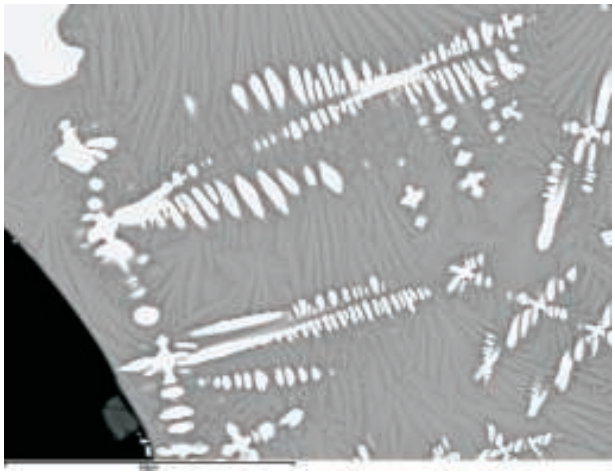

d

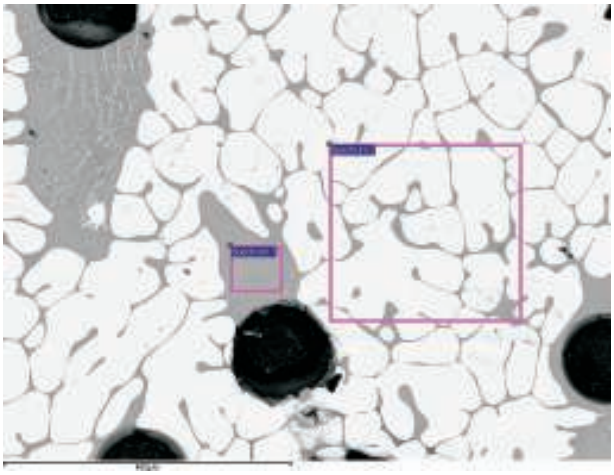

e

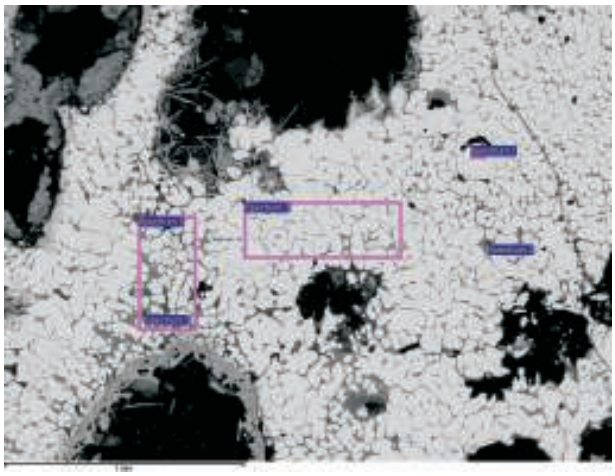

f

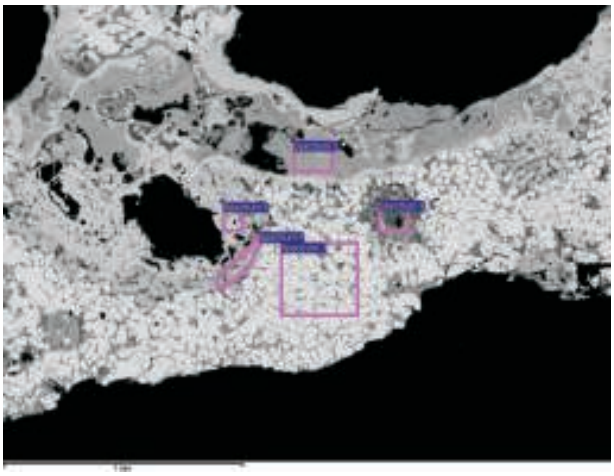

g

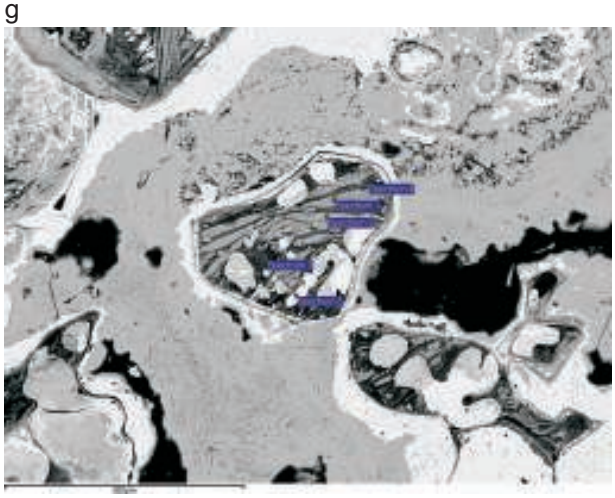

h

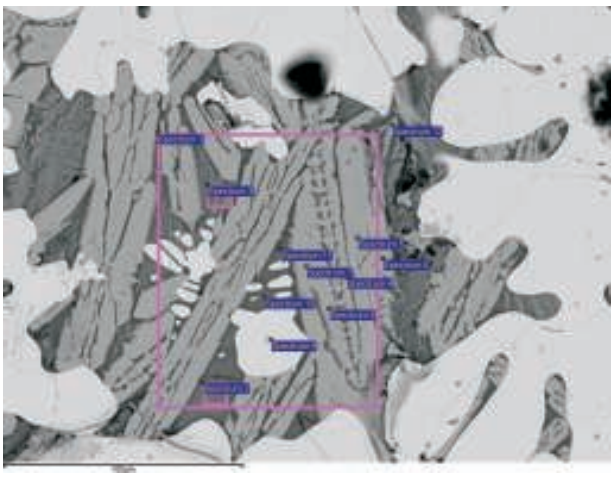

a

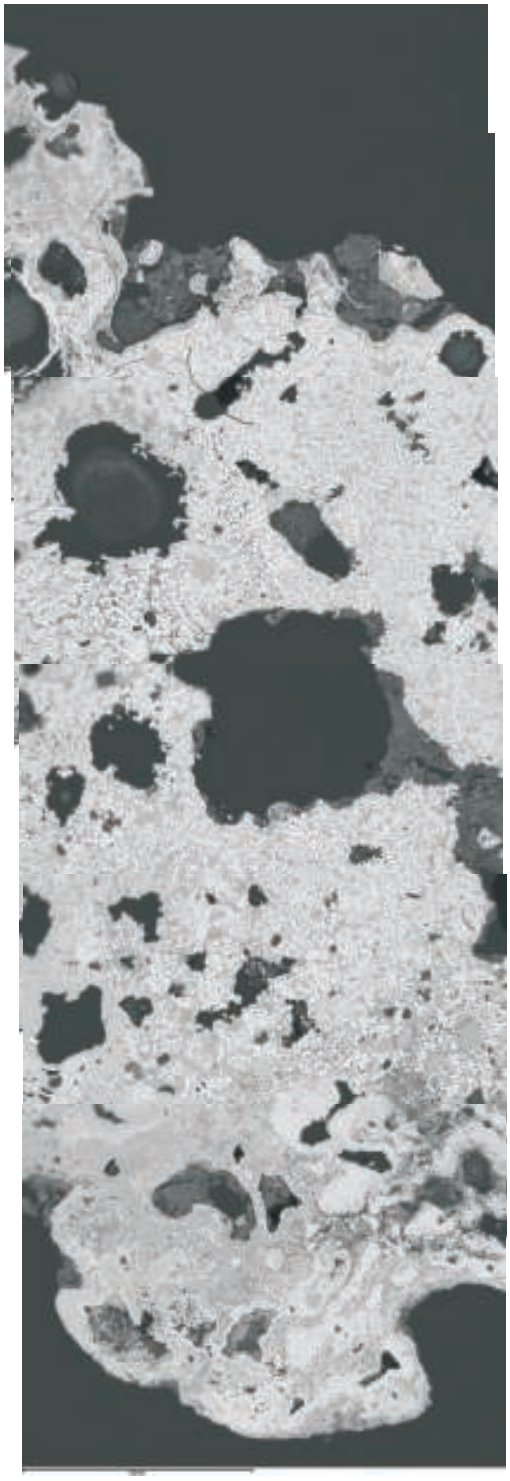

5mm

b

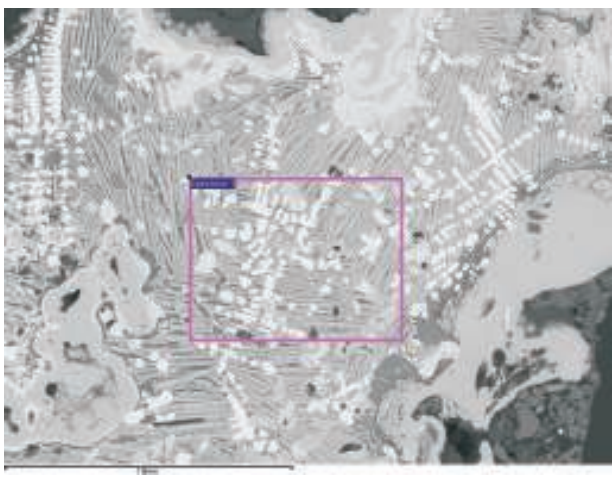

c

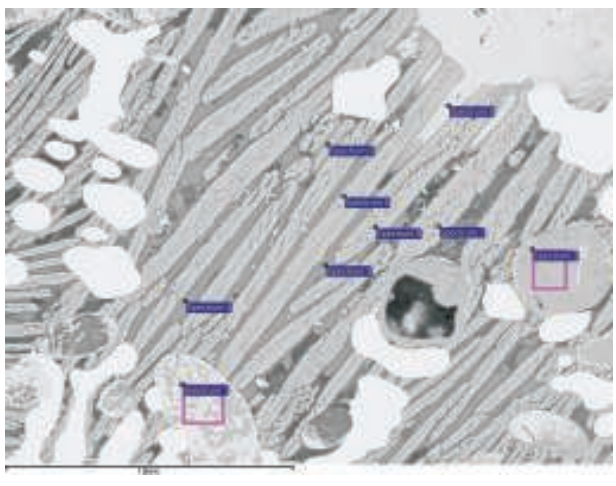

a

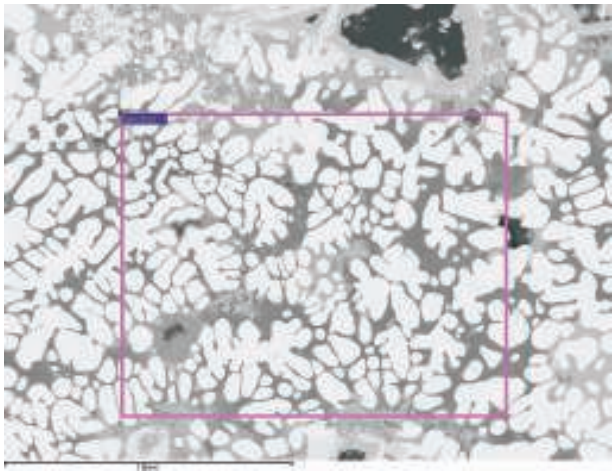

b

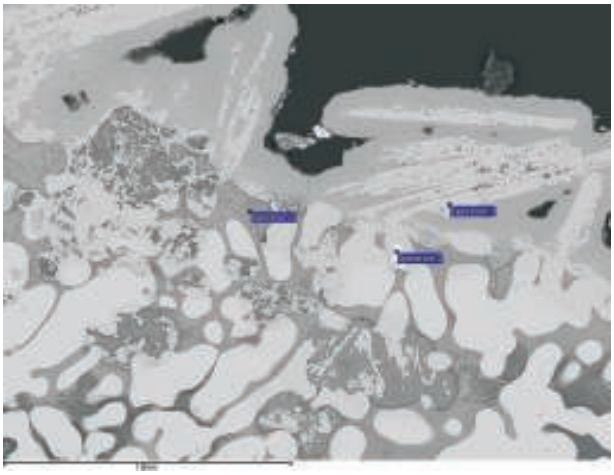

c

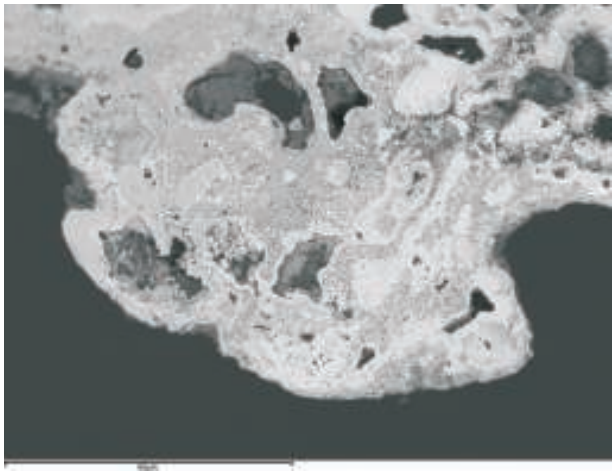

d

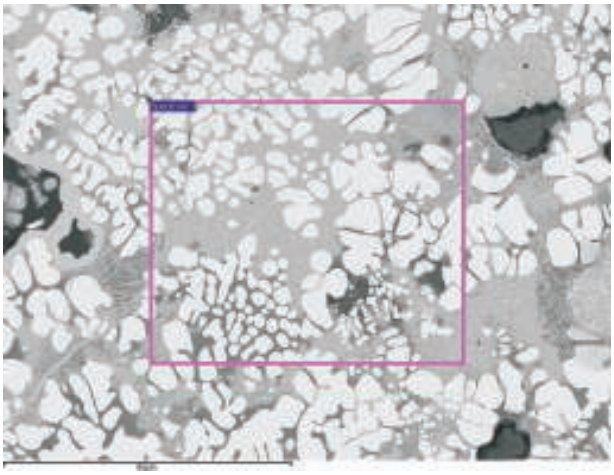

e

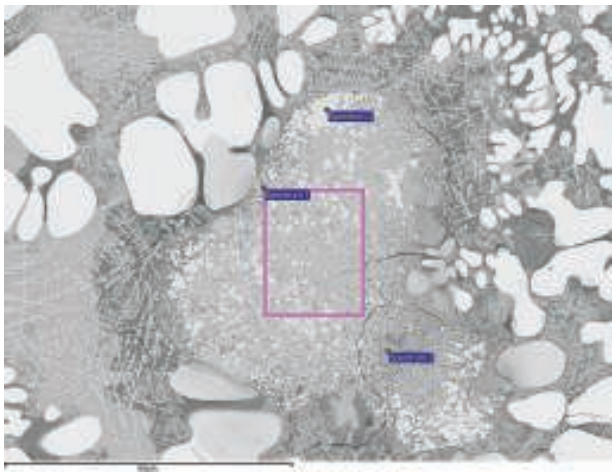

a

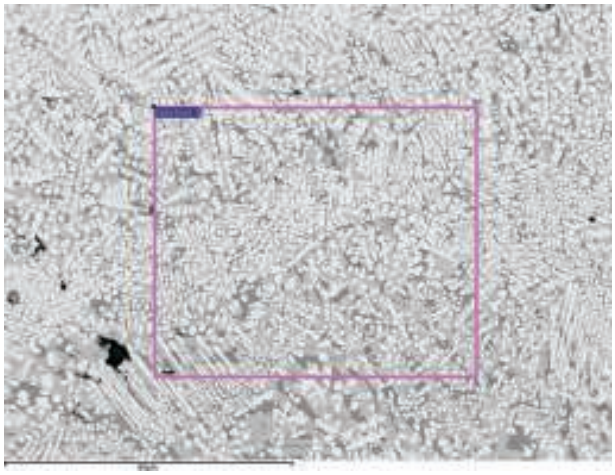

b

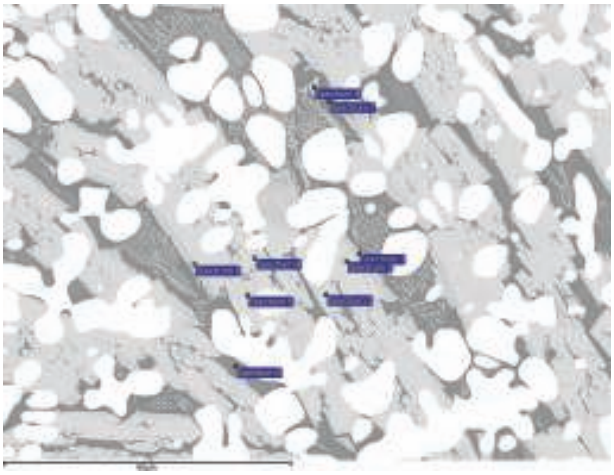

c

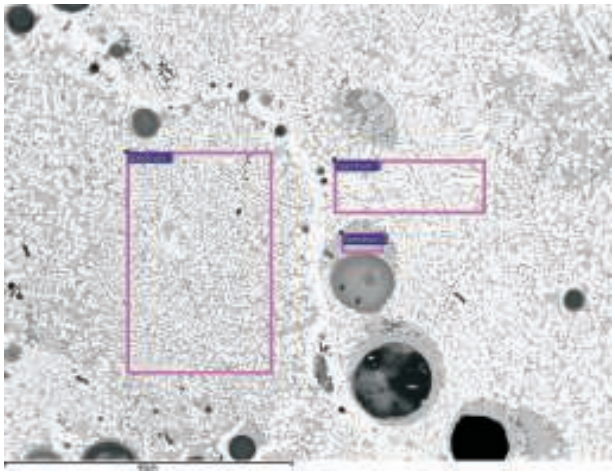

d

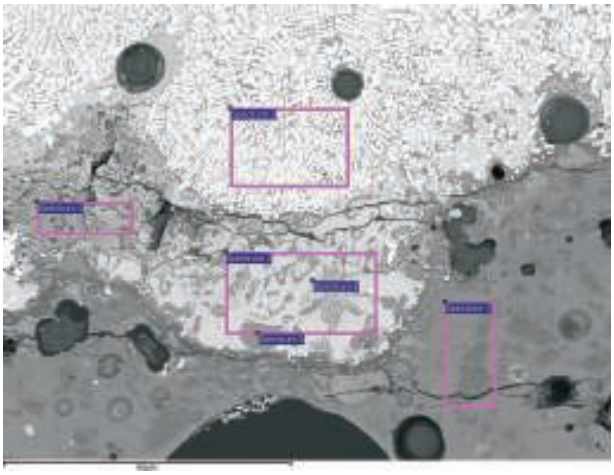

e

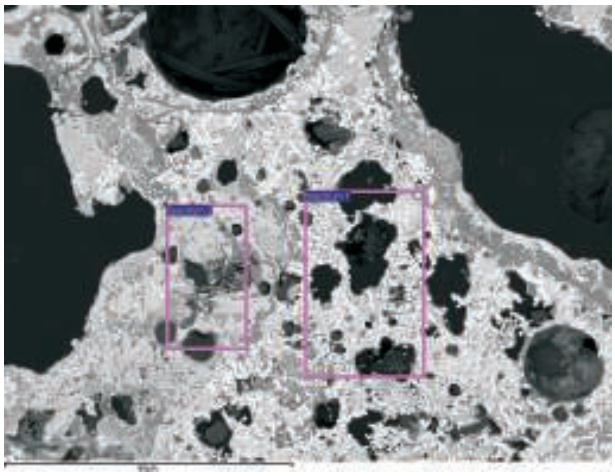

f

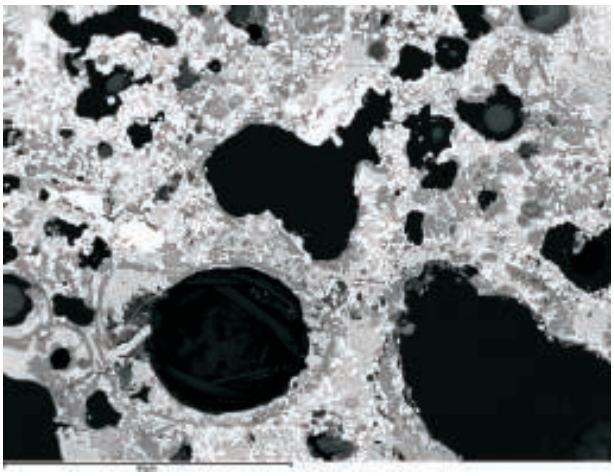

g

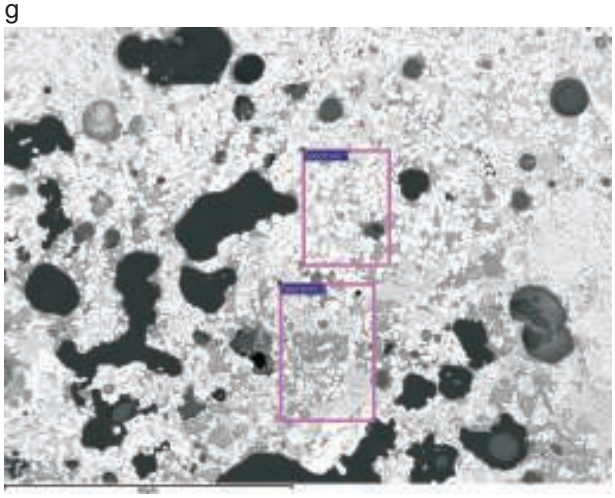

h

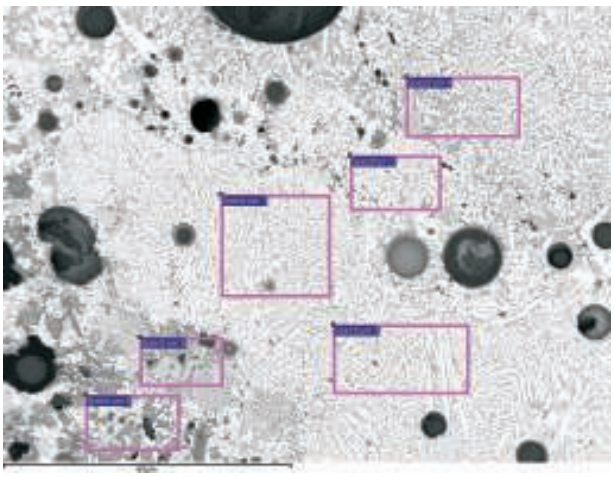

a

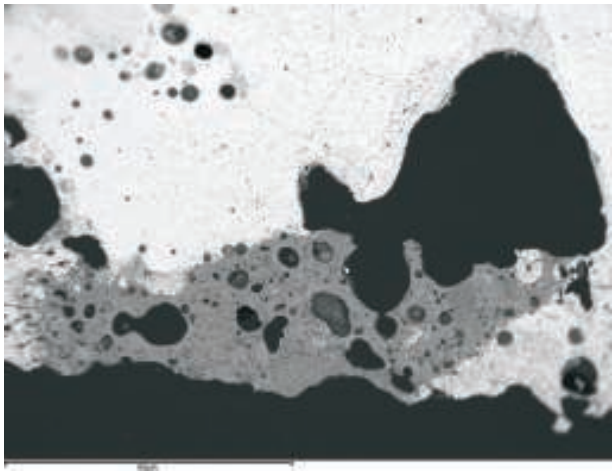

a

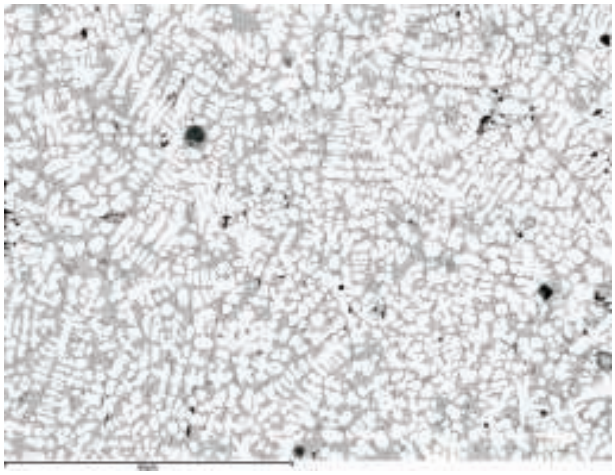

b

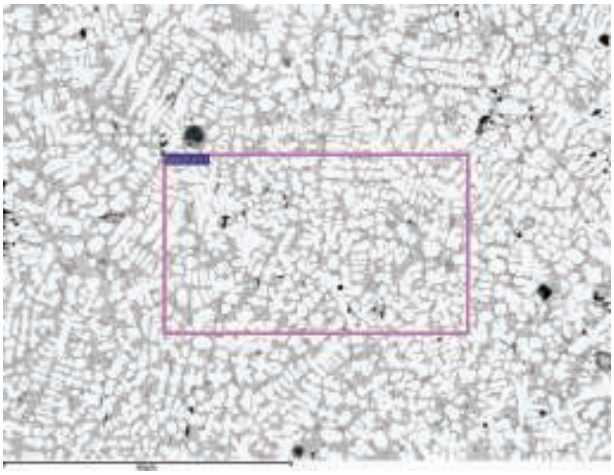

c

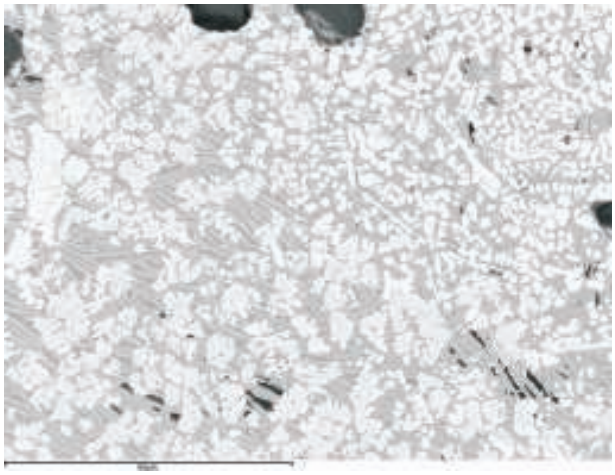

d

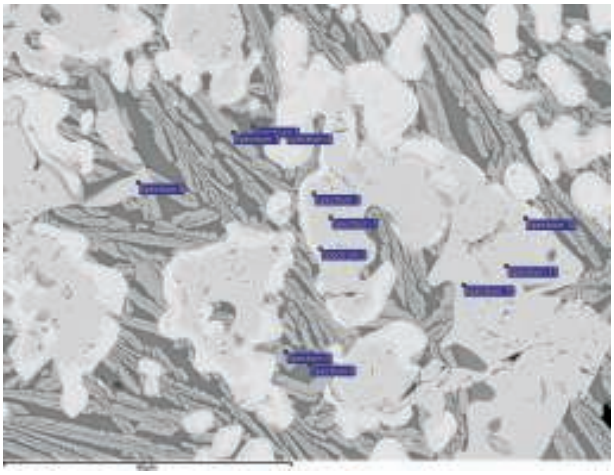

e

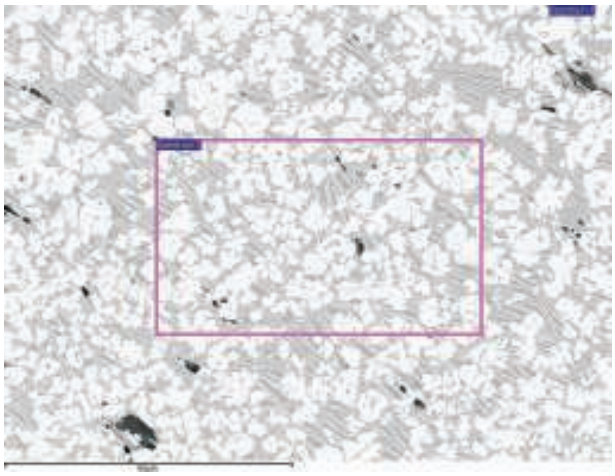

f

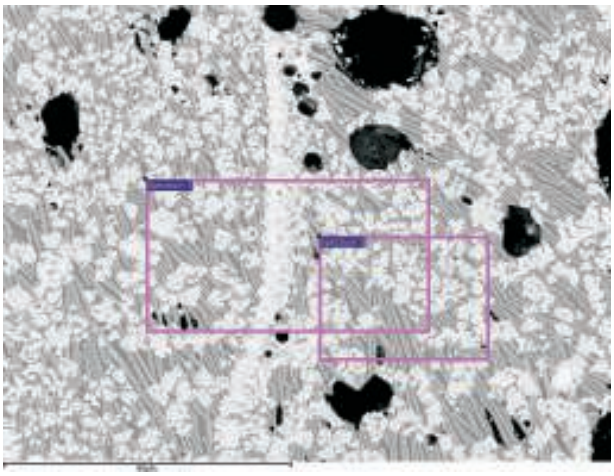

g

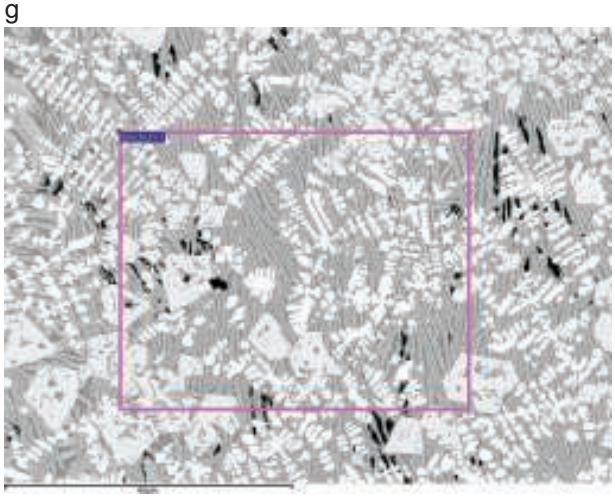

h

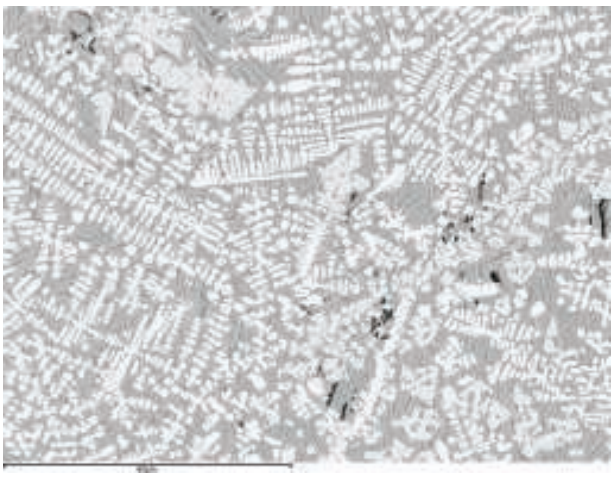

a

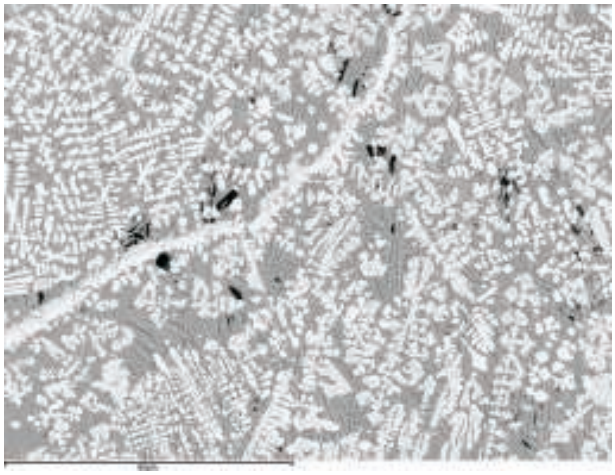

b

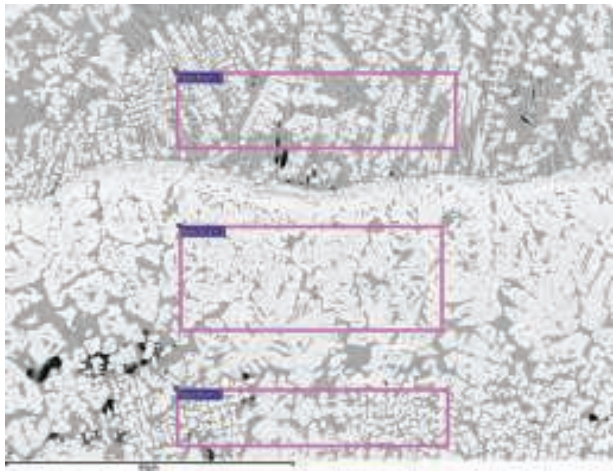

c

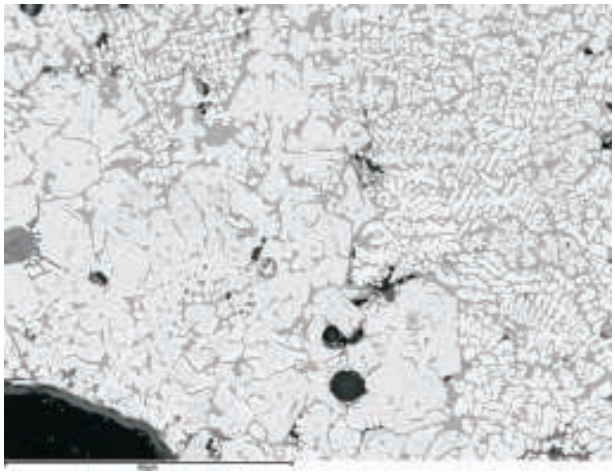

d

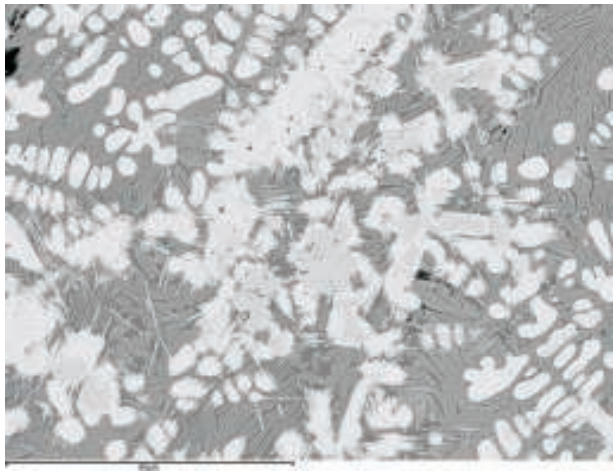

e

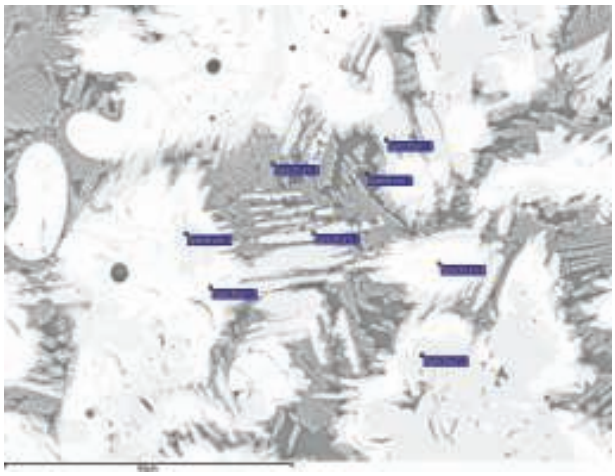

f

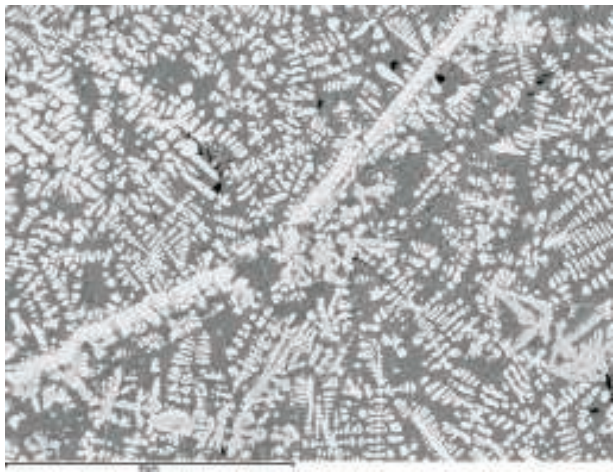

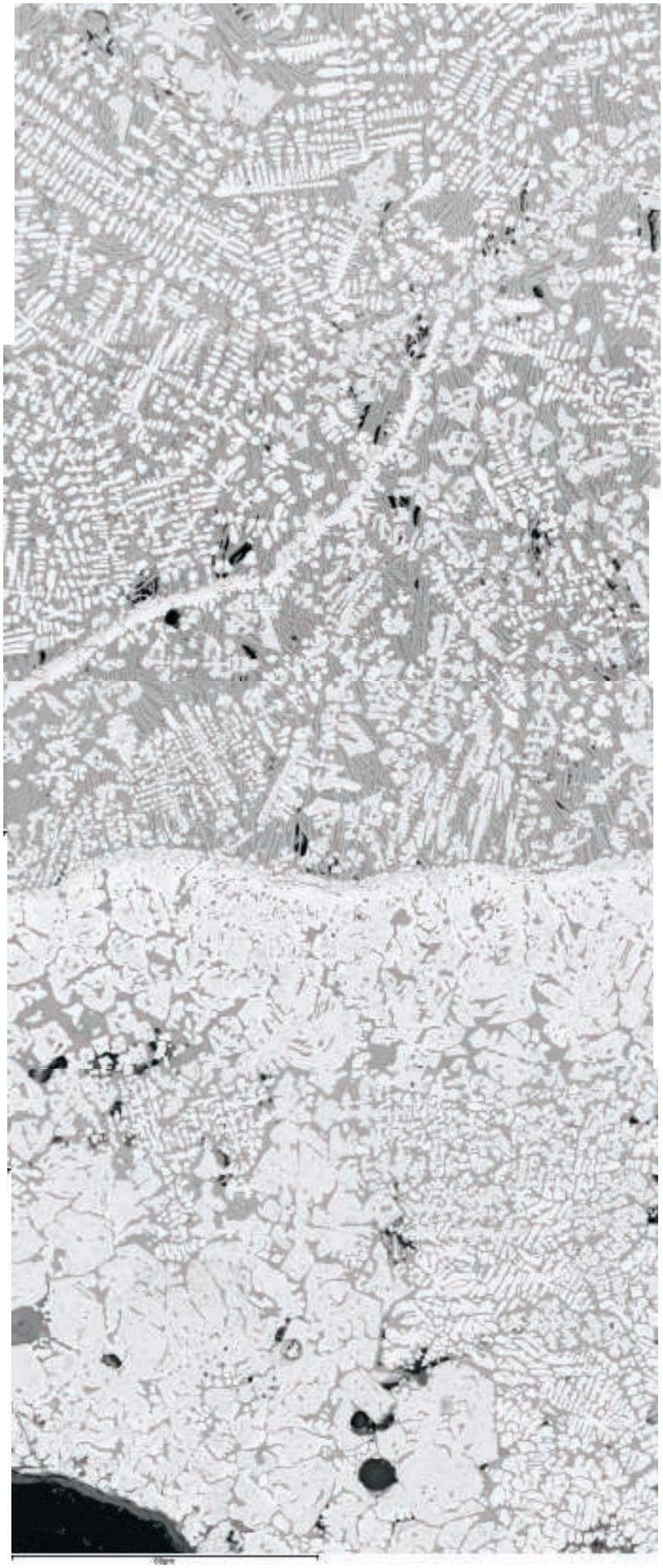

1mm

a

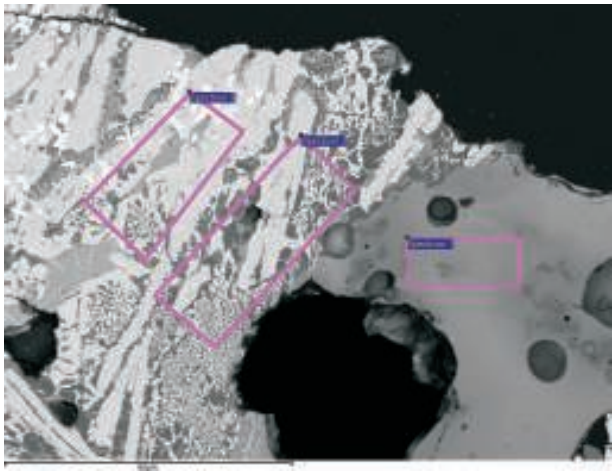

b

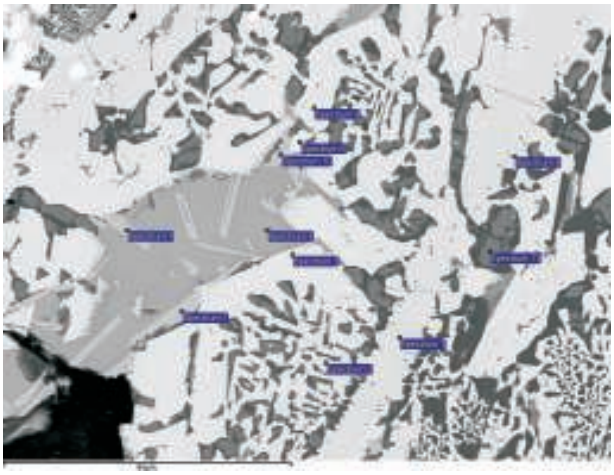

c

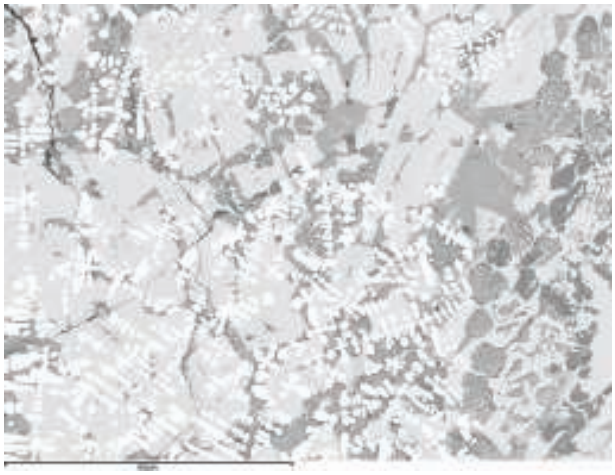

d

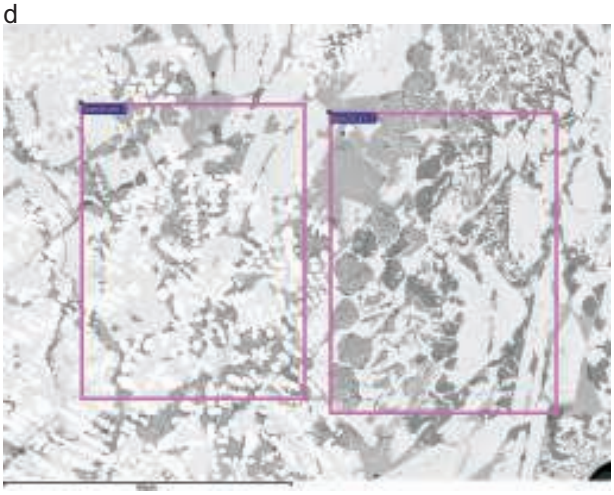

e

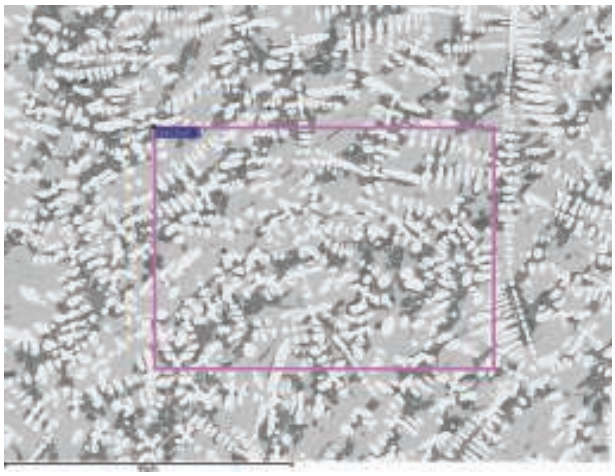

f

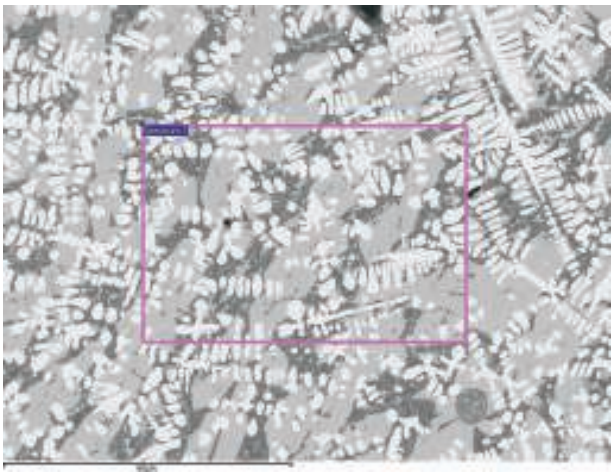

g

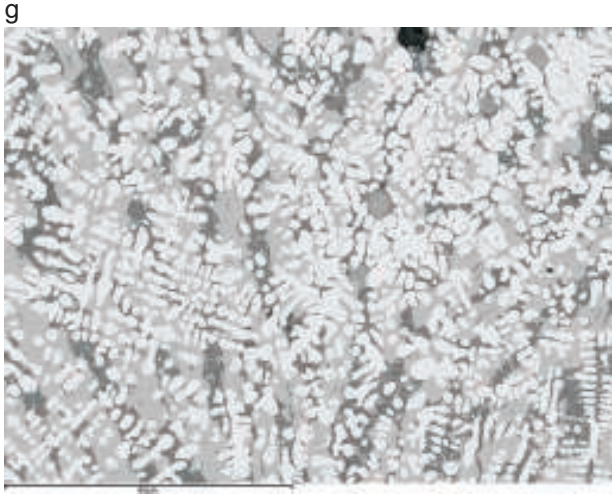

h

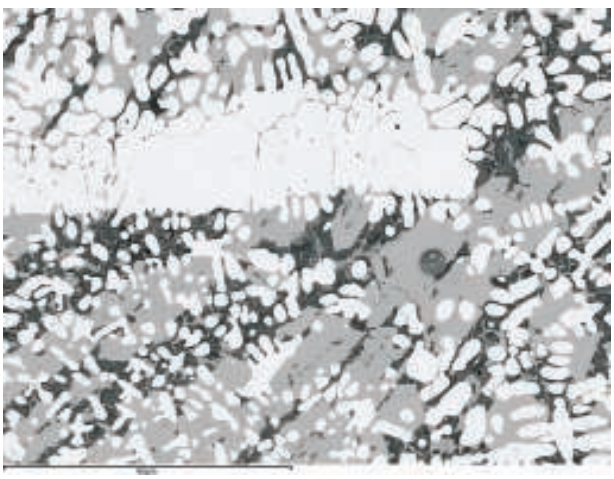

a

Plate A31

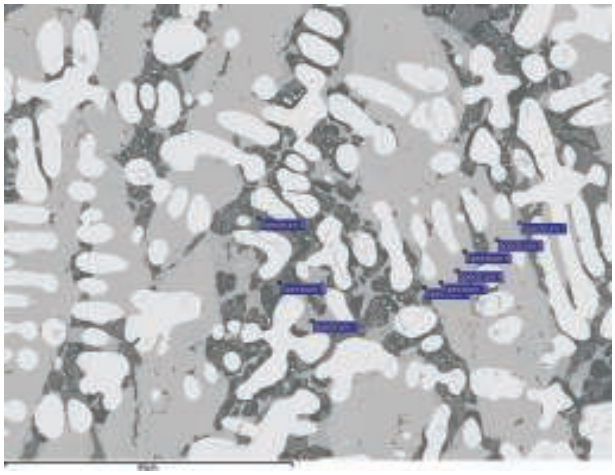

APPENDIX B
EDS ANALYSIS ARCHIVE

EDS data archive

Table B1: Archive of all EDS analyses ..... p. 68

Table B2: EDS Data for analysed representative areas
.....p. 77

					Atom%																	Wt%																	
					O	Na	Mg	Al	Si	P	S	Cl	K	Ca	Ti	V	Cr	Mn	Fe	Ni	Cu	Ba	O	Na	Mg	Al	Si	P	S	Cl	K	Ca	Ti	V	Cr	Mn	Fe	Ni	Cu	Ba	total
A1	SOI 1	#1	area	typical	59.00	0.29	0.45	2.21	11.24	0.12			0.82	1.30	0.00			0.15	24.44				22.17	0.15	0.26	1.40	7.41	0.08			0.75	1.22	0.00			0.19	32.07				65.71
A1	SOI 1	#2	area	error	58.57		0.52	1.52	11.85				0.62	1.06					25.85				39.64		0.53	1.74	14.08				1.03	1.80					61.08				119.91
A1	SOI 1	#3	area	typical	59.12	0.40	0.44	2.15	11.43	0.11	0.00		0.91	1.48	0.00				23.96				34.37	0.33	0.39	2.11	11.67	0.13	0.00		1.29	2.15	0.00				48.63				101.08
A1	SOI 2	#1	area	small typical	58.52	0.42	0.39	2.22	11.71	0.12	0.00		1.09	1.67	0.07				23.80				36.24	0.37	0.36	2.32	12.73	0.14	0.00		1.65	2.58	0.12				51.44				107.95
A1	SOI 2	#2	point	ol core	59.02		1.28	0.13	13.34					0.50				0.12	25.60				35.36		1.17	0.13	14.03					0.75				0.25	53.54				105.23
A1	SOI 2	#3	point	ol inner	59.07		1.13	0.19	13.38					0.60				0.08	25.54				34.95		1.02	0.19	13.89					0.89				0.17	52.74				103.85
A1	SOI 2	#4	point	ol outer	59.74		0.67	0.00	13.39					0.85				0.09	25.25				35.29		0.60	0.00	13.89					1.26				0.17	52.07				103.29
A1	SOI 2	#5	point	ol outer	58.81		0.82	0.11	13.38					0.79				0.14	25.96				35.19		0.74	0.11	14.05					1.19				0.28	54.21				105.76
A1	SOI 2	#6	point	ol outer	58.44		1.00	0.10	13.71					0.62	0.00			0.00	26.12				34.96		0.91	0.10	14.40					0.93	0.00			0.00	54.54				105.84
A1	SOI 2	#7	point	i/s ol + glass	60.88	0.45	0.00	4.38	15.20	0.27	0.10		2.94	4.75	0.00			0.00	11.03				41.64	0.44	0.00	5.05	18.25	0.36	0.14		4.91	8.14	0.00			0.00	26.33				105.26
A1	SOI 2	#8	point	i/s ol + glass	57.47	0.65	0.00	4.47	13.96	0.22	0.15		2.30	4.13	0.06			0.00	16.59				37.11	0.60	0.00	4.86	15.83	0.27	0.19		3.62	6.68	0.12			0.00	37.40				106.69
A1	SOI 2	#9	point	oxide of lobe margin	54.91			0.56	0.84				0.11	0.36	0.11				43.12				24.85			0.43	0.66				0.12	0.41	0.15				68.12				94.74
A1	SOI 3	#1	area	typical	58.63	0.28	0.51	2.16	11.50	0.11	0.00		0.93	1.45	0.00				24.43				31.84	0.22	0.42	1.98	10.96	0.11	0.00		1.23	1.97	0.00				46.31				95.04
A1	SOI 5	#1	area	typical	57.82	0.38	0.44	2.29	11.84	0.16			1.05	1.57	0.06			0.10	24.28				31.07	0.29	0.36	2.08	11.17	0.17			1.38	2.12	0.10			0.18	45.56				94.48
A1	SOI 6	#1	area	typical	57.71	0.34	0.39	2.22	11.75	0.10	0.00		1.08	1.58	0.06			0.08	24.69				32.30	0.28	0.33	2.09	11.55	0.11	0.00		1.47	2.21	0.10			0.15	48.24				98.84
A1	SOI 8	#1	point	ol outer	60.78		0.43	0.75	13.24				0.64	1.95				0.08	22.12				37.22		0.40	0.77	14.23				0.96	2.99				0.18	47.29				104.04
A1	SOI 8	#2	point	to inner	59.13		0.98	0.17	13.44					0.71				0.12	25.46				34.39		0.86	0.16	13.73					1.04				0.23	51.69				102.11
A1	SOI 8	#3	point	to inner	59.41		1.10	0.41	13.28				0.20	0.88				0.11	24.61				35.27		0.99	0.41	13.85				0.29	1.31				0.22	51.00				103.34
A1	SOI 8	#4	point	to core	58.91		1.18	0.23	13.36					0.67				0.10	25.55				34.38		1.05	0.22	13.69					0.97				0.20	52.05				102.56
A1	SOI 8	#5	point	to core	58.65		1.19	0.15	13.46					0.57				0.10	25.87				34.52		1.07	0.15	13.91					0.85				0.19	53.15				103.84
A1	SOI 8	#6	point	to inner = 3	57.85		0.87	0.21	12.38					0.68				0.08	27.92				33.09		0.76	0.20	12.43					0.98				0.15	55.76				103.38
A1	SOI 8	#7	point	glass	61.05	0.81	0.00	7.90	15.57	0.37	0.16		4.29	3.48	0.06				6.31				43.67	0.84	0.00	9.53	19.56	0.51	0.23		7.50	6.24	0.12				15.77				103.97
A1	SOI 8	#8	point	glass	60.45	0.82		7.69	15.87	0.40	0.17		4.51	3.40	0.08				6.60				41.67	0.81		8.94	19.21	0.53	0.24		7.61	5.87	0.17				15.89				100.93
A1	SOI 8	#9	point	K	60.15	0.42	0.13	1.92	13.22	0.22			0.71	7.97					15.26				40.99	0.41	0.13	2.20	15.82	0.29			1.18	13.61					36.30				110.93
A1	SOI 8	#10	point	glass?	60.14	0.75		7.52	15.90	0.37	0.10		4.19	2.91	0.07				8.05				41.93	0.75		8.84	19.45	0.50	0.14		7.15	5.08	0.14				19.60				103.58
A1	SOI 10	#1	area	typical	58.56	0.42	0.35	2.70	11.99		0.00		1.35	1.98	0.00				22.65				37.44	0.39	0.34	2.91	13.46		0.00		2.11	3.17	0.00				50.55				110.37
A1	SOI 11	#1	area	typical	58.70	0.38	0.48	2.26	12.04	0.11	0.00		1.04	1.57					23.42				31.85	0.30	0.40	2.06	11.47	0.12	0.00		1.38	2.13					44.36				94.06
A2	SOI 1	#1	area	typical	56.56	0.36	0.40	2.41	11.72	0.10	0.00		0.99	1.79	0.06			0.08	25.54				30.32	0.28	0.32	2.18	11.03	0.10	0.00	1.29	2.40	0.10	0.14			47.80	95.98				
A2	SOI 3	#1	area	typical	57.12	0.36	0.50	2.24	11.67	0.00			0.97	1.77	0.00			0.09	25.29				33.88	0.30	0.45	2.24	12.16	0.00			1.41	2.62	0.00			0.19	52.37				105.61
A2	SOI 4	#1	area	typical	56.70	0.27	0.62	2.42	11.81	0.11	0.00		1.07	1.90	0.00			0.14	24.98				31.58	0.21	0.52	2.27	11.54	0.11	0.00		1.45	2.65	0.00			0.27	48.55				99.16
A2	SOI 5	#1	area	typical	56.81	0.43	0.50	2.41	11.90				1.05	1.87	0.06			0.07	24.90				30.93	0.34	0.41	2.21	11.37				1.40	2.55	0.10			0.13	47.31				96.76
A2	SOI 6	#1	point	altered M	53.00			0.57	0.25				0.00	0.00	0.08				46.11				23.81			0.43	0.19				0.00	0.00	0.11				72.30				96.84
A2	SOI 6	#2	point	altered M	52.72			0.65	0.33						0.10				46.19				24.58			0.51	0.27						0.15				75.18				100.70
A2	SOI 6	#3	point	ol core	58.17		1.39	0.20	13.65					0.69				0.12	25.78				32.88		1.20	0.19	13.54					0.98				0.24	50.87				99.89
A2	SOI 6	#4	point	ol inner	57.67		0.67	0.36	14.31				0.14	1.51				0.10	25.23				32.73		0.58	0.34	14.26				0.20	2.15				0.20	49.98				100.45
A2	SOI 6	#5	point	ol outer	58.08		0.96	0.15	13.78					0.90				0.16	25.98				32.00		0.80	0.13	13.33					1.24				0.31	49.96				97.78
A2	SOI 6	#6	point	ol margin	58.37		0.34	0.74	13.98				0.24	2.39				0.00	23.95				33.22		0.29	0.71	13.96				0.34	3.41				0.00	47.58				99.51
A2	SOI 6	#7	point	ol core	58.41		1.46	0.17	13.63					0.76				0.14	25.44				33.31		1.27	0.16	13.64					1.08				0.28	50.63				100.37
A2	SOI 6	#8	point	ol inner	58.12		1.45	0.12	13.65					0.69				0.16	25.81				33.09		1.25	0.12	13.64					0.99				0.31	51.28				100.68
A2	SOI 6	#9	point	ol outer	58.06		0.53	0.12	13.75					1.32				0.12	26.10				32.90		0.46	0.11	13.67					1.87				0.23	51.63				100.88
A2	SOI 6	#10	point	glass/late ol	59.37	0.60	0.00	5.06	15.81	0.27			3.18	5.30				0.07	10.32				38.66	0.56	0.00	5.56	18.08	0.34			5.07	8.65				0.16	23.47				100.55
A2	SOI 6	#11	point	glass/late ol	60.32	0.41	0.15	4.79	15.91	0.28			2.89	5.22					10.02				38.42	0.38	0.14	5.15	17.79	0.35			4.49	8.34					22.29				97.35
A2	SOI 6	#12	point	w?	52.33			0.47	0.38				0.00	0.10	0.12				46.59				24.11			0.36	0.31				0.00	0.12	0.17				74.93				100.00
A2	SOI 6	#13	point	w?	51.63			0.46	0.30					0.13	0.17			0.10	47.21				22.10			0.33	0.23					0.14	0.22			0.14	70.53				93.69
A2	SOI 6	#14	point	weathering?	60.52	0.49		5.61	16.27	0.32			3.12	5.21	0.07				8.39				38.53	0.45		6.02	18.18	0.39			4.85	8.31	0.13				18.65				95.51
A2	SOI 6	#15	point	weathering?	64.56	0.37	0.11	6.36	17.51	0.25	0.00	0.09	2.36	1.62	0.08				6.70				41.56	0.34	0.11	6.90	19.79	0.31	0.00	0.13	3.71	2.61	0.14				15.05				90.65

					O	Na	Mg	Al	Si	P	S	Cl	K	Ca	Ti	V	Cr	Mn	Fe	Ni	Cu	Ba	O	Na	Mg	Al	Si	P	S	Cl	K	Ca	Ti	V	Cr	Mn	Fe	Ni	Cu	Ba	total
B1	SOI 1	#1	area	typical	58.45		0.53	3.00	12.23				1.35	1.58	0.08			0.09	22.69				32.27		0.45	2.79	11.85				1.82	2.18	0.13			0.17	43.73				95.38
B1	SOI 1	#2	area	typical	58.85	0.33	0.60	3.26	12.56				1.23	1.54	0.07				21.56				36.35	0.29	0.56	3.39	13.62				1.85	2.39	0.14				46.49				105.09
B1	SOI 2	#1	area	typical	58.93		0.57	3.35	13.02				1.65	1.51	0.00				20.97				35.62		0.52	3.42	13.82				2.43	2.29	0.00				44.25				102.34
B1	SOI 3	#1	point	ol core	58.50		1.51	0.15	13.51					0.60				0.10	25.63				34.57		1.36	0.15	14.02					0.88				0.21	52.87				104.05
B1	SOI 3	#2	point	ol inner	58.42		1.22	0.15	13.56					0.68				0.08	25.89				34.38		1.09	0.14	14.01					1.00				0.17	53.18				103.97
B1	SOI 3	#3	point	ol outer	58.73		0.72	0.20	13.57					0.92				0.13	25.73				34.64		0.65	0.20	14.04					1.36				0.27	52.96				104.12
B1	SOI 3	#4	point	ol outer	58.22		0.73	0.15	13.65					0.88	0.00			0.12	26.25				33.87		0.65	0.14	13.93					1.29	0.00			0.24	53.30				103.42
B1	SOI 3	#5	point	main ol margin	58.05		0.52	0.17	13.72					1.46				0.13	25.95				33.03		0.45	0.16	13.70					2.09				0.25	51.53				101.22
B1	SOI 3	#6	point	K og	59.35		0.00	0.11	13.31	0.15				9.20				0.08	17.79				36.23		0.00	0.12	14.27	0.18				14.07				0.18	37.91				102.95
B1	SOI 3	#7	point	K og	59.57		0.20	0.12	13.13	0.19				9.29					17.51				36.63		0.18	0.13	14.17	0.23				14.31					37.58				103.24
B1	SOI 4	#1	area	typical	59.93	0.22	0.75	2.79	11.97	0.09	0.00		0.67	0.82	0.09			0.00	22.66				32.94	0.17	0.63	2.58	11.55	0.09	0.00		0.90	1.13	0.16			0.00	43.48				93.64
B1	SOI 5	#1	point	glass	60.71	0.48		9.86	15.16	0.47	0.09		4.66	3.63	0.13				4.80				42.19	0.48		11.55	18.50	0.63	0.13		7.92	6.32	0.28				11.64				99.65
B1	SOI 5	#2	point	glass	60.90	0.44		9.33	15.84	0.38	0.08		4.66	3.54	0.06				4.76				41.25	0.43		10.66	18.83	0.50	0.11		7.72	6.01	0.12				11.24				96.88
B1	SOI 5	#3	point	ol margin	58.61		0.62	0.19	13.70					0.78				0.10	26.00				33.11		0.53	0.18	13.59					1.10				0.20	51.26				99.98
B1	SOI 5	#4	point	ol outer	58.78		1.75		13.43					0.49				0.09	25.46				33.36		1.51		13.38					0.70				0.17	50.44				99.55
B1	SOI 5	#5	point	ol inner	58.46		1.99		13.45					0.53				0.13	25.44				33.43		1.73		13.50					0.76				0.25	50.79				100.47

| | | |

| | | |

| | | |

| | | |

| | | |

| | | |

| | | |

| | | |

				atom% O	Na	Mg	Al	Si	P	S	Cl	K	Ca	Ti	Mn	Fe
A1	SOI 1	#1	typical	59.00	0.29	0.45	2.21	11.24	0.12			0.82	1.30	0.00	0.15	24.44
A1	SOI 1	#3	typical	59.12	0.40	0.44	2.15	11.43	0.11	0.00		0.91	1.48	0.00		23.96
A1	SOI 3	#1	typical	58.63	0.28	0.51	2.16	11.50	0.11	0.00		0.93	1.45	0.00		24.43
A1	SOI 5	#1	typical	57.82	0.38	0.44	2.29	11.84	0.16			1.05	1.57	0.06	0.10	24.28
A1	SOI 6	#1	typical	57.71	0.34	0.39	2.22	11.75	0.10	0.00		1.08	1.58	0.06	0.08	24.69
A1	SOI 10	#1	typical	58.56	0.42	0.35	2.70	11.99		0.00		1.35	1.98	0.00		22.65
A1	SOI 11	#1	typical	58.70	0.38	0.48	2.26	12.04	0.11	0.00		1.04	1.57			23.42
A2	SOI 1	#1	typical	56.56	0.36	0.40	2.41	11.72	0.10	0.00		0.99	1.79	0.06	0.08	25.54
A2	SOI 3	#1	typical	57.12	0.36	0.50	2.24	11.67	0.00			0.97	1.77	0.00	0.09	25.29
A2	SOI 4	#1	typical	56.70	0.27	0.62	2.42	11.81	0.11	0.00		1.07	1.90	0.00	0.14	24.98
A2	SOI 5	#1	typical	56.81	0.43	0.50	2.41	11.90				1.05	1.87	0.06	0.07	24.90
B1	SOI 1	#1	typical	58.45		0.53	3.00	12.23				1.35	1.58	0.08	0.09	22.69
B1	SOI 1	#2	typical	58.85	0.33	0.60	3.26	12.56				1.23	1.54	0.07		21.56
B1	SOI 2	#1	typical	58.93		0.57	3.35	13.02				1.65	1.51	0.00		20.97
B1	SOI 4	#1	typical	59.93	0.22	0.75	2.79	11.97	0.09	0.00		0.67	0.82	0.09	0.00	22.66
B1	SOI 7	#1	typical	56.99	0.52	0.52	3.80	12.12	0.17			1.49	2.03	0.09	0.07	22.19
B2	SOI 3	#1	typical	57.42		1.08	2.70	13.51	0.24	0.11		0.25	2.42	0.09	0.11	22.07
B2	SOI 3	#2	typ with margins	58.34		0.91	3.41	13.03	0.16			0.70	1.88	0.09		21.48
B2	SOI 4	#1	typical	58.29	0.38	0.57	4.62	13.37	0.15	0.00		1.78	1.33	0.11	0.07	19.34
B3	SOI 4	#2	typical	57.13	0.38	0.71	3.61	13.71	0.11	0.00		1.32	1.36	0.08	0.07	21.51
B2	SOI 6	#1	typical	59.48		1.25	2.52	12.32				0.81	0.73			22.88
C1	SOI 1	#1	typical	58.66	0.00	0.59	3.14	11.85	0.09	0.07		0.64	1.80	0.10	0.08	22.98
C1	SOI 2	#1	typical	58.60	0.27	0.38	3.88	12.08	0.11	0.00	0.00	1.06	1.76	0.09	0.09	21.68
C1	SOI 3	#1	typical	58.66		0.27	4.49	12.36				1.59	1.78	0.11	0.09	20.66
C2	SOI 1	#1	typical	57.12	0.00	0.85	2.11	11.00	0.16			0.18	1.45	0.00	0.09	27.04
C2	SOI 2	#1	typical	55.31	0.36	0.76	2.56	12.94	0.15			1.25	2.40	0.08	0.10	24.08
C2	SOI 3	#1	typical	55.89	0.00	0.73	2.63	13.08	0.11			1.16	2.50	0.08	0.00	23.82
C2	SOI 5	#1	typical	55.92		0.80	2.67	11.44	0.17			0.59	1.83	0.07	0.11	26.40
C2	SOI 6	#1	typical	58.12		0.88	2.17	10.03	0.14	0.00			1.05	0.11	0.00	27.51
C2	SOI 7	#1	typical	55.71	0.00	0.79	2.53	13.01				1.25	2.42	0.00	0.11	24.17
D1	SOI 2	#1	typical	54.88	0.35	0.49	2.57	10.60	0.14	0.00		1.02	1.65	0.00	0.00	28.30
D1	SOI 3	#1	typical	55.01	0.32	0.54	2.30	10.52	0.15	0.00		1.04	1.67	0.07	0.00	28.38
D1	SOI 5	#1	typical	55.32	0.00	0.64	2.17	9.89				0.78	1.42	0.00	0.07	29.72
D1	SOI 6	#1	typical	55.24	0.00	0.67	2.15	10.13	0.15	0.07		0.70	1.37	0.00	0.00	29.52
D2	SOI 39	#1	slag by iron	57.16	0.36	0.57	2.38	9.66	0.16	0.00		1.35	1.29	0.00	0.00	27.06
D2	SOI 41	#1	slag by iron	59.24		0.63	1.35	4.81	0.00	0.00	0.00	0.18	0.33	0.00	0.08	33.38
D2	SOI 41	#2	slag by iron	59.55		0.75	2.29	8.52	0.11		0.36		0.64		0.13	27.65
D2	SOI 41	#4	slag by iron	60.95		0.64	1.34	6.32			0.32		0.41	0.00	0.00	30.02
D2	SOI 45	#1	slag nr iron	56.88	0.00	0.65	1.57	5.92	0.12	0.00	0.00	0.60	0.80	0.08	0.10	33.28
D2	SOI 45	#2	slag nr iron	56.49	0.00	0.59	1.54	5.92		0.00	0.08	0.64	0.80	0.00	0.08	33.85
D2	SOI 43	#1	SI	59.48		0.28	1.67	5.26	0.00		0.22		0.23	0.08	0.00	32.80
D2	SOI 43	#2	SI	56.59	0.31	0.65	2.02	8.32	0.14			1.06	1.01	0.00	0.14	29.75
D2	SOI 43	#3	SI	56.18	0.00	0.76	2.05	6.99	0.11			0.82	0.80	0.00	0.11	32.20
D2	SOI 44	#1	SI	57.77	0.00	0.75	2.23	9.17	0.16	0.08	0.00	0.90	1.04	0.06	0.18	27.65
E1	SOI 1	#1	typical	57.61	0.00	0.54	2.11	9.54		0.08		0.73	1.29	0.06	0.00	28.04
E1	SOI 4	#1	typical	57.20	0.00	0.59	2.13	8.96				0.77	1.14	0.00	0.11	29.10
E1	SOI 5	#1	typical	56.58	0.25	0.66	2.17	8.16				0.74	1.25		0.10	30.09
E1	SOI 6	#1	typical	57.51	0.34	0.56	2.39	8.99		0.00		0.80	1.14		0.08	28.20
E2	SOI 1	#1	typical	56.96	0.25	0.75	3.38	11.73		0.00	0.00	1.09	0.81	0.09	0.07	24.87
E2	SOI 2	#1	typical	56.19	0.41	0.62	3.88	12.11		0.08		1.22	0.89	0.00	0.13	24.47
E2	SOI 4	#1	typical	55.70	0.35	0.66	3.70	12.16	0.00	0.00		1.20	0.88	0.00	0.15	25.20
E2	SOI 5	#1	typical	55.12	0.39	0.71	3.63	12.17		0.09		1.11	0.87	0.08	0.15	25.69
F1	SOI 3	#1	typical	56.84	0.37	0.64	2.42	11.38		0.07		0.96	2.91	0.00	0.08	24.33
F1	SOI 3	#2	typical	57.04	0.00	0.62	2.39	11.22	0.00	0.07		0.89	2.91	0.08	0.11	24.67
F1	SOI 3	#3	typical	57.17	0.26	0.56	2.45	11.36	0.10	0.00		0.81	2.93	0.00	0.00	24.35
F1	SOI 4	#1	typical	57.25	0.34	0.54	2.23	11.30	0.00	0.00		0.99	2.94	0.09	0.00	24.31
F1	SOI 4	#2	typical	57.03	0.53	0.56	2.31	12.02		0.00		1.07	3.09	0.00	0.00	23.40
F1	SOI 5	#1	typical	57.26	0.26	0.53	2.43	10.92	0.13	0.00		0.90	3.15	0.07		24.34
F1	SOI 5	#2	typical	57.46	0.00	0.60	2.42	11.02	0.11			0.96	3.18	0.00		24.25
F1	SOI 6	#1	typical	56.63	0.00	0.60	2.31	11.36				0.93	3.17	0.00	0.09	24.91
F1	SOI 6	#2	typical	56.15	0.25	0.64	2.33	11.74				1.00	3.15	0.00	0.07	24.68
F1	SOI 7	#1	typical	56.61	0.24	0.66	2.22	10.74	0.12			0.88	2.63	0.06	0.00	25.83
F1	SOI 7	#2	typical	57.29	0.33	0.58	2.30	11.19				0.94	2.75	0.00		24.62
F1	SOI 8	#1	typical	56.98	0.26	0.54	2.08	10.55	0.00	0.00		0.83	2.64	0.00		26.13
F1	SOI 8	#2	typical	56.45	0.28	0.61	2.34	11.70	0.10	0.00		1.06	2.88	0.00	0.08	24.50
F2	SOI 1	#1	typical	55.91	0.00	0.54	2.67	11.65	0.13			1.02	2.51	0.00	0.11	25.44
F2	SOI 2	#1	typical	55.70	0.42	0.47	2.63	11.23	0.08	0.00	0.06	0.92	2.29	0.08		26.13
F2	SOI 3	#1	typical	55.66	0.33	0.46	2.59	11.45	0.09	0.00		1.00	2.38	0.00	0.00	26.04
F2	SOI 3	#2	typical	55.99	0.25	0.54	2.75	11.56	0.00	0.07		1.02	2.43	0.00	0.00	25.39
F2	SOI 4	#1	typical	55.67	0.34	0.51	2.62	11.44	0.10	0.00		0.94	2.38	0.07	0.00	25.92
G1	SOI 1	#1	typical	55.17	0.32	0.67	1.63	9.87	0.18			0.60	1.48		0.00	30.06

G1	SOI 2	#1	typical	54.33	0.33	0.55	1.90	9.14	0.10	0.00	0.00	0.84	0.99	0.00	0.00	31.82
G1	SOI 3	#1	W free	57.55	0.39	0.98	1.42	13.69	0.16	0.00		0.61	1.24		0.08	23.88
G1	SOI 3	#2	typical	56.39	0.26	0.68	1.84	10.73	0.11	0.09		0.72	1.26		0.08	27.84
G1	SOI 6	#1	W-rich	54.59	0.32	0.27	1.71	7.10	0.18	0.00		0.51	1.43	0.00	0.00	33.89
G1	SOI 6	#2	typical	57.00	0.52	0.46	2.79	9.59	0.21	0.10	0.08	0.99	1.68	0.00		26.57
G2	SOI 66	#1	typical	56.46	0.27	0.58	2.33	10.99	0.20			0.81	1.56	0.00	0.09	26.70
G2	SOI 69	#1	typical	54.54	0.33	0.63	1.56	8.08	0.09			0.52	1.05	0.00	0.00	33.21
G2	SOI 70	#1	typical	54.74	0.00	0.62	1.45	8.31	0.14			0.37	1.10		0.00	33.26
G2	SOI 71	#2	typical	56.26	0.30	0.69	2.08	10.41	0.13			0.61	1.02			28.49
G2	SOI 72	#1	typical	57.08	0.00	0.51	3.77	13.45	0.15			1.96	1.52			21.45
H	SOI 14	#4	in pore	56.99	0.86	0.54	2.35	13.76	0.40	0.16		2.25	3.83	0.08	0.11	18.65
H	SOI 14	#5	in pore	56.84	0.97	0.61	2.61	15.17	0.33	0.17		2.57	4.35	0.00	0.16	16.23
H	SOI 14	#6	typical	53.45	0.38	0.61	1.33	6.20	0.18	0.00		0.90	1.49	0.00		35.48
H	SOI 14	#7	typical	54.23	0.72	0.72	1.81	9.25	0.19	0.10	0.00	1.41	2.39		0.11	29.07
H	SOI 15	#1	typical	53.37	0.50	0.46	1.27	5.89	0.13	0.09		0.76	1.49	0.07		35.99
H	SOI 17	#1	in pore	59.23	0.62	0.60	2.57	15.34	0.34	0.13		2.04	4.85		0.07	14.21
H	SOI 17	#2	typical	52.36	0.00	0.64	0.81	3.06				0.43	0.70	0.00	0.09	41.91
H	SOI 18	#2	typical	52.55	0.41	0.58	0.65	2.76				0.25	0.60			42.20
H	SOI 18	#3	typical	54.84	0.00	0.48	1.31	6.53	0.18	0.00	0.09	0.60	1.46			34.52
H	SOI 19	#1	typical	53.66	0.32	0.46	0.90	3.47			0.00	0.32	0.46			40.41
H	SOI 21	#1	pore fill	58.18	0.55	0.50	1.99	12.59	0.11	0.07		1.22	2.11		0.00	22.68
I	SOI 7	#1	fine ols	58.13	0.49	0.60	3.13	10.24	0.17	0.07	0.00	0.55	1.60	0.08	0.00	24.95
I	SOI 9	#1	typical	55.09		0.33	3.49	8.87	0.00			0.31	0.75	0.06	0.00	31.11
I	SOI 13	#1	typical	55.30	0.44	0.76	3.12	8.61	0.20	0.00		0.77	1.54	0.06	0.00	29.20
J	SOI 1	#1	typical	55.25	0.40	0.57	2.75	8.51				0.79	2.03	0.08		29.62
J	SOI 3	#1	typical	54.89	0.72	0.60	2.69	9.59	0.12			1.22	2.77	0.08	0.00	27.33
J	SOI 3	#2	typical	52.99	0.47	0.55	1.89	6.59				0.70	1.71	0.00	0.00	35.10
J	SOI 3	#3	ol-L in pore	57.63	0.37	0.84	3.89	15.62				2.49	2.84		0.08	16.24
J	SOI 4	#1	ceramic	64.80	0.39	0.73	4.12	26.99		0.00	0.00	1.89		0.16	0.00	0.93
J	SOI 4	#2	marginal slag	58.67	0.79	0.58	3.64	14.67	0.23	0.07	0.12	2.24	4.19	0.08	0.00	14.71
J	SOI 4	#3	typical	54.18	0.82	0.35	2.64	8.45				1.11	2.44	0.11	0.00	29.90
J	SOI 4	#4	marginal slag	64.79	1.48	0.11	3.97	15.08	0.67		0.05	0.17	1.99	0.18		11.50
J	SOI 5	#1	typical - W	57.48	0.73	0.61	2.35	11.67	0.00	0.00	0.17	1.16	2.77	0.00		23.05
J	SOI 5	#2	typical - pore	61.17	0.45	0.53	3.12	13.60	0.15	0.13	0.00	1.57	2.89	0.06		16.31
J	SOI 7	#1	typical - W	54.65	0.80	0.56	2.93	9.39	0.13	0.10		1.09	2.09	0.07		28.17
J	SOI 7	#2	typical - pore	56.21	0.77	0.29	5.21	13.32	0.13			2.80	1.52	0.06		19.70
J	SOI 8	#1	dense W	54.33	0.46	0.47	2.32	8.54				1.02	2.15			30.70
J	SOI 8	#2	dense W	53.86	0.40	0.50	2.39	8.38	0.16			1.08	2.21			31.03
J	SOI 8	#3	dense W	54.52	0.00	0.70	2.48	9.10				1.17	2.16			29.87
J	SOI 8	#4	typical	56.21	0.00	0.54	3.55	11.81				1.86	2.68			23.36
J	SOI 8	#5	F+L	59.63	0.48	0.41	3.51	14.40	0.14	0.00		2.17	3.62		0.06	15.60
J	SOI 8	#6	L/W dom	56.23	0.65	0.18	6.15	14.04	0.10	0.06		3.72	1.80	0.00	0.06	17.02
K	SOI 2	#1	typical	55.54	0.34	0.53	2.06	7.43				0.74	1.05			32.31
K	SOI 3	#1	typical	56.39	0.43	0.44	2.79	9.64		0.00	0.00	1.16	1.34	0.00	0.10	27.71
K	SOI 5	#2	typical	57.63	0.39	0.51	2.56	9.05				1.06	1.25	0.07		27.48
K	SOI 6	#1	incl 'scale'	57.32	0.28	0.49	2.59	9.28				1.06	1.34	0.07	0.12	27.44
K	SOI 6	#2	typical	57.33	0.43	0.39	2.76	10.23	0.09			1.27	1.47	0.07	0.08	25.89
K	SOI 7	#1	typical	57.24	0.32	0.51	2.77	10.81	0.08			1.36	1.66		0.00	25.25
K	SOI 10	#1	typical	57.50	0.57	0.49	2.10	10.50	0.15			1.63	2.05			25.01
K	SOI 10	#2	typical	55.80	0.31	0.30	1.16	4.26				0.82	1.00		0.00	36.35
K	SOI 10	#3	typical	56.65	0.49	0.39	1.06	8.16	0.11			1.56	2.12			29.45
L	SOI 2	#1	ceramic glass	62.51	1.74	0.99	4.63	22.75	0.09	0.00		3.22	1.35	0.20	0.06	2.46
L	SOI 2	#2	typical	59.52	3.91	0.87	4.33	15.16				0.42	0.64	0.07		15.08
L	SOI 2	#3	typical	58.24	1.51	0.76	3.42	13.91				0.69	1.72	0.12	0.00	19.63
L	SOI 5	#1	typical	59.21	1.35	0.45	5.12	14.57	0.13			2.28	1.52	0.06		15.30
L	SOI 5	#2	typical	56.77	1.06	0.68	3.84	11.88	0.12	0.06		1.37	1.56	0.10	0.07	22.48
L	SOI 6	#1	typical	56.00	0.65	0.75	3.12	10.79	0.00			1.34	1.46			25.90
L	SOI 7	#1	typical	55.44	0.73	0.72	3.28	10.90	0.13	0.00		1.47	1.48	0.00	0.09	25.76
L	SOI 8	#1	typical	53.27	0.43	0.78	2.74	8.77	0.12	0.00	0.00	1.11	1.17	0.00	0.00	31.60

GeoArch

geoarchaeological, archaeometallurgical & geophysical investigations

Unit 6, Block C,
Western Industrial Estate,
Caerphilly,
CF83 1BQ

Office: 029 20881431
Mobile: 07802 413704

E-Mail: Tim.Young@GeoArch.co.uk
Web: www.GeoArch.co.uk